EXPERIMENTAL STUDY OF STRUCTURE AND PHASE TRANSITIONS IN SOME LIQUID CRYSTALS

BY

BULBUL GOGOI

A THESIS SUBMITTED
IN
FULFILMENT OF THE REQUIREMENT FOR
THE DEGREE OF
DOCTOR OF PHILOSOPHY

TO
DEPARTMENT OF PHYSICS
NORTH EASTERN HILL UNIVERSITY
SHILLONG - 793 022
DECEMBER, 2002

DEDICATED

TO

MY WELL WISHERS

NORTH – EASTERN HILL UNIVERSITY

DEPARTMENT OF PHYSICS

Date 19/12/02

I Mr. Bulbul Gogoi, hereby declare that the subject matter of this thesis is the record of work done by me, that the contents of this thesis did not form basis of the award of any previous degree to me or to the best of my knowledge to anybody else, and that the thesis has not been submitted by me for any research degree in any other University/Institute.

This is being submitted to the North – Eastern Hill University for the degree of Doctor of Philosophy in Physics.

(Candidate)

(Head) 19.12.02

Prof. & Head,
Physics Department,
N.E.H.U, Shillong-793022.

19.12.02

(Supervisor)

Prof. A. L. Verma
Department of Physics
NEHU, Shillong

(Joint-Supervisor)

Dr. P. R. Alapati
Department of Physics
NERIST, Itanagar

ACKNOWLEDGEMENT

It gives me immense pleasure to wish to express my deepest sense of gratitude and indebtness to my revered supervisor **Professor A. L. Verma**, Department of Physics, NEHU, Shillong (presently Director, NERIST) for his supervision and guidance for this research work. I am highly grateful to him for his encouragement, kind advice and help without which this work would not have been possible to complete.

I always feel great pleasure to work under the guidance and joint-supervision of **Dr. P. R. Alapati**, Department of Physics, NERIST, Itanagar. Let me acknowledge him that practically I come to know first about the fascinating subject, 'liquid crystal' only from him. His constant encouragement and care in every respect during the period of my research work make sure to materialize my dream. Again, in particular, I owe to him for the two research project fellowships (one CSIR and one DST, New Delhi) under him, which provides me the necessary financial support to carry out this work smoothly. Also, I am simultaneously grateful to the funding agency, **CSIR** and **DST** New Delhi.

I take opportunity to thank **Dr. Ayon Bhattacharjee** and **Dr. H. H. Thanga**, Department of Physics, NEHU for their extreme co-operation of my Raman Spectroscopy work at NEHU. My sincere thanks go to all the faculty members of the Department of Physics, NERIST for their help and encouragement during course of this work.

I acknowledge gratefully to my indebtness to **Mr. T. K. Ghosh, Mr. B. P. Deka** and **Mr. O. S. Rathore** for their co-operation and help during my research work. I also

extend my hearty thanks to **Mr. N. N. Chutia, Dr. P. R. Gajurel, Dr. P. Bhuyan, Mr. S. Singh, Mr. L. Behera** and other research scholars and friends of NERIST.

Finally I would like to extend my hearty thanks to madam, **Dr. S. Alapati** and **my family members** and those others who directly or indirectly help me to complete this work.

(BULBUL GOGOI)

CONTENTS

PREFACE

Liquid crystals, a state of condensed matter between that of three dimensional periodic crystalline solids and isotropic liquids, have experienced an explosive growth during the last couple of decades. They were was discovered by an Austrian botanist, *Friedrich Reinitzer in 1888 and later, Lehman identified these liquid crystalline phases in* cholesteryl compounds and named these as "intermediate phases" or mesophases. The most essential requirement for the occurrence of mesomorphism is that the molecule must be geometrically anisotropic in shape, like a rod or a disc. At the same time the molecule must also possess some rigidness of the long axis and strong dipoles. Liquid crystals possess the dual characteristics of solids and liquids, i.e., anisotropic properties of crystalline solids and flow properties of isotropic liquids. Not surprisingly, the intensive materials programme has quite frequently brought to light new materials with hitherto unknown liquid crystalline phases, particularly, the many exotic phases of smectic types and its successful applications in the electrooptical displays. This has stimulated phase transition and structural studies of these systems by Polarizing Thermal Microscopy, Calorimetric studies, X- ray diffraction, Nuclear Magnetic Resonance, Electron Spin Resonance, Neutron Scattering, Raman and FT-IR spectroscopy, Dielectric and Dilatomertic studies etc. The research area is interdisciplinary among chemists, physicists and technologists with a common goal for developing its useful applications.

In the present work discussed in this thesis, Laser Raman spectroscopy and dilatometric measurement techniques were employed to study the structure and phase transition of five liquid crystal compounds. Also, Differential Scanning Calorimetry and dilatometric techniques have been applied to explore tricritical point in Sm A – Sm C phase transition in the binary mixtures of Terepthalylidene-bis-p-n-alkylanine (TBAA) homologues series.

In Laser Raman spectroscopy, variation of some physical quantities are found to affect the polarizability tensor that results in changes in measurable parameters of bands from certain vibrational modes in the Raman spectrum of the system. Laser Raman spectroscopy has been found to be very effective in the study of phase transitions in liquid crystals. In the past couple of decades Raman spectroscopy has been extensively used in the study of liquid crystals to extract structural information, more specifically on the molecular structure and intra/inter-molecular interactions in the liquid crystalline phases. Also, the density measurement studies by either vibration densitometer or classical dilatometer is an important experimental technique for the study of phase transitions and related thermodynamical parameters. The density of the liquid crystalline compound varies with the variation of temperature in liquid crystals. A first order transition is associated with a discontinuity in the density values at the transition whereas the second order transition is accompanied by a continuous change in the density values.

The liquid crystal materials chosen for this thesis work are the liquid crystal dimers, α,ω-bis(4-n-alkylanilinebenzylidene-4′-oxy)alkane, popularly known as m.OnO.m homologues series of compounds for its rich smectic mesomorphism and their

ability to act as model compounds for semi-flexible main chain liquid crystal polymers and also for their quite fascinating and unusual properties. The transitional properties of these dimers depend on the length and parity of the flexible spacer as well as the nature of linking group of the mesogenic units. In particular, the nematic-isotropic transition temperatures are found to exhibit a dramatic alternation on the number of carbon atoms as the alkyl spacer changes from odd to even. However, though a large number of schiff base liquid crystal dimers have been synthesized and characterized in the recent past, the detailed study of various rare and new phase transitions exhibited by the dimers and the detailed structural evaluations have not yet been carried out. Therefore, we have taken up the study of molecular dynamics and phase transitions of few symmetric liquid crystal dimers using Laser Raman spectroscopy and density measurement techniques.

We have also studied another well-known schiff base liquid crystalline compounds, Terepthalylidene-bis-p-n-alkylanine (TBAA) homologues series.This series is popularly known as TBAA homologues series and is interesting for its rich variety of polymorphism with wide thermal ranges. One of the TBAA series compound, TBBA exhibits six mesophases which offers the possibility to study the liquid crystalline modifications of different types and different phase transitions in a single compound. The other interesting aspects of these homologues series are the specific identification of Sm G and Sm H in a single compound, identification of Sm F and Sm I phases, identification of two or three second order phase transitions (Sm A-Sm C, Sm I - Sm F, Sm F-Sm G) in addition to the first order transitions (I - Sm A, Sm C - Sm I, Sm G - K) in a single compound. However, the TBDA, one of the higher homologue of the TBAA

series exhibits a weakly first order Sm A - Sm C phase transition whereas the TBBA, the lower homologue exhibits a second order Sm A - Sm C phase transition. This implies that there exists a tricritical point (where the first order transition becomes second order) at the Sm A – Sm C phase transition in the binary mixtures of TBBA and TBDA. In order to explore tricritical point at the Sm A – Sm C phase transition, we have employed Differential Scanning Calorimetry and the density measurement techniques with varying temperature in the binary mixtures of TBBA and TBDA of different weight percent. The only other study of the Sm A – Sm C tricritical point in TBAA homologues series was reported using x-ray diffraction studies on binary mixtures of TBDA and TBOA where TBOA exhibits a second order Sm A – Sm C transition. However, density studies reported earlier confirm this to be a weakly first order transition in TBOA which prompted us to study the Sm A – Sm C tricritical point of the binary mixtures of TBBA and TBDA, where TBBA has been well established to exhibit a second order Sm A – Sm C phase transition

The thesis is presented in six chapters:

Chapter – 1 sets out a brief introduction to liquid crystals and their classifications. An overview of the structural description of different liquid crystalline phases has also been presented. The importance of schiff base liquid crystal dimers and TBAA homologues series are described briefly. A general focus on phase transitions in liquid crystals and types of experimental techniques used are also discussed. The prime

experimental techniques, Laser Raman spectroscopy and density measurement by bicapillary pyknometer have been briefly discussed.

Chapter – 2 gives the description of the experimental techniques used in the present study. The methods of preparation of liquid crystal dimer and TBAA compounds are discussed. A brief discussion on DSC is given in the light of phase transition and transition enthalpy data. The thermal polarizing microscope and its accessory like heating block, for varying the temperature are described briefly. In order to carry out the temperature dependant Raman studies, a device having temperature variation facility is designed and fabricated, a brief description of this is also given. A brief description of different components used in Laser Raman Spectroscopy and Density measurement is also presented.

Chapter – 3 describes the phase transition studies of five liquid crystal dimers viz. 7.O4O.7, 7.O5O.7, 10.O4O.10, 10.O10O.10 and 10O.12O.10 by DSC and density measurements. Compounds 7.O4O.7, 7.O5O.7 and 10.O10O.10 exhibit Sm A and Sm F phases and Compound 10.O4O.10 exhibits Sm C and Sm F phases while the compound 10.O12O.10 exhibits only G phase. The synthesis and identification of the phases exhibited by these compounds are described in chapter 2, while the entropy studies are described in this chapter. DSC studies revealed that the entropy values of different phase transitions of the dimers are larger than that of other monomeric compounds (twice that of monomeric compounds). Further, the entropy value of even spacer dimer (7.O4O.7) at the Isotropic – Sm A transition is nearly double compared to the odd spacer dimer (7.O5O.7). These very large entropy values suggest that, both the orientational and

translational ordering in the smectic A phase are high for even spacers and also reflect the alternation of entropies in varying the flexible spacer for any given length of terminal chain. The phase transitions Sm A – Sm F and I – G phase are rare kind of transitions. Only two compounds (10.O12O.10 being the second compound) are known to exhibit the I – G transition so far. The other compound is 18.O14; in which the I – G transition has been studied by density measurements. The nature of phase transitions is discussed from the changes in the density across the phase transitions and the calculated thermal expansion coefficients in the liquid crystalline phases of all the dimers studied. A comparison of the estimated pressure dependence of transition temperatures using Clausius – Clapeyron equation with those reported in literature are also presented. All the transitions are found to be first order in nature but smaller jump were observed than expected in the density across certain transitions.

Chapter – 4 describes our results of the study of molecular dynamics using Laser Raman spectroscopy on 7.O4O.7 and 7.O5O.7. Laser Raman studies on two compounds of the series, α,ω-bis(4-alkylaniline benzylidene -4′-oxy)alkane, which were carried out in the spectral regions of 1140 – 1220 $cm^{-1}$and 1550 – 1650 cm^{-1} as a function of temperature, are presented. Compounds, 7.O4O.7 and 7.O5O.7, exhibit Sm A and Sm F phases. The Raman spectra of these liquid crystal dimers have been analyzed. This Raman spectra at the room temperature remarkably highlight the odd – even effect. We have explained the results on the basis of the bending dynamics of these compounds, and its manifestation in the odd – even effect at the molecular level by assuming a semi-rigid core region of the dimeric molecule. We find that the odd spacer dimer (7.O5O.7)

satisfied the molecular model, whereas the even spacer dimer (7.O4O.7) is established to behave like monomeric compounds such as nO.ms. In both the cases, the dynamics about the C = N bond have a profound effect on the molecular shape in different phases and phase behaviour which have been discussed.

Chapter – 5 describes the tricritical behaviour of the Sm A – Sm C phase transition where a first order transition becomes second order transition in the TBAA homologues series. The only other study of the Sm A – Sm C tricritical point in TBAA homologues series was reported using x-ray diffraction studies on binary mixtures of TBDA and TBOA, where TBOA was found to undergo a second order Sm A – Sm C transition. However, density studies reported confirm this to be a weakly first order transition in TBOA. On the other hand, the TBNA and TBDA, higher homologues of the TBAA series, exhibit a weakly first order Sm A – Sm C phase transition, whereas the TBBA, the lower homologue exhibits a clearly second order Sm A – Sm C phase transition within the series. For this reason, we have chosen to study binary mixtures of TBBA and TBDA, where TBBA has been well established to exhibit a second order Sm A – Sm C phase transition. These imply the existence of a tricritical point. In order to investigate the tricritical point (TCP) of the Sm A – Sm C phase transition, binary mixtures of TBBA and TBDA (of different weight percent) of few compositions have been studied as tricritical point is approached using DSC and density measurements as a function of temperature. The results of these studies clearly suggest the decisive role played by the Sm A thermal range in determining the nature of the Sm A – Sm C transition and governing the TCP, since the transition becomes weakly first order as the

thermal range of Sm A decreases. The TCP for TBOA was reported in the thermal range of 9.4°C, which is much lower than that of our TBDA+TBBA mixture (present study) where the Sm A thermal range is about 17°C.

Chapter – 6 deals with the summary and the major conclusions drawn from each chapter in this thesis. The major conclusions from the present thesis can be mentioned as follows.

1. Synthesized the liquid crystal dimers (7.O4O.7, 7.O5O.7, 10.O4O.10, 10.O10O.10 and 10O.12O.1) and TBAA compounds (TBBA and TBDA) and characterized the phases and phase transition temperatures using the Polarizing Thermal Microscopy and Differential Scanning Calorimetry.
2. Characterized the two very rare phase transitions, Sm A – Sm F and I – G in addition to I –Sm A, Sm C – Sm F phase transitions using density measurements. The density jump and a peak in the thermal expansion coefficient in all the transitions confirm the first order nature of the transition but smaller jumps were observed (than expected) in the density across certain transitions.
3. Study of molecular dynamics using laser Raman spectroscopy on two liquid crystals dimers (7.O4O.7 and 7.O5O.7). The Raman spectra of these compounds at room temperature remarkably highlight the odd – even effect. Odd spacer dimer (7.O5O.7) satisfies the semi – rigid core of the molecular model, whereas the even spacer dimer (7.O4O.7) is established to behave like monomeric compounds such as nO.ms. In both the cases, the dynamics about the C = N bond

have a profound effect on the molecular shape in different phases and phase behaviour.

4. The results of the TCP studies on TBBA and TBDA mixtures clearly indicate the decisive role played by Sm A thermal range in determining the nature of the Sm A – Sm C transition. The transition becomes weakly first order as the thermal range of Sm A decreases. The earlier report on TCP for TBOA was found in the thermal range of 9.4°C, which is much lower than that of our TBDA+TBBA mixture where the Sm A thermal range is about 17°C.

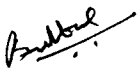

BULBUL GOGOI

NERIST, Itanagar

LIST OF TABLES

LIST OF PLATES

LIST OF FIGURES

CHAPTER - 1

1. GENERAL INTRODUCTION

"Liquid Crystal" *may be defined as a thermodynamically stable phase characterized by anisotropy of properties without the existence of a three dimensional crystal lattice.* For many organic materials, the transition from the solid to the liquid phase does not occur in a single step but takes place in a cascade of transitions [1]. The molecular ordering in these intermediate phases, known as '***mesophases***,' lies between that of a solid and an isotropic liquid. These ordered fluid mesophases are commonly called liquid crystals and are most often composed of elongated molecules. In these mesophases, the molecules show some degree of rotational order (and in a few cases partial translational order as well) even though the crystal lattice does not exist. Lack of a lattice requires that these mesophases be fluid; they are, however, *'ordered fluid phases'*. It is this simultaneous possession of liquid-like (fluidity) and solid-like (molecular order) character in a single phase that makes liquid crystals unique and gives rise to so many interesting properties as well as technological applications. A most fascinating aspect of liquid crystals is that their study, which began as basic research with purely academic interests, has led to the development of a host of devices with very versatile applications. The research area of liquid crystals is interdisciplinary and is of equal interest to physicists, chemists, mathematicians and technologists for the development of high quality electro-optic devices.

Liquid crystals were discovered by an Austrian botanist, F. Reinitzer [2] in the year 1888. Later, Lehman [3] identified liquid crystalline phases in some cholesteryl compounds and termed them as intermediate phases. Liquid crystalline phases are generally characteristic of materials composed of molecules which are highly anisotropic in shape (i.e., anisometric) [4] and are commonly exhibited by rod or disc

shaped molecules. This anisometry is essential since the molecules exhibiting liquid crystalline character should not only possess some rigidity but should also be able to rotate around the long molecular axis, sweeping a cylindrical volume, thereby undermining the importance of rotational order/disorder.

A liquid crystal generally comprises of anisometric organic molecules possessing some rigidity in the structure. The general structure of a liquid crystalline compound is shown below [5].

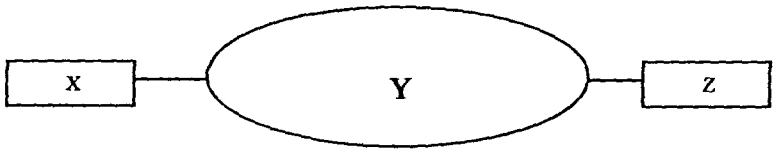

In this figure, X and Z represent the zigzag tails of the liquid crystal, which may be R (R= alkyl chains), RO, CN, NO_2, Cl, etc. Y is the central rigid part called core. Y is generally composed of phenyl rings, substituted phenyl rings (Aromatic), Aro-CH=N-Aro, Aro-N=N(O)-Aro Aro-CH=N-Aro=N-Aro, Aro-COO-Aro, etc. The properties regarding the liquid crystalline nature exhibited by the two molecules possessing the same molecular formula but different atomic arrangement are subtle. For example, the compounds (1) and (2),

(1) $CH_3CH_2CH_2CH_2CH_2O$AroCN

(2) $CH_3CH_2OCH_2CH_2CH_2$AroCN

possess the same formula with identical chain lengths and rod like shapes, but differ only in the location of oxygen. The compound (1) exhibits a mesomorphic phase between 53 °C and 65 °C while compound (2) does not show any liquid crystalline properties.

1.1 CLASSIFICATION OF LIQUID CRYSTALS.

Depending on the process by which transition of intermediate phases occur, the liquid crystals can be broadly classified into two categories viz. Thermotropic and Lyotropic liquid crystals. The term 'thermotropic' implies that the transition to the mesophases are brought about by thermal process i.e. thermotropic liquid crystals are formed due to variation of temperature (cooling or heating) while the lyotropic liquid crystals show mesomorphic behaviour due to influence of solvent on a solid or liquid and are biologically very important. However, modern texts prefer to classify liquid crystals on the basis of their molecular structures into four comprehensive groups which are:

a) Calamitic Liquid Crystals [6-10].

b) Discotic Liquid Crystals [11-15].

c) Lyotropic Liquid Crystals [16-20].

d) Defect Phases [21-25].

Based on structure and symmetry these liquid crystalline groups are further classified into different mesophases. Since the present thesis deals with the study of phase transitions as well as molecular dynamics in thermotropic mesophases, a brief description of various order parameters used to classify the liquid crystals is given in the next section.

1.1.1 ORDER PARAMETERS

When a system undergoes a phase transition, one cannot describe the two different phases by a single analytical function. Hence an extra parameter is required for describing the system in a low symmetry phase. This parameter which is used to quantify the positional or orientational order of the liquid crystalline molecules is thus

appropriately termed as order parameter. A very important feature of order parameter is that, while describing the order of the molecules in the liquid crystalline materials, it also allows orientational deviation of the individual molecules from the director [26]. Typically the value of order parameter in liquid crystalline materials lie within a range of 0.3 to 0.9 depending on the temperature, with a value of unity for perfect order and a value of zero for the isotropic phase. The order parameters commonly considered in the study of liquid crystals are discussed here briefly, which will help us in the discussion on classification of liquid crystals.

1.1.1.1 Orientational order:

The orientational order can be described as a measure of the tendency of the molecules to align along the director on a long range basis. In a nematic liquid crystal, for example, with a preferred direction $\hat{n}$ for the long molecular axis (called the director) an average orientational distribution function f(θ) exists, where θ is the angle between the long axis of the molecule and the director. This distribution function can be expanded in a series of Legendre polynomials as,

$$f(\theta) = S_0 P_0(\cos\theta) + S_2 P_2(\cos\theta) + S_4 P_4(\cos\theta) + S_6 P_6(\cos\theta) + ... + \qquad (1.1)$$

The Legendre polynomials are denoted by $P_n(\cos\theta)$ and S_n are the coefficients describing the orientational distribution function. Only even powers of the Legendre polynomials are retained since the director can be defined in either of two opposite directions, $\hat{n}$ or $-\hat{n}$. The dominant parameter is S_2 and when properly normalised, i.e.,

$$S_2 = \frac{1}{2}\left\langle 3\cos^2\theta - 1 \right\rangle, \qquad (1.2)$$

then S_2 can be used as the orientational order parameter.

1.1.1.2 Bond Orientational order:

This is an order parameter which describes a line joining the centres of nearest neighbour molecules without requiring a regular spacing along that line. Thus, a relatively long range order with respect to the line of centres becomes possible by only short range positional order along that line. This order parameter plays a very important role in the phase transitions of the hexatic phases. Thus a bond orientational order with six-fold symmetry in the plane of the layer actually is an expression for the arrangement of the hexagonal net i.e. the net is arranged in the same way from layer to layer, but there is no real positional correlations of the molecules between the layers. To represent mathematically, the bond angle variation can be expressed as,

$$\psi_6 = I_6 e^{6i\phi} \qquad (1.3)$$

Where ϕ is the azimuthal angle and I_6 is the complex order parameter.

1.1.1.3 Translational order:

Positional order is used to describe the extent to which the position of an average molecule or group of molecules shows translational symmetry. For example, the layering tendency of the molecules can be described by an average density of the centres of mass $\rho(z)$, which sinusoidally varies along the normal to the layers. The amplitude of the sinusoidal part, ψ, describes the amount of positional order and can be used as an order parameter:

$$\rho(z) = \rho_0\left[1 + \psi\cos\left(\frac{2\pi z}{d}\right)\right] \qquad (1.4)$$

where ρ_0 is the average density, and d is the distance between the layers.

On the basis of these order parameters and other properties, the liquid crystals are broadly classified into the following categories.

1.1.2 Calamitic Liquid Crystals:

These are the most common type of thermotropic liquid crystals and are composed of rod-like molecules with one molecular axis much longer than the other two. Depending on the structure and symmetry, calamitic liquid crystals are further divided into three main classes, viz., the nematic liquid crystals, the cholesteric liquid crystals and the smectic liquid crystals.

i) **Nematic liquid crystals**:

Liquid crystalline compound possessing only nematic phase is called nematic liquid crystal. If we consider liquid crystalline compounds in terms of the translational and orientational ordering of their individual molecules, then in nematic liquid crystals, there is only orientational ordering, but no translational ordering between the molecules. To be more specific, in the nematic phase the molecular centre of mass positions are disordered as in a liquid but have a statistically parallel orientation of the molecular long axes of each molecule along the director ($\hat{n}$). Therefore, the molecular ordering in nematics is long range orientational order and there is no regular arrangement of the ends of the molecules. In the state of thermal equilibrium, the nematic phase has a symmetry ∞/mm and is therefore uniaxial. The direction of the director ($\hat{n}$) is arbitrary. The molecular arrangement of nematic liquid crystals is shown in Fig. 1.1a.

In some nematics, there exists a short-range smectic-like order in addition to the characteristic long-range orientational order. These nematics are termed as cybotactic nematics, skewed cybotactic nematics (N_{SC}) or normal cybotactic nematics

(N_{nc}). In the first case, the smectic like order involves not only the layered arrangement of the molecules but also significant tilt of the molecules whereas in the second case, the molecules are parallel to the layer normal of the smectic like groups. The nematic phase exhibits schlieren, threaded, marbled, pseudo-isotropic and homogeneous textures when viewed through crossed polarizer.

ii) **Cholesteric or spontaneously twisted nematic liquid crystals:**

The cholesteric mesophase is similar to the nematic mesophase except that it is composed of optically active molecules. In this phase, the different layers orient at a slight angle relative to each other (rather than parallel as in nematic). So the directors in each layer are twisted with respect to those of the preceding layers to form a continuous helix about the layer normal. Cholesteric phase is also known as "spontaneously twisted nematic phase". The term cholesteric has been borrowed from the word cholesterol since this phase was first reported in the derivatives of cholesterol. The cholesteric liquid crystals are uniaxial (positive or negative) and exhibit focal conic with Grandjean steps, homogeneous and isotropic textures. Apart from optical activity, this phase also exhibits circular dichroism. (Fig. 1.1b).

iii) **Smectic liquid crystals:**

Smectic liquid crystal phases are characterized by a one dimensional density wave along the average director giving rise to a layered structure. These liquid crystals have stratified structures but a variety of molecular arrangements are possible within each stratification [27-30]. There exists a number of smectic phases, but two of the most important cases occur when the director is parallel to the layer normal giving rise to orthogonal phases, and when the director is making an angle to the layer normal giving rise to the tilted phases. The smectic mesophase forms a one-

dimensional periodic lattice in which the molecular arrangement within the individual layers are two-dimensional (liquids like). The interlayer attractions are weak as compared with the lateral forces between molecules and, as a consequence, the layers are able to slide over one another relatively easily. There are various modifications of the smectic phases, each with different combination of in-plane order and tilt angle. These have been named as the smectic A, B, C, D, E, F, G, H, I, J and K phases designated as, Sm A, Sm B, Sm C, Sm D, Sm E, Sm F, Sm G, Sm H, Sm I, Sm J and Sm K or S_A, S_B, S_C, S_D, S_E, S_F, S_G, S_H, S_I, S_J, and S_K, with the letters denoting the chronological order of discovery of these phases. The sequence of their appearance is S_A, S_D, S_C, S_B, S_E, S_I, S_F, S_G, S_G' (S_J), S_H and S_H' (S_K) with decreasing temperature. S_B, S_G, S_J, S_E, S_H and S_K are found to be more crystalline than liquid crystalline phases. Therefore, at present, these phases are treated as soft crystalline phases and designated as the B phase, G phase, J phase, E phase, H phase and K phase. If a compound exhibits both nematic as well as smectic phases, the nematic phase always appears on the higher temperature side. No single compound is found to exhibit all the smectic phases (modifications) so far. However, the maximum number of phases that a single compound can exhibit are found to be six so far, by terepthalylidene-bis-p-n-butyl aniline (TBDA) as well as N (p-n-pentoxy benzylidene) p-n-hexylaniline (5O.6). The structural identification of each smectic phase is briefly discussed below and their molecular arrangements are shown in the Fig. 1.1c.

SMECTIC A:

The molecular arrangement in this phase involves a parallel arrangement of the rod-like molecules with their ends in line to form layers in which the long axes of the molecules tend to be orthogonal to the layer planes. Rotational motion of the

molecules is fairly free, but there is no long range packing of the centres of gravity of the molecules in the planes of the smectic layers. The layers are therefore liquid like in nature. The movement of the molecules from one layer to another, i.e., diffusion of molecules, occurs quite freely and the layers are free to slide on one another. The S_A phase is uniaxially positive. This phase usually exhibits pseudo-isotropic or homeotropic texture in which the smectic layers are parallel to the supporting surface and the optic axis is perpendicular to it. The characteristic textures observed are battonnets, focal conic fan and polygonal. If a liquid crystalline compound has S_A phase in addition to other smectic phases, the S_A phase is always found to be at the higher end of the temperature range.

SMECTIC B:

The smectic B phase generally exists along with S_A phase and occurs upon cooling the S_A phase. The molecules tend to be orthogonal to the layer planes and lamellar spacing is approximately equal to the molecular length. The layers in S_B phase are highly structured unlike in the case of S_A phase. The molecular centres lie on a hexagonal network and the molecules are free to rotate about their long axes. The dimensions of the hexagonal network are, however, small in relation to the size of the molecules, so that the molecular rotation can hardly be regarded as free, but is probably cooperative [31]. Three types of molecular stackings in smectic B phase are reported to be possible [32], namely AAA... (monolayer), ABA...(bilayer), which is also the most common one, and ABCA...(trilayer). The correlation between these layers was also reported in some compounds. Experimental studies [33] established a hexatic B phase which is different from the crystal S_B phase in a few compounds. The hexatic B exists at a higher temperature than the crystalline S_B phase and has short-

range in-plane positional ordering and long range bond orientational ordering, both within and between the layers. Some compounds exhibit both types of smectic B phases [34]. If S_B follows the S_A phase upon cooling, S_B phase adopts all the textures exhibited by S_A phase with some modifications. This phenomenon is known as paramorphosis. However, the natural texture of S_B phase is mosaic, while the S_A -S_B transition is accompanied by the appearance of transient transition bars across the fans or focal conics while cooling from S_A phase. Hexatic B to crystal S_B phase transition also exhibits paramorphotic texture with difference in fans.

SMECTIC C:

This phase is the tilted analogue of the S_A phase i.e., the smectic layers have a liquid like, unsaturated arrangement of molecules where the molecular long axes or the directors ($\hat{n}$) are tilted with respect to the layer normal at an angle (θ) that varies from compound to compound. Three different tilt angles viz., one associated with the central atomic core region and the other two with the end alkyl chain regions of the smectic layers, are differentiated [35,36]. The tilt angle is temperature dependent [37] in some compounds and is temperature independent in some other compounds. The S_C phase either exhibits broken focal conic fan or schileren textures.

SMECTIC D:

Only a very few compounds [38,39] are known to exhibit this phase and the common variants observed are I- S_D- S_C or I- S_A -S_D- S_C. Diele et al [39] proposed a structural model for this phase with a cubic close packing of spherical units with each unit consisting of several molecules. No characteristic texture was observed because this phase is found to be optically isotropic. However, in the compound 4-hexyloxy-3-nitrobiphenyl-4-carboxylic acid, which exhibits S_D phase between S_A and S_C phases, a

mosaic texture is observed initially which later transforms into an isotropic texture spontaneously.

SMECTIC E:

This phase is commonly observed [40] in the sequence N- S_A – S_B – S_E with decreasing temperature. The X-ray diffraction studies indicate (i) a high degree of order in smectic layers with a distinctly non-hexagonal lattice, (ii) orthogonal arrangement of molecules with respect to the layers, and (iii) a three dimensional lattice. In some of the S_E modifications optically biaxial properties are observed [41]. Goodby [42] has reported it to be optically uniaxial. Some compounds exhibiting S_E phase are found to possess an orthorhombic cell in the S_E layers. This phase exhibits mosaic and the paramorphotic fan textures with concentric curves across the fans.

SMECTIC F:

This phase is observed in the homologues of pyridene derivatives [43], higher homologues of terepthalydene bis-p-n-alkylaniline (TB$\overline{A}$A) series [43], Schiff base liquid crystal dimers [44] and a few N (p-n-alkoxy benzylidene) p-n-alkylaniline (nO.m) compounds [45] and in α-ω-bis(alkyaniline benzylidene-4′-oxy)alkane (m.OnO.m) homologues series [69]. The S_F phase has long range order of tilt direction (similar to S_C phase) and has a quasi-two-dimensional structure, with essentially no correlation of molecular positions between layers. The molecules are packed in hexagonal layers with their long axes tilted with respect to the layer planes. It has a C-centred monoclinic lattice with long range three-dimensional order of the lattice direction but does not have long range positional ordering. Shift distortions of the hexagonal net occur between layers, indicating poor correlation between the layers. However, since mono-domains can be obtained with a uniform tilt direction,

the hexagonal symmetry is apparently preserved through the bulk of the sample, and it may be concluded that the layers are free to slide over, but not free to rotate relative to one another, i.e., the phase has extensive three dimensional bond orientational ordering. The S_F phase exhibits stripped or chequered fan and schlieren textures under polarizing thermal microscope.

SMECTIC G:

The smectic G phase is more crystalline in nature and found almost all the nO.m and some of m.OnO.m compounds at low temperature. It has a pseudo-hexagonal structure with a local herringbone order. This phase, of course, has a three-dimensional structure but with a considerable disorder, i.e., the layer distribution is not sharp as in the case of crystals. Presumably this is associated with orientational disorder of the molecules about their long axes. As the layer thickness does not change discontinuously at the S_F -S_G transition, no change in tilt is expected and hence the tilt in S_G phase is of the same magnitude as in the S_F phase. The S_G phase exhibits paramorphotic focal conic fan or characteristic mosaic texture.

SMECTIC H:

Sakagami et al [46] had first differentiated S_G and S_H phases in the well known terepthalylidene bis-p-n-butylaniline (TBBA) and its higher homologues which are rich in S_G and S_H phases. In the S_H phase, the layers are highly structured and it is analogous to S_E phase with a tilt of the molecules. The arrangement of the molecules in the layers can be described as monoclinic when compared with the orthorhombic orthogonal arrangement of molecules in the S_E phase. The characteristic textures of S_H are mosaic which are different in the areas of the mosaic of S_G and the paramorphotic focal conic fan.

SMECTIC I:

Higher homologues of the TB$\bar{A}$ A series (alkyl = nonyl, decyl, dodecyl) [47] exhibit the S_I phase. Esters like 4-(2'methylbutyl)phenyl 4'-n-octyloxybiphenyl-4'-carboxylate (8OSI) and amines, like N,N'-bis- (4'-n-heptyloxy benzylidene)-1, 4-phenylenediamine (7OBPD) also exhibit the S_I phase. The molecules are tilted in the layers and the tilt angle in this phase is equal to the tilt angle in the lower temperature S_G and S_F phases. It has more or less similar structure to that of the S_F phase. The only difference is that S_F phase has an in-plane short-range positional ordering whereas the S_I phase has a typical long range positional ordering. However, the S_F and S_I phases also differ in the direction of molecular tilt relative to the hexagonal packing of the molecular long axes. For the S_F phase the hexagon is tilted towards an edge, while for S_I phase, the tilt is towards an apex of the hexagon. The S_I phase exhibits broken fan, mosaic and schlieren textures.

SMECTIC J AND SMECTIC K:

Gane et al [48] first observed these phases in bis-(4'-heptyloxybenzylidene)-1,4'-phenylenediamine (HEPTOBPD) and confirmed that these are not new liquid crystalline phases, but two disordered crystal phases which are analogous to S_G and S_H phases except for the direction of tilt. Both the phases have monoclinic symmetry (with b>a) and pseudo-hexagonal packing of the molecules that are tilted towards the apex of the hexagon. The distortion from the hexagonal packing is greater in the lower temperature phases. Leadbetter et al [49] confirmed the existence of S_J phase in 4-n-hexylphenyl 4-n pentyl phenyl 4-n-decyloxybenzothiolate.

Some of the smectic phases exhibit ferroelectricity when they are composed of chiral molecules. The potential applications of these ferroelectric liquid crystals are so

immense that it is studied as a new branch of material science and technology. It is separately discussed in forthcoming sections later.

1.1.3 Discotic liquid crystals:

Discotic phases are formed on heating compounds that are composed of relatively flat, disc-shaped molecules. These have been recognized as a distinct class of liquid crystalline compounds where the short axis of the molecules maintains a preferred orientation. Evidence for the formation of the mesomorphic phases by disc-like molecules dates back to 1960 [50-52]; however, identification of the discotic phase was made by Chandrasekhar et al [11,13] in 1977 with benzene-hexa-*n*-alkanoate compounds. Investigations have revealed that not only does the extended columnar discotic system exists, discotic analogues of the nematics are also well recognized now a days. Polymorphism of the columnar discotic systems is also possible depending upon the nature of the lateral packing of the columns and the tilt angle of the column with respect to the normal to molecular planes. Some discotic liquid crystals, analogous to smectic liquid crystals, possess no positional order parallel to the director, making them behave like one-dimensional liquids. In the columnar phase the molecules are more likely to be found in columns rather than between the columns. This phase possesses the orientational order of the nematic phase and also positional order in directions perpendicular to the director. The structures of a few discotic liquid crystals are shown in the Fig. 1.2.

1.1.4 Lyotropic liquid crystals:

Lyotropic liquid crystals are made up of two or more components. Generally, one of the components is an amphiphillic (containing a polar head group attached to one or more long hydrocarbon chains) and the other is water. A familiar example of

such a system is soap (sodium dodecylsulphate) in water. As the water content is increased several mesophases are obtained. These phases differ from other liquid crystalline phases because these are multi-component systems and the concentration of the various components of the system is an important parameter in exhibiting the liquid crystalline properties by these systems [19,20,53].

A few modifications of lyotropic liquid crystals have been identified. In the lamellar, or the neat phase, water is sandwiched between the polar heads of adjacent layers, while the hydrocarbon tails, which are disordered or are in a liquid-like configuration, are in a non-polar environment. In the cubic, or the viscous isotropic phase, the layers are bent to form spherical units with a body-centred cubic arrangement. In the hexagonal or middle phase, the layers are rolled up into cylindrical units of indefinite length arranged parallel to one another in a hexagonal array. A nematic type ordering has also been observed in some soap systems. In hydrophobic dominated compositions, such as aerosol OT-water system, inverted middle and inverted viscous isotropic phases can occur in which the tails point outward towards the hydrophobic medium while water is trapped inside. Cholesteric liquid crystals are formed by the solutions of synthetic polypeptides, e.g., poly-γ-benzyl-L-glutamate, in organic liquids when the concentration exceeds a certain critical value. Lyotropic liquid crystals occur abundantly in nature, being ubiquitous in living systems. (Fig. 1.3.)

1.1.5 Defect phases:

One of the most important recent developments in the science of liquid crystals is the appreciation of liquid crystal phases which are possible only through the incorporation of periodic and non-periodic defects [54,55]. Defects in a liquid

crystalline phase are points, lines or surfaces at which the orientational or positional ordering is not defined. These defects, thought to be energetically unfavourable, are a part of the structure of the new phases. These phases can be thought of as super structures in which individual regions exhibit liquid crystallinity and the regions are separated by defects. These defects may have the order of an isotropic liquid in analogy with a 'melted lattice.' Two of the important defect phases are the smectic twist grain boundary (TGB) phase and the blue phases formed by some highly chiral molecules. In the TGB phase, the tendency of the molecules to form a twisted phase is frustrated by an additional tendency to form layers. The result is a smectic A structure periodically interrupted by the grain boundaries where the smectic A structure twists by a small angle. In blue phases, regions with liquid crystalline order slightly different from the chiral nematic phase are separated by a lattice of line defects. A few of the defect phases are shown in Fig. 1.4.

1.2 FERROELECTRIC LIQUID CRYSTALS

The ferroelectric effect was first observed in 1921 by Valasek [56] during experiments on crystals of Rochelle salt (potassium sodium tartarate). A ferroelectric material is characterized by an electric dipole moment even in the absence of an external electric field. In these materials the centre of positive charge does not coincide with the centre of negative charge, resulting in the development of spontaneous polarization [57]. This spontaneous polarization, which is the most characteristic property of a ferroelectric material, usually vanishes above a certain temperature called the Curie temperature. There is an intimate relationship between the ferroelectric properties and the atomic arrangement of the ferroelectric materials. Two viewpoints contribute to the understanding of occurrence of ferroelectricity. One

is the idea of polarization catastrophe where the local field caused by polarization increase faster than the elastic restoring force on an ion in the crystal, thereby leading to an asymmetrical shift in ionic positions. The other idea is that the static dielectric constant increases when the transverse optical phonon frequency decreases. Both of these ideas have been used to describe the origin of ferroelectricity in different types of materials [58].

In 1975, the American physicist Meyer using symmetry arguments suggested that the tilted smectic phases made up of chiral molecules should also exhibit ferroelectricity. [59,60] Ferroelectricity in the tilted smectic phases requires the molecules to be chiral. The concept of chirality and how it influences the tilted smectic phase, is discussed in the following section. We have confined our discussion to the chiral smectic S_C^* phase since materials exhibiting this phase are used for device applications. However, the same arguments apply equally to other tilted chiral smectic phases like S_F^*, S_I^* and also the crystal smectic phases H*, J*, K* and G*.

The ferroelectric liquid crystals, the first group of compounds with fluid properties, can be thought of as the most recent members of the already rich family of ferroelectric materials,. They are very similar to the ferroelectric solids in some respects, like, they exhibit spontaneous polarization, have a Curie point and their macroscopic polarization vanishes as the system approaches this temperature. The electro-optic properties of the ferroelectric liquid crystals are widely different from those of the other kinds of liquid crystals. Ferroelectric liquid crystals switch at a very fast rate (~ 1μs) with a large change in the refractive index ($\Delta n \sim 0.1$). With such a fast response, ferroelectric liquid crystals have opened new avenues in the field of display technology. Today commercial applications of the ferroelectric liquid crystals include

flat panel displays, miniature xerographic devices and high-resolution printheads, etc., to name a few. The molecular alignment and structure of ferroelectric liquid crystals are shown in Fig 1.5.

1.3. Importance of Schiff base Liquid Crystal

The first room temperature liquid crystal compound that exhibits only the nematic phase was N(p-n-methyloxybenzylidene)p-n-butylaniline [68], popularly known as MBBA. It was reported in 1969 and has paved the way for a new era in liquid crystals research and applications. In this present thesis we have chosen some schiff base liquid crystal dimers and TBAA compounds to study molecular structures and phase transitions.

1.3.1 Liquid Crystal Dimers

The liquid crystal dimers are different from conventional low molar mass mesogens in that they are composed of molecules, in which two anisotropic mesogenic groups are linked by a flexible spacer. They have been attracting a great deal of interest in recent years not only from their ability to act as model compounds for semi-flexible main chain liquid crystal polymers but also because they exhibit quite fascinating and unusual properties [69,70,71]. The transitional properties of the dimers depend on the length and parity of the spacer as well as the nature of linking group of the mesogenic units. In particular, the nematic-isotropic transition temperatures are found to exhibit a dramatic alternation on the number of carbon atoms as the alkyl spacer changes from odd to even. However, the odd-even effect thought to be a characteristic of dimer does not always occur and can also vanish when rod-like molecules are replaced by disc-like groups. Both theories and

experiments, of varying degree of sophistication have been developed to understand the phase transition behaviour of the dimers. The liquid crystal dimers are classified into two categories: symmetric and non-symmetric. In the former class of dimers, the mesogenic groups are identical and in the latter, the mesogenic groups are not identical. However, though a large number of schiff base liquid crystal dimers have been synthesized and characterized in the recent past, the detailed study of various rare and new phase transitions exhibited by the dimers and the detailed structural evaluations have not yet been carried out. Therefore, in the present thesis density measurement studies as a function of temperature of few symmetric liquid crystal dimers as well as study of molecular dynamics using Laser Raman spectroscopy was taken up. The general molecular structure of symmetric liquid crystal dimer is shown in Fig 1.6a.

1.3.2. TBAA Compounds

Terepthalydene-bis-p-n-alkylanine, popularly known as TBAA homologues series is one of the well known and interesting series of schiff base liquid crystalline compounds for its rich variety of polymorphism with wide thermal ranges [72,73]. One of the TB*4*A series compound, TBBA exhibits six mesophases which offers the possibility to study the liquid crystalline modifications of different types and different phase transitions in a single compound. The other interesting aspects of these homologues series are the specific identification of S_G and S_H in a single compound [74,75], identification of S_F and S_I phases [76,77], identification of two or three second order phase transitions (S_A-S_C, S_I-S_F, S_F-S_G) in addition to the first order transitions (I-S_A, S_C-S_I, S_G-K) in a single compound. However, the TBDA, one of the higher homologue of the TBAA series exhibits a weakly first order S_A-S_C phase

transition whereas the TBBA, the lower homologue exhibits a second order S_A- S_C phase transition. These imply the existence of a tricritical point, where the first order transition becomes second order. In order to explore tricritical point the binary mixtures of TBBA and TBDA of different weight percent have been chosen to study the variation of density as tricritical point is approached. Few compositions of these binary mixtures were chosen to study DSC and density measurements as a function of temperature. The general molecular structure of the TB*n*A series is shown in Fig 1.6b.

1.4. Phase Transition studies in Liquid Crystals

The liquid crystal phases are described by their positional as well as orientational ordering. The nematic liquid crystals possess long range orientational ordering whereas the smectic phases possess either three or two or one-dimensional periodic ordering (positional) of the molecules in addition to the orientational ordering. At any temperature, the state of the system can be described by an equilibrium value of the molecular parameters and fluctuations about that value. When the system transforms from one phase into other phase, it can be indicated by either a continuous or discontinuous change in the equilibrium value of the molecular property. A continuous change in the molecular property defines a second order transition while a discontinuous change defines first order transition. However, due to weakly first order nature of most mesophase transitions, large pretransitional effects, reminiscent of second order behaviour are usually observed in the region of transition point. In general, an nth-order phase transition is one in which it is the nth derivative of the chemical potential μ, with respect to temperature T and pressure P, which first becomes discontinuous at the point of transition. For an a-b equilibrium phase transition, $\mu^a(T,P) = \mu^b(T,P)$; the zeroth derivative is thus continuous. The $\mu(T,P)$

surfaces of the a and b phases intersect (first order) or "make contact" (second order) over a range of T and P. For a first order phase transition ($\partial\mu/\partial T$ and $\partial\mu/\partial P$ discontinuous), enthalpy ΔH (or entropy ΔS) and volume ΔV changes are observed. The projection of the line of intersection of the μ surfaces onto the P-T plane provides a consistency relation between dT/dP and $T\Delta V/\Delta H$ through the Clausius-Clapeyron equation. For a second order transition, both ΔH and ΔV are zero, but $\partial^2\mu/\partial T^2$, $\partial^2\mu/\partial T\partial P$ and $\partial^2\mu/\partial P^2$ lead to a change in the constant pressure heat capacity ΔC_p, expansion coefficient $\Delta\alpha$ and isothermal compressibility $\Delta\chi$, respectively.

With liquid crystals, change in the order parameters (s) must also be considered. At the first order nematic – isotropic transition, the orientational order parameter ηchanges discontinuously. The smectic A phase may be characterized by an additional order parameter σ. According to Mc Millan theory, η and σ may change discontinuously or continuously, depending on whether the smectic A – nematic transition is first order or second order transition respectively.

1.5. Experimental studies on liquid crystals.

Studies on liquid crystals have been conducted using a number of experimental techniques such as X-ray diffraction [78,79], Dilatometric analysis [80,81], Nuclear Magnetic Resonance (NMR) [82,83], Electron spin resonance (ESR) [84,85], Fourier Transform Infrared Spectroscopy (FTIR) [86,87] and Raman Spectroscopy [88,89]. These techniques have divulged an enormous volume of experimental data, which has been interpreted to understand the phase transitions in liquid crystalline systems and the associated changes in the various physical and chemical properties, including the electro-optic properties. In this regard, both Laser

Raman and FTIR spectroscopies have proved to be very important techniques as they are able to provide information both at the microscopic (molecular) as well as the macroscopic levels. In Laser Raman spectroscopy, variation of some physical quantities are found to affect the polarizability tensor that results in changes in measurable parameters of certain vibrational modes of the Raman spectrum of the system. Laser Raman spectroscopy has been found to be very effective in the study of phase transitions in liquid crystals. Therefore, in this thesis, Raman studies have been employed in the study of phase transitions and molecular dynamics of two symmetric liquid crystal dimers.

The density measurement studies by either vibration densitometer or classical dilatometer is an important experimental technique for the study of phase transitions. The density of the liquid crystalline compound varies with the variation of temperature. A first order transition is associated with a discontinuity in the density values at the transition whereas the second order transition is related to a continuous change in the density values.

1.5.1. Laser Raman spectroscopy and Density studies on liquid crystals.

Raman spectroscopy is one of the most important techniques used in the study of vibrational dynamics of the liquid crystals. Apart from being bond specific, the variation of physical quantities of the liquid crystalline phases affect the polarizability tensor which are reflected as changes in measurable parameters in the Raman spectra. In the past couple of decades, Raman spectroscopy has been extensively used in the study of liquid crystals to extract spectral information [90-104], more specifically on the molecular structure [90-98] and intra/inter-molecular interactions [105-107] in the liquid crystalline phases. During recent past, most of the studies using Raman

techniques have concentrated on the ferroelectric [108,109] and polymer liquid crystals [110]. However, many basic aspects of the orientational and conformational changes during the process of phase transitions in non-ferroelectric liquid crystals are yet to be explored.

Density measurement as a function of temperature is an important experimental technique to study the phase transitions. A specially designed bicapillary Pyknometer was used for the density studies. The capillaries with a diameter of about 0.35 mm and about 40 cm long are arranged at the top of a bulb in a "U" shape. The capacity of the pyknometer is about 2 to 3 CC. The bulb contains 98% of the total volume of the sample. The accuracy in density is ± 0.1 kg m^{-3}. The pyknometer was calibrated by measuring the molar volume of water at different temperatures. The mass of the liquid crystal sample was determined using a microbalance with an accuracy of ± 0.001mg. For filling the sample in the pyknometer, the pyknometer was kept inside the heating chamber at a higher temperature of 10 to15°C above the mesophase-isotropic transition temperature of the liquid crystal sample and cooled down slowly until the sample level reaches the mark in the capillaries at isotropic phase. Special precautions were taken for removing excess sample and bubbles in the pyknometer. The sample level in the capillaries of the pyknometer was observed with the help of a cathetometer in the cooling cycle with a cooling rate of 2°C hr^{-1}.

The interest concerning the nature of smectic C – smectic A phase transition has grown steadily since de Gennes suggestion that the smectic C- smectic A transition may be continuous by symmetry reasons and proposed an analogy with superfluid helium [111]. The development of displays containing chiral smectic C liquid crystals has further reinforced and stimulated research efforts on the chiral

smectic C- smectic A as well as chiral smectic C- cholesteric transitions. Most of the studies regarding the density studies stress on the order of phase transition. There are some examples of phase transitions, I – N, I - S_A, I – S_G, S_A - S_F S_C - S_I, S_G – K which show first order nature of transition whereas the transitions of N - S_A, S_A – S_C, S_I – S_F, S_F - S_G shows second order nature of the transition as confirmed by density studies. In addition, tricritical nature of some of the transitions viz., S_A – N, S_F – S_I and S_A – S_C was also reported.

REFERENCES

1. de Gennes, P. G., and Prost, J., *"The Physics of Liquid Crystals"*, Oxford University Press, 2nd ed., 1993.

2. Reinitzer, F., *Monatsch. Wiener. Chem. Ges.*, **9**, 421,1888.

3. Lehmann, O., *Z. Physics. Chem.*, **4**, 462, 1889.

4. Blinov, L. M., *"Electro-optical and magneto-optical properties of Liquid Crystals"*, John Wiley and Sons Ltd, 1st ed., 1983.

5. Priestley, E. B., Wojtowicz, and P. J., Sheng, P., *"Introduction to Liquid Crystals"*, Plenum Press, 1974.

6. Friedel, G., *Ann. Physique*, **18**, 273, 1922.

7. Bouligand, Y., (a) *J. Phys. (Paris)*, **30**, 90, 1969, (b). *J. Phys. (Paris)*, **33**, 525, 1972, (c) *J. Phys. (Paris)*, **34**, 603, 1973, (d) *J. Microscop. (Paris)*, **17**, 145, 1973.

8. Leadbetter, A. J., *"Thermptropic Liquid Crystals"*, (ed. Gray, G. W.) Wiley, Chichester, 1987.

9. Pershan, P. S., *"Structure of Liquid Crystal Phases,"* World Scientific, Singapore, 1988.

10. Birgeneau, R. J., and Lilster, J. D., *J de Physique Lettres*, **39**, 399,1978.

11. Chandrasekhar, S., Sadasiva, B. K., and Suresh K. A., *Pramana*, **9**, 471, 1977.

12. Levelut, A. M., *J. Chim. Phys.*,**88**, 149, 1983.

13. Chandrasekhar, S., *Phil Trans Roy Soc London*, **A309**, 93, 1983.

14. Ohta, K., Muroki, M., Takagi, A., Hatad, K. I., Ema, H., Yamamoto, I., and Matsuraki, K., *Mol. Cryst. Liq. Cryst.*, **140**, 131, 1981.

15. Ribeiro, A. C., Martins, A. F., and Giroud-Godquin, M. A., *Mol. Cryst. Liq. Lett.*, **5**, 133, 1988.

16. Luzzati, V., and Tardieu, A., *Ann. Rev. Phys. Chem.*, **25**, 79, 1974.

17. Friberg, S, *J. Am. Oil. Chem. Soc.*, **48**, 578, 1971.

18. Lawson, K. D., and Flautt, T. J., *J. Am. Chem. Soc.*, **89**, 5489,1967.

19. Khetrapal, C. L., Kunwar, A. C., Tracey, A. S., and Diehl, P., *"NMR- Basic, Principles and progress,"* **9**, (eds. Diehl, P., Fluck, E., and Kosfield, R.) Springer-Verlag, Berlin, 1975.

20. Safran, S., " *Statistical Thermodynamics of Surfaces, Interfaces and Membranes*", Addision Wesley, 1994.

21. Brazovskii, S. A., and Dmitriev, S. G., *Zh. Eksp. Teor. Fiz.*, **69**, 979, 1975.

22. Hornreich, R. M., Luban, M., and Shtrikman, S., *Phys. Rev. Lett.*, **35**, 1678, 1975.

23. Wright, D. C., and Mermin, N. D., *Rev. Mod. Phys.*, **61**, 385, 1975.

24. de Gennes, P. G., *Solid State Commun.*, **10**, 753, 1972.

25. Halperin, B. I., Lubensky, T. C., and Ma, S. K., *Phys. Rev. Lett.*, **32**, 292, 1974.

26. Collings, P .J., and Patel, J. S., *"Handbook of Liquid Crystals Research"*, Oxford University Press, 1997.

27. Sackmann, H. and Demus, D., *Mol. Cryst. Liq. Cryst.* **21**, 239, 1973.

28. Coates, D., and Gray, G. W., *Microscop.*, **24**, 117, 1973.

29. Gray, G. W., and Goodby, J. W., *"Smectic Liquid Crystals : Textures and Structures"*, Leonard Hill, London, 1984.

30. Demus, D., and Richter, L., *"Textures of Liquid Crystals"*, Verlag Chemie, New York, 1978.

31. Gray, G. W., *Mol. Cryst. Liq. Cryst.*, **66**, 270, 1981.

32. Goodby, J. W., Gray, G. W., Leadbetter A. J., and Mazid, M. A., *"Liquid Crystal of one and two dimensional order"* (eds. Helfrich, W., Heppke,) G., Springer-Verlag, New York, pp-3 1980.

33. Goodby, J. W., and Pindak, R., *Mol. Cryst. Liq. Cryst.*, **75**, 233, 1981.

34. Poeti, G., Fanelli, E., and Guillon, D., *Mol. Cryst. Liq. Cryst.*, **82**, 107, 1982.

35. Bartolino, R. Doucet, J. and Durand, G., *Ann. Phys.*, **3**, 389, 1978.

36. Taylor, T. R., Fergason, J. C., and Arora, S. L., *Phys. Rev. Lett.*, **24**, 359, 1970.

37. Luckhurst, G. R., Timmimi, B.A., Pisipati, V.G.K.M., and Rao, N.V.S., *Mol. Cryst. Liq. Cryst. Letter*, **1**, 45, 1985.

38. Demus, D., Kunicke, G., Nelson and Sackmann, H., *Z. Naturfrosch*, **23A**, 84, 1968.

39. Diele, S., Brand, P., and Sackmann, H., *Mol. Cryst. Liq. Cryst.*, **17**, 163, 1972.

40. Goodby J. W., and Gray, G. W., *Mol. Cryst. Liq. Cryst.*, **56**, 43, 1979.

41. Biering, A., Demus, D., and Gray, G. W., and Sackman, H., *Z. Naturforsch*, **23A**, 84, 1986.

42. Goodby, G. W., *Liq., Cryst., Ordered fluid*, **4**,175, 1984.

43. Sackman, H., *"Advances in Liquid Crystals"*, (ed. Bata, L.) p-27, 1981.

44. Attard, G. S., Date, R. W., Imrie., C. T., Luckhurst, G. R., Roskilly, S. J., Seddon, J. M., and Tayler, L., *Liq. Cryst*, **16**, 525, 1994.

45. Alapati, P.R., Potukuchi, D.M., Rao, P.B., Rao. N.V.S., Pisipati, V.G.K.M., and Paranjpe, A.S., *Liq. Cryst.*, **5**, 545, 1989.

46. Sakagami, S., Takase, A., and Nikamizo, M., *Mol. Cryst. Liq. Cryst.*, **36**, 261, 1976.

47. Weigelben, A., Ritcher, L., Deresch, J., and Demus, D., *Mol. Cryst. Liq., Cryst.*, **59**, 329, 1980.

48. Gane, P. A. C., Leadbetter, A. J., Wrighton, P. G., Goodby, J. W., Gray, G. W., and Tajbkhsh, A. R., *Mol. Cryst. Liq. Cryst.*, **100**, 67, 1983.

49. Leadbetter, A. J., Tucker, P. A., Gray, G. W., and Tajbakhsh, *Mol. Cryst. Liq. Cryst. Lett.*, **1**, 19, 1985.

50. Brook, J. D., and Tayler, G. H., in *"Chemistry and Physics of Carbon"*, Vol-3, (ed. Philip, L.Walker Jr.), pp-243-283, New York.

51. Tanford, C., *"The Hydrophobic Effect"*, Wiley, New York, 1973.

52. Tanford, C., *J. Phys. Chem.*, **78**, 2469, 1974.

53. Renn, S. R., and Lubensky, T. C., *Phys. Rev. A.*, **38**, 2132, 1988.

54. Brazovskii, S. A., and Filev, V. M., *Zh. Eksp. Teor. Fiz.*, **75**, 1140, 1978.

55. Sethna, J. P., *Phys. Rev. B.*, **31**, 6278, 1985.

56. Valasek, J., *Phys. Rev.*, **17**, 425, 1921.

57. Halblutzel, J., *Helv. Phys. Acta.*, **12**, 489, 1939.

58. Kittel, C., *"Introduction to Solid State Physics"*, Wiley Eastern Limited, 5th ed., 399, 1987.

59. Meyer, R. B., Liebert, L., Strzelecki, L., and Keller, P. *J., Physique. Lett.*, **36**, 69, 1975.

60. Meyer, R. B., *Mol. Cryst. Liq. Cryst.*, **40**, 74, 1976.

61. Brand, H. R., Cladis, P. E., and Fin, P. L., *Phys. Rev. A.*, **31**, 361, 1985.

62. Clark, N. A., and Lagerwall, S. T., *"Liquid Crystals of One and Two-Dimensional Order"*, (eds. Helfrich, W, Heppke, G.) p-222, Berlin, Springer, 1980.

63. Clark, N. A., and Lagerwall, S. T., *Appl. Phys. Lett.*, **36**, 899.1980.

64. Chandani, A. D. L., Ouchi, Y., Takezoe, H., Fukuda, A., Terashima, K., Furukawa, K., and Kishi, A., *Japan. J. Appl. Phys. Lett.*, **29**, 987, 1990.

65. Gorecka, E., Chandani, A. D. L., Ouchi, Y., Takezoe, H., and Fukuda, A., *Japan. J. Appl. Phys.*, **29**,131,1990.

66. Inui, S., Kawano, S., Saito, M., Takanishi, Y., Hiraoka, K., ., Ouchi, Y., Takezoe, H., and Fukuda, A., *Japan. J. Appl. Phys. Lett.*, **29**, 987,1990.

67. Goodby, J. W., Blinc, R., Clark. N.A., Lagerwell, S. T., Osipov, M. A., Pikin, S. A., Sakurai, T., Yoshino, K., and Zeks, B., *"Ferroelectric Liquid Crystals: Principles, Properties and Applications "*, Gordon and Breach, Philadelphia, 1991.

68.Meyer, R. B., *Mol. Cryst. Liq. Cryst.*, **40**, 74, 1976.

69. Date, R. W., Imrie, C. T., Luckhurst, G. R. and Seddon, J. M., *Liq. Cryst.*, **12**, 203, (1992)

70. Attard, G. S., Date, R. W., Imrie, C. T., Luckhurst, G. R., Roskilly, S. J., Seddon, J M. and Tayler, L., *Liq. Cryst*, **16**, 529, (1994)

71. Ferrarini, A., Luckhurst, G. R., Nordio, P. L. and Roskilly, S. J., *Che. Phys. Lett.* **214**, 409, (1993)

72. Weigelben, A., Rictcher, L., Deresch, J.and Demus, D., *Mol Cryst. Liq. Cryst.*, **59**, 329, (1980)

73. Rao, N. V. S., Pisipati, V. G. K. M., Murthy, J. S. R., Bhaskara Rao, P. and Alapati, P. R., *Liq. Cryst.*, **5**, 539, (1989)

74. Sakagami, S., Takase, Ed. A., Nakamizo, M., *Mol. Cryst. Liq. Cryst.*, **36**, 261, (1976)

75. Leibert, L., "Liq. Cryst. solid state phys. Suppl.", 14, Academic Press, New York, (1978)

76. Goodby, J. W., Gray, G. W. and Mosley, A., *Mol. Cryst. Liq. Cryst. Lett.*, **41**, 183, (1978)

77. Diele, S., Demus, D. and Sackmann, H., *Mol. Cryst. Liq. Cryst. Lett.*, **56**, 217, (1980)

78. Kaganer, M. V., Ostrovskii, B. I., and de Jeu, W. H., *Phys. Rev. A*, **44**, 8158, 1991.

79. Hou, J., Tashiro, K., Kobayashi, M., and Inoue, T., *J. Phys. Chem.*, **96**, 484, 1992.

80. Rao, N. V. S., Pisipati, V. G. K. M., Alapati, P. R., and Potukuchi, D. M., *Mol. Cryst. Liq. Cryst.*, **162B**, 119, 1988.

81. Kiefer, R., and Baur, G., *Liq. Cryst.*, **7**, 815, 1990.

82. Martins, A. F., Esnault, P., and Volino, F., *Phys. Rev. Lett.*, **57**, 1745, 1986.

83. Fan, S. M., Luckhurst, G. R., and Picken, S. J., *J. Chem. Phys.*, **101**, 3255, 1994.

84. Rananavare, S. B., Pisipati, V. G. K. M., and Freed, J. H., *Liq. Cryst.*, **3**, 752, 1988.

85. Luckhurst, G. R., and Poupko, R., *Chem. Phys. Lett.*, **29**, 191, 1974.

86. Verma, A. L., Zhao, B., Ziang, S. M., Shen, J. C., and Ozaki, Y., *Phys. Rev.E.*, **56**, 3053, 1997.

87 Verma, A. L., Zhao, B., Terauchi, H., and Ozaki, Y., *Phys. Rev. E.*, **59**, 1868, 1999.

88. Galbiati, E., and Zerbi, G., *J. Chem. Phys.*, **84**, 3509, 1986.

89. Kirov, N., Dozov, I., and Fontana, M. P., *J. Chem. Phys.*, **83**, 5267, 1985.

90. Schnur, J. M., *Phys. Rev. Lett.*, **29**, 1141, 1972.

91. Amer, N. M., and Shen, Y. R., *Phys. Rev. Lett.*, **27**, 718, 1970.

92. Borer, W. J., Mitra, S. S., and Brown, C. W., *Phys. Rev. Lett.*, **27**, 379, 1971.

93. Chang, R., *Mol. Cryst. Liq. Cryst.*, **12**, 105, 1971.

94. Schnur, J. M., Sheriden, J., and Fontana, M., in *"Liquid crystals"* ed. Chandrasekhar, S., 1975.

95. Bulkin, B. J., and. Prochaska, F. T., *J. Chem. Phys.*, **54**, 635, 1971.

96. Schnur, J. M., and Fontana, M., *J. Phys. (Paris).*, **35**, L53, 1974.

97. Fontana, M., and Bini, S., *Phys. Rev. A* **14**, 1555, 1976.

98. Yoshida, H., Nakajima, Y., Kobinata, S., and Maeda, S., *J. Phys. Soc. Jpn.*, **50**, 3525,1981.

99. Dalmolen, L. G. P., Egberts, E., and de Jeu, W. H., *J. Phys. (Paris).*, **45**, 129, 1984.
100. Wrobel, D., Biophys. Chem., 26, 91, 1987.

100. Wrobel, D., Biophys. Chem., 26, 91, 1987.

101. Vanwinkle, D. H., Dierkker, S. B., and Clark, N. A., *J. Chem. Phys.*, **91**, 5212, 1989.

102. Watanabe, K., and Klein, M. L., *J. Phys. Chem.*, **95**, 4158, 1991.

103. Yokovenko, S. Y., Minko, A. A., Arnscheidt, B., and Pelzl, J., *Liq. Cryst.*, **19**, 449, 1995.

104. Shao, Y., and Zerda, T. W., *J. Phys. Chem. B.*, **102**, 3387, 1998.

105. Dash, S. K., Singh, R. K., Alapati, P. R., and Verma, A. L., *Mol. Cryst. Liq.Cryst.*, **319**, 147, 1997.

106. Dash, S. K, Singh, R. K., Alapati, P. R., and Verma, A. L., *J. Phys. Condensed Matter*, **9**, 7809, 1997.

107. Dash, S. K., Singh, R. K., Alapati, P. R., and Verma, A. L., *Liq. Cryst.*, **25**, 459, 1998.

108. He, L., Shen, Z. X., Yin, Z., Zhang, M. S., Li, W. S., and Tang, S. H., *Ferroelectrics.*, **230**, 345, 1999.

109. Clarke, M. J., Meyer, S. C., and Coles, H. J., *Ferroelectrics.*, **245**, 707, 2000.

110. Mihara, T., and Koide, N., *Mol. Cryst. Liq. Cryst.*, **367**, 605, 2001.

111. de Gennes, P. G., *Mol. Cryst. Liq. Cryst.*, **21**, 49, (1973)

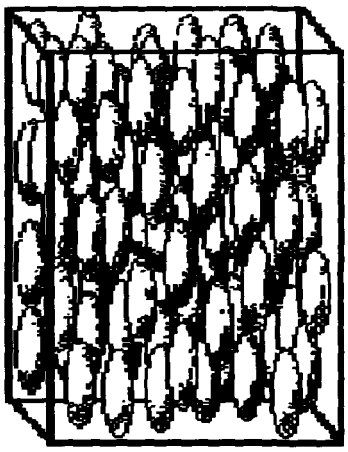

Nematic

Fig. 1.1a Nematic liquid crystals

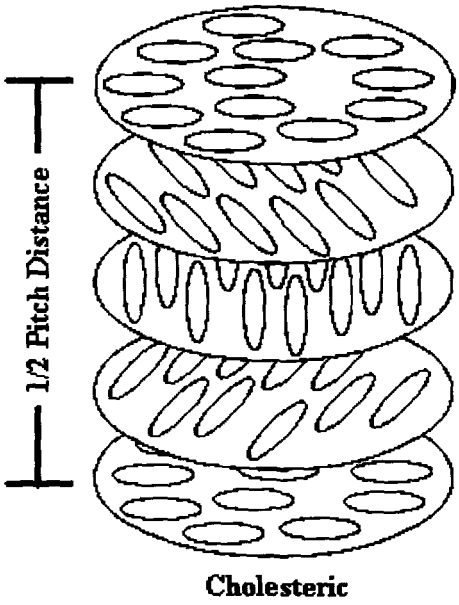

Cholesteric

Fig 1.1b Cholesteric liquid crystals

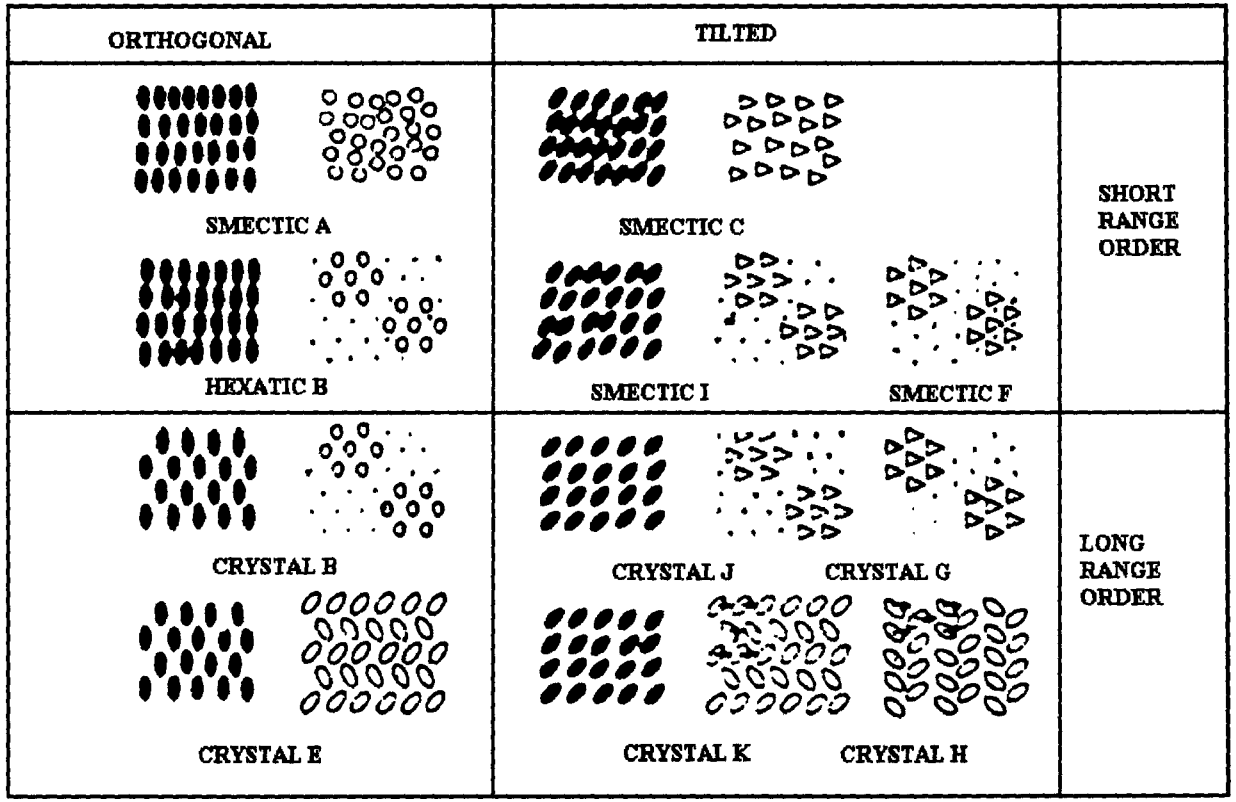

The structures of lamellar smectic mesophases. The side of the lath-like molecules are shown by black ellipses.

Fig 1.1c Various types of Smectic liquid crystals

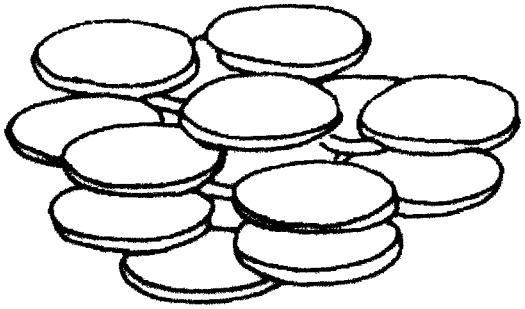

(a) Discotic Phase. (Nematic type)

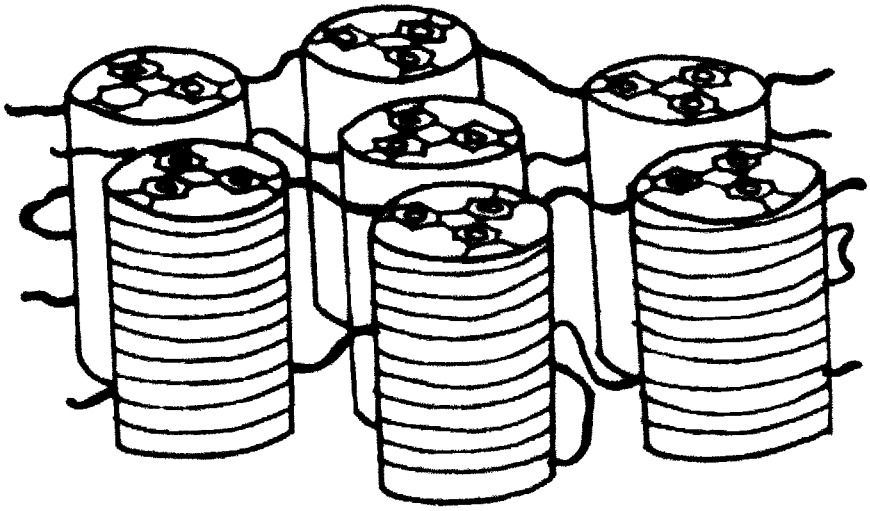

(b) Discotic phase (columnar type).

Fig. 1.2 Two different types of discotic liquid crystals

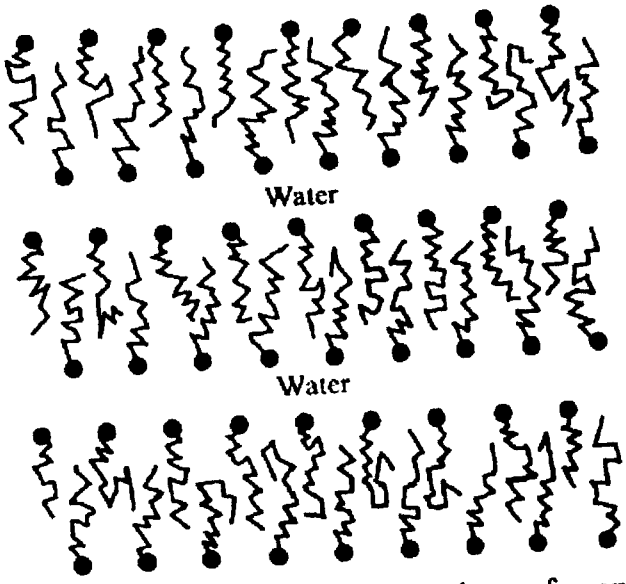

(a) The lamellar or neat phase of soaps.

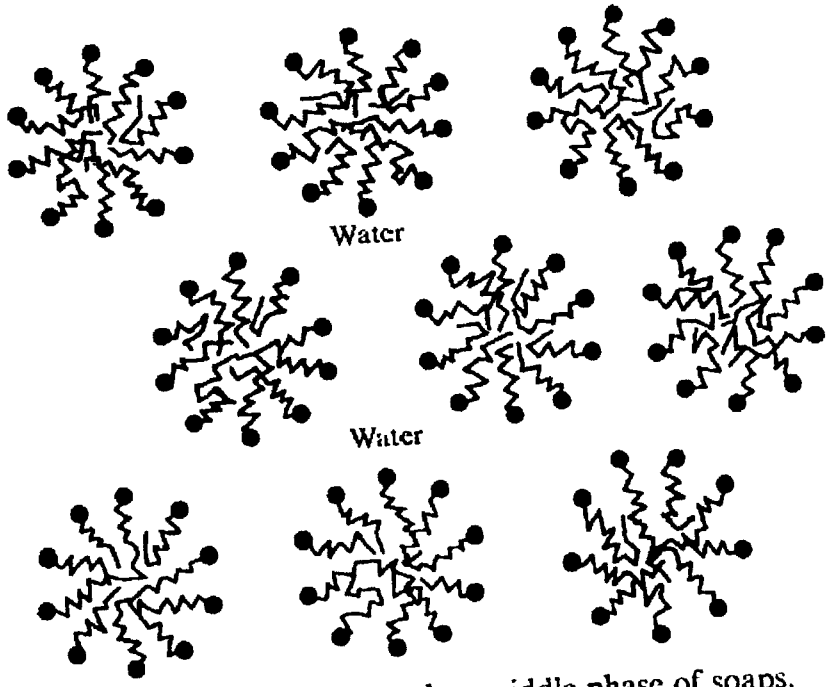

(b) The hexagonal or middle phase of soaps.

Fig 1.3 Different types of Lyotropic liquid crystals.

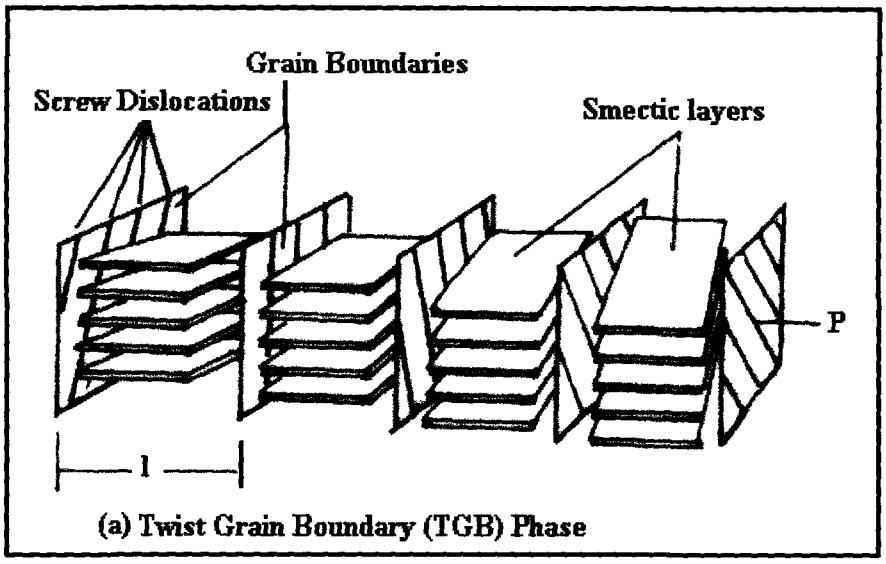

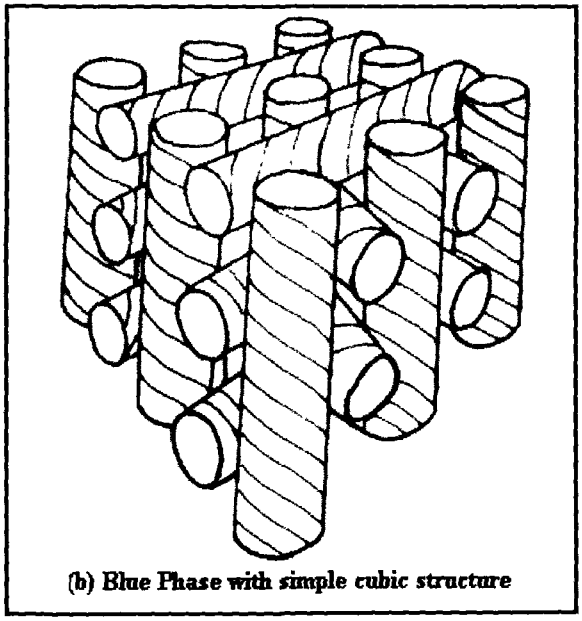

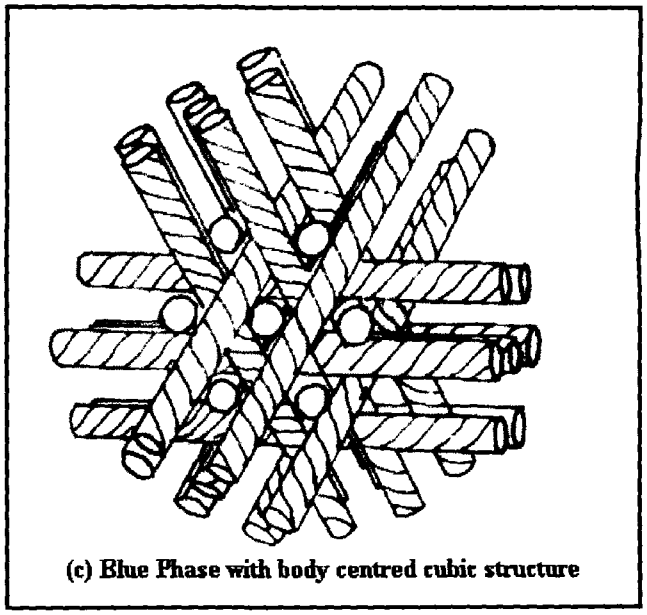

Fig 1.4 Different types of defect phases

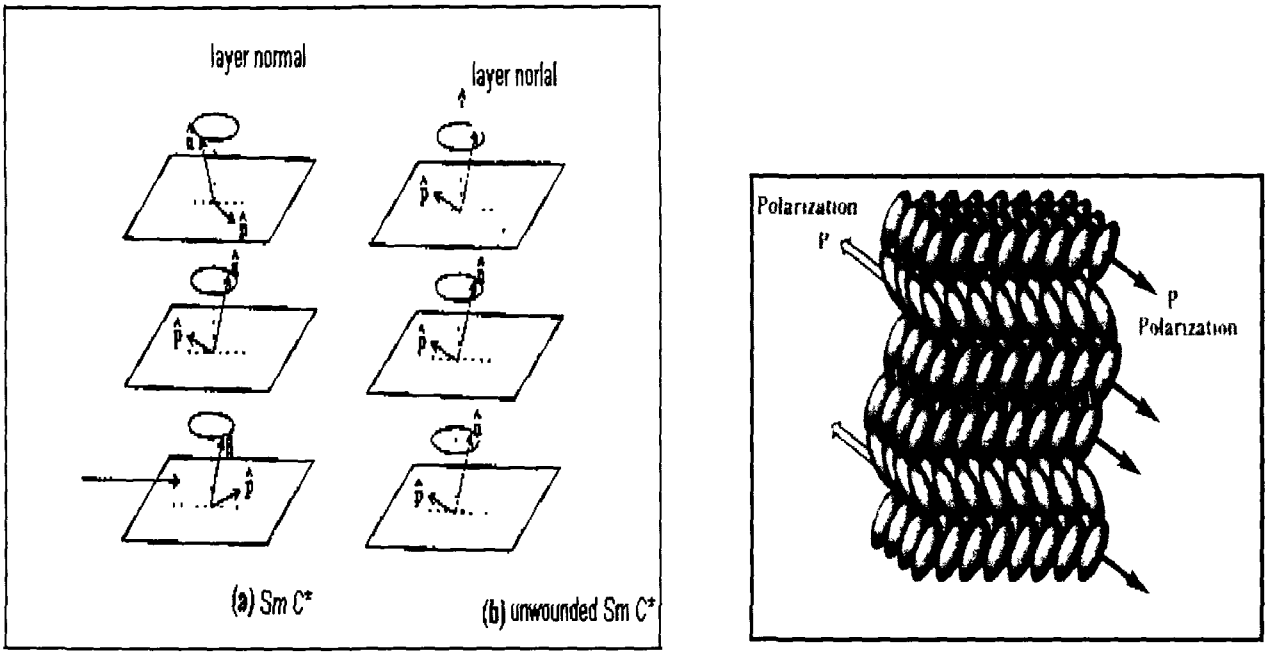

Fig. 1.5 Molecular alignment and structure of ferroelectric liquid crystals.

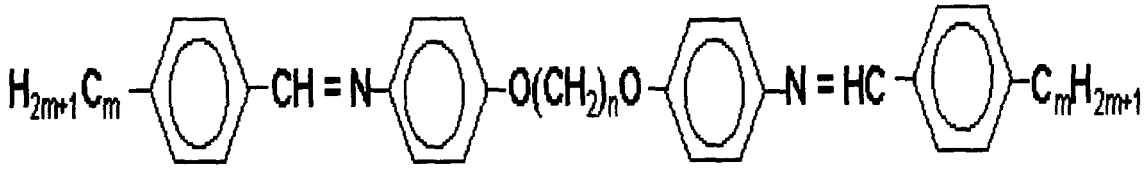

(a)

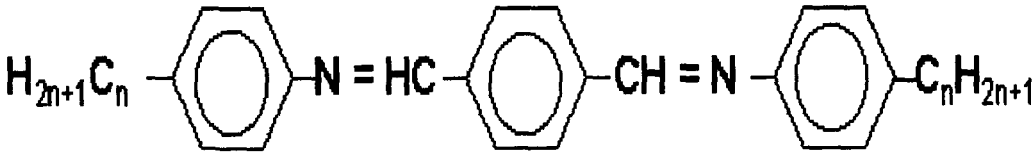

(b)

Fig. 1.6 (a) Molecular structure of symmetric liquid crystals

(b) Molecular structure of Terepthalylidene-bis-p-n-alkylaniline

CHAPTER - 2

EXPERIMENTAL TECHNIQUES :

In this chapter we discuss briefly about the methods of preparation of liquid crystal samples in this study, identification of phases and phase transition temperatures, density measurements, Raman spectroscopic studies, experimental techniques and instruments employed in this thesis. The liquid crystal compounds are synthesized in our laboratory. The phase transition temperatures are determined by observing the optical textures under a polarizing microscope attached with a heating block which was designed and fabricated in our workshop. The density measurements and the vibrational spectral measurements are carried out by using a bicapillary pyknometer and Raman spectrometer respectively.

2.1. Preparation of Samples

In this thesis, five compounds of symmetric liquid crystal dimers, α,ω-bis(4-n-alkylaniline benzylidene-4′-oxy)alkane have been studied for their phase transitional behaviour. Two compounds of the same series have been studied for their dynamical behaviour. Binary mixtures of two compounds of Terephthalylidene-bis-p-n-alkylaniline (TBAA) homologues series are studied to explore the Tricritical point (TCP) of Sm A – Sm C transition. Due to their interesting properties and behaviour, following compounds have been selected. In case of symmetric liquid crystal dimers, which are popularly known as mO.nO.m homologues series, five compounds, viz.7.O4O7, 7.O5O.7, 10.O4O.10, 10.O10O.10, 10O.12O.10 have been studied and in case of TBAA homologues series, seven binary mixtures of TBBA and TBDA have been studied. All of

the above compounds are synthesized using imported chemicals (Aldrich Chemical Co., USA and TCI, Japan), following the standard procedures [1-3] in our laboratory.

(1) **Preparation of Symmetric Liquid Crystal Dimer (m.OnO.m) compounds**

(Molecular structure of m.OnO.m)

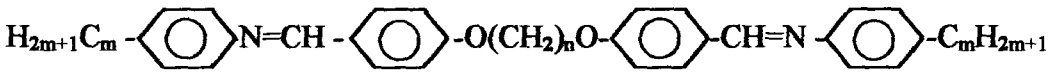

(Synthesis route of mO.nO.m homologues series)

STEP - I

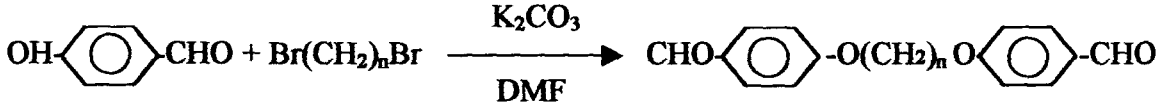

STEP -II

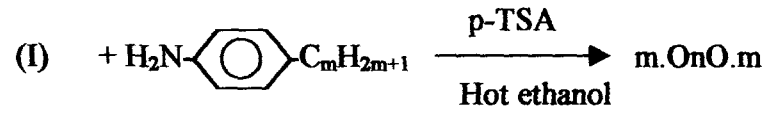

STEP–I: A mixture of 4 hydroxybenzyldehyde (0.053 mol), an α,ω-dibromoalkane (0.025 mol) and anhydrous potassium carbonate (0.063 mol) in N,N-dimethylformamide (25 ml) was refluxed with stirring for three hours. The cooled reaction mixture was then poured in to water (300 ml). The resulting precipitate was filtered off and washed thoroughly with water. The crude product was recrystallized twice from ethanol and dried.

STEP –II: 4-n-alkylaniline (0.0084 mol) was added to a stirred solution of the α, ω-bis(4-formylphenyl-4′-oxy)alkane (0.004 mol) (product of STEP – I) in the presence of a few crystals of p-tolune sulphonic acid (p-TSA) in hot ethanol. The mixture was

allowed to cool to room temperature and stirred for further three hours. The resulting precipitate was filtered off, washed thoroughly with cold ethanol and dried. In general, all the compounds were recrystallized from ethyl acetate until the transition temperatures were found constant and reproducible. Various phases and phase transition temperatures were characterized by observing their optical textures under a polarizing microscope attached with an indigenously constructed hot stage. The phase and phase transition temperatures are in excellent agreement with the reported literature values [1,2]

(II) **TBAA Homologues Series**

The general molecular structure and synthesis route of TBAA homologues series are given below.

(Molecular structure)

(Synthesis route of TBAA homologues series)

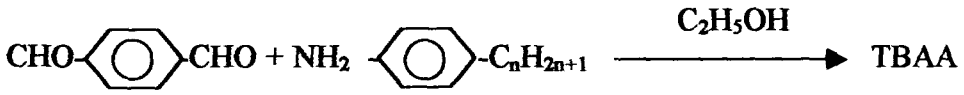

Two TBAA homologues (TBBA and TBDA) were prepared by condensation of p-n-alkylaniline (0.2 mol) and Terephthaldehyde (0.1 mol) by refluxing with a mixture of ethanol and benzene (50:50) in the presence of a few drops of glacial acetic acid. After refluxing the reactants for 4 hours the solvent was removed by distillation under reduced pressure and later the pure compound was recrystallized from absolute ethanol-benzene mixture until the observed transition temperatures were found constant and reproducible.

Various phases and phase transition temperatures were characterized by observing their optical textures under a polarizing microscope attached with an indigenous hot stage. The phases and phase transition temperatures are in excellent agreement with the reported literature values [3].

2.2. Polarizing Thermal Microscopic Studies

Liquid crystals are found to be birefringent, for their anisotropic nature i. e. they exhibit the property of double refraction. Due to this reason, liquid crystals exhibit different optical textures characteristic of each phase between the crosspolarizers. Polarizing microscope attached with hot stage was used for the determination of transition temperatures and the identification of various phases. The optical textures of the synthesized compounds were observed by using the polarizing microscope [Model – METZ –782 POL]. To observe the textures above the room temperature, a heating block is necessary and the design and construction details of the heating block are given hereunder.

Gray [4] described a good design for the heating block in which the liquid crystal sample is held between two glass plates and can be placed along with the thermometer. Based on that idea, a heating block has been designed and fabricated (shown in Fig. 2.1) and found fruitful results.

A cylindrical brass block of 5.5 cm diameter and 3 cm thickness was taken and a central hole of 2 cm diameter was drilled along its axis. The block was cut equally into two pieces (discs) with a groove to keep both of the parts intact. A slide slot at the upper side of the bottom piece symmetrically situated with respect to central hole of dimension

5.5 cm × 2.5cm × 0.4cm was made to place the sample slide. Keeping both the discs intact, a thermometer hole was drilled along side of the slide slot for measurement of temperature. Another circular hollow groove of diameter 5.2 cm with a depth of 1 cm was made on the lower side of the bottom disc for keeping the heating mantle. The heating mantle, which is well insulated with heat resistant nylon, was arranged in the bottom disc of the block and closed by extra aluminum sheet and the heating wires were taken out from the circular disc. The temperature of the block was varied by controlling the supply voltage to the heating wire. The liquid crystal sample which was held between the glass slide and cover slip and the thermometer were placed in their respective positions of the heating block, which was arranged on the stage of the polarizing microscope for viewing the textures.

2.3. Differential Scanning Calorimetric (DSC) Studies

Differential Scanning Calorimetry is a technique of recording the energy necessary to establish zero temperature difference between a substance and a reference material against either time or temperature as the two specimens are subjected to identical temperature regimes in an environment heated or cooled at a controlled rate. DSC data play an important role for the study of the nature of phase transition i.e. to measure the enthalpy (entropy) directly with temperature and record the transition temperatures. The DSC studies presented in this thesis were carried out on two different differential scanning calorimeters available at RRL, Jorhat (Perkin Elmer DSC – 4) and NEHU, Shillong (Perkin Elmer DSC –7). Fig. 2.2 shows an example of the DSC scan of liquid

crystal dimer (10.O12O.10). The phases and phase transition temperatures and transition enthalpies of all the compounds studied are shown in Table 2.1.

2.4. Density measurement Studies

Measurement of density of liquid crystal compounds as a function of temperature using a specially designed bicapillary pyknometer (shown in Fig. 2.3) is a well established technique. Two capillaries with a diameter of about 0.35 mm and about 40 cm long are arranged at the top of a bulb in a "U" shape. The capacity of the pyknometer is about 2 to 3 CC. The bulb contains 98% of the total volume of the sample. The accuracy in density measurement is ± 0.1 kg m^{-3}.

To determine the density of the liquid crystal materials at different temperatures, a hot oven with a provision for observing the levels of liquid crystal compound in the pyknometer was designed and fabricated in our laboratory. The oven was constructed as described below: three polished aluminum sheets of 0.4 cm thick, 40 cm long and 20 cm width were arranged in rectangular shape with one side open, for the arrangement of glass with panel for observation. The backside of three aluminum sheets were covered with winding heating coil and were connected to porcelain terminals placed at the top of the block. The heating coil was again shielded with asbestos sheets to provide thermal insulation. Top and bottom of the block was also shielded with the asbestos sheet with two holes at the top for inserting pyknometer and thermometer. The whole assembly was kept in a wooden box with a glass window on the front side for opening and observing the pyknometer. The temperature of the block was monitored with the help of imported thermometers of temperature resolution of 0.1°C.

The pyknometer was calibrated by measuring the molar volume of water at different temperatures. The mass of the liquid crystal sample was determined using a microbalance with an accuracy of ±0.001mg. For filling the sample in the pyknometer, the pyknometer was kept inside the heating chamber at a higher temperature of 5 to 10 °C above the mesophase-isotropic transition temperature of the respective liquid crystal sample. The sample is placed in one of the cups which melts and goes to liquid state and flows down into the bulb due to capillary action. Once the bulb is filled, the sample raises in the second capillary upto the top again. Then the sample is cooled down slowly until the sample attains the desired temperature. At this stage excess sample is removed from the cups. Now as the sample is cooled down slowly the level in the capillary tubes falls slowly. The sample level in the capillaries of the pyknometer was monitored by a cathetometer in the cooling cycle with a cooling rate of 2 °C hr^{-1}. The experimental set up of the density studies is shown in Plate 2.1.

2.5. Raman spectroscopic technique

2.5.1. Raman effect

Light incident upon a molecule can interact with the molecule either by the absorption of light or by scattering phenomena. When a substance is irradiated by an intense beam of monochromatic light of frequency ν_o, most of the incident radiation passes through the sample undeflected. But, a small part will be scattered by the molecules in all directions, except in the direction of the incident beam. It is found that a major portion of the scattered light has the same frequency (ν_o) which is called Rayleigh scattering or elastic scattering, and its intensity is proportional to the fourth power of

frequency of the incident radiation. Apart from the Rayleigh line, the scattered light contains radiation of frequencies different from frequency of incident radiation. These spectra radiations due to inelastic scattering, are characteristic of the molecule on which light is incident and is known as Raman scattering. A Raman band is not characterized by its absolute wavenumber $\nu_o + \nu_r$, but by the magnitude of wavenumber shifts $|\Delta\nu|$ from ν_o where $|\Delta\bar{\nu}| = |\bar{\nu}_o - \bar{\nu}| = \bar{\nu}_r$. Raman scattering is always accompanied by Rayleigh scattering. The pattern of frequencies on the lower frequency side, known as Stokes lines are mirrored by an identical pattern of lesser intensity on the higher frequency side of the exciting line, and is known as the anti-Stokes lines (Fig. 2.4). As the anti-Stokes Raman scattering originates from higher vibrational levels of ground electronic state, the intensity of such Raman lines is much weaker compared to those from Stokes Raman scattering and is governed by Boltzmann distribution. A Raman band is characterized not only by its wavenumber shift but also by its polarization characteristics, shape and bandwidth. These parameters provide useful structural information [5-7].

It is found that generally Raman frequencies correspond to the vibrational and rotational transitions of the scattering molecule. Raman effect can be understood by considering the light scattering process as collisions of photons of incident light with the scattering molecules, as it is an extremely feeble two-photon process.

2.5.2. Parameters of Raman profiles:

In order to obtain useful information from the Raman spectra, a number of parameters of Raman profiles need to be analyzed. Some of the basic features obtained in Raman spectroscopy are peak position, integrated intensity and linewidth. These are

extremely helpful in applicational aspects of Raman spectroscopy in different fields such as molecular dynamics, structural phase transitions and molecular order parameter calculations. In view of this, the spectroscopic origin of these parameters are discussed below briefly.

2.5.2.1. Peak Positions:

If the Raman spectra originate from molecular vibrations, then the Raman bands characterize a particular mode of vibration at certain frequency involving mainly a group of atoms. However, depending upon the symmetry properties of molecular vibration, Raman modes may be active, inactive or weakly active. The peak positions usually indicate energy of vibration of the molecules. Shift in peak position, therefore, indicate increase or decrease of energy of the bond that mainly contributes to vibration. Peak positions of certain characteristic modes are sensitive towards different physical parameters such as temperature, pressure, solvents and other perturbations which affect the intermolecular interactions and bonding arrangements.

2.5.2.2 Integrated Intensity:

The integrated intensity of Raman bands provides information about molecular structure. It shows the modulation of the molecular polarizability by a vibration. Placzek's theory [8], which treats molecules as quantum objects and electromagnetic fields classically, satisfactorily describes the Raman effect with the condition that the exciting frequency differs considerably from the frequencies of electronic as well as of vibrational transitions. If a sample is irradiated by a laser radiation whose electric vector is oriented perpendicularly to the plane of irradiation and observation, then the observed

radiant power is proportional to the absolute differential Raman scattering cross-section (or integral Raman scattering coefficient) $\left(\frac{d\sigma}{d\Omega}\right)$, where σ is the cross-section and Ω is the solid angle. In case of 'Stokes line' of a Raman-active vibration of frequency ν, scattering coefficient is given by [9],

$$\left(\frac{d\sigma}{d\Omega}\right)_{\perp} = \frac{\pi^2 b^2 (\nu_o - \nu)^4}{45\varepsilon_o^2 \nu \left[1 - e^{\frac{\eta c \nu}{kT}}\right]} g_j \left(45\alpha'^2 + 7\gamma'^2\right) L \qquad (2.1)$$

(α' and γ' are changes in polarizability tensor corresponding to the isotropic and anisotropic invariants respectively.)

Here ν_0 and ν represent the frequency of the exciting radiation and the excited vibration, respectively and g_j is the degeneracy of the vibration. The expression g_j $(45\alpha'^2+7\gamma'^2)$ is known as the *scattering activity*, $b^2 = h/8\pi^2 c\nu$ is the square of the 'zero point amplitude' of the vibration. Therefore, equation (2.1) can be rewritten in simplified form as:

$$\left(\frac{d\sigma}{d\Omega}\right)_{\perp} = \frac{\pi^2 b^2 (\nu_o - \nu)^4}{8c\varepsilon_o^2 \nu \left[1 - e^{\frac{\eta c \nu}{kT}}\right]} g_j \left(\alpha'^2 + \frac{7}{45}\gamma'^2\right) L \qquad (2.2)$$

In equation (2.2), L represents internal *field factor* that is given by

$$L = \frac{1}{3^4}\left[\left(\frac{n_R}{n_o}\right)\left(n_R^2 + 2\right)^2 \left(n_o^2 + 2\right)^2\right] \qquad (2.3)$$

where n_o and n_R are the refractive indices at the wavelength of the exciting and Raman scattering radiation respectively. The increase of the incident and scattered electric field

due to the dielectric constant of the scattering medium are generally taken into account by the internal field factor [10]. Therefore, barring L, the differential Raman scattering cross-section of a vibration of degeneracy g_j, frequency ν, excited by radiation with frequency ν_o, could be represented by:

$$\left(\frac{d\sigma}{d\Omega}\right)_{\perp} = \frac{\pi^2 b^2 (\nu_o - \nu)^4}{8c\varepsilon_o^2 \nu \left[1 - e^{-\frac{hc\nu}{kT}}\right]} g_j \left(\alpha'^2 + \frac{7}{45}\gamma'^2\right) \qquad (2.4)$$

Now, redefining ν_o as the reference frequency ν_{ref}, and dividing the above equation by $(\nu_{ref}-\nu)^4$ one gets

$$\left(\frac{d\sigma}{d\Omega}\right)_{\perp} (\nu_{ref} - \nu)^{-4} = \frac{h}{8c\varepsilon_o^2 \nu \left[1 - e^{-\frac{hc\nu}{kT}}\right]} g_j \left(\alpha'^2 + \frac{7}{45}\gamma'^2\right) \qquad (2.5)$$

The left hand side of equation (2.5) is known as *'absolute normalized Raman scattering cross-section'* and is equal to the intensity of the observed band. From equation (2.5) it is also inferred that intensity of the scattered radiation is proportional to ν^4 of the exciting frequency.

2.5.2.3 Width of spectral lines (Linewidth)

It is a well-known fact that all the spectral lines have an *intrinsic linewidth*, which is independent of any detection system used for their observation. This intrinsic linewidth has got its origin from the fact that an atom or a molecule, in an excited state, has got a finite life time and accordingly it has some energy (or frequency) spread. This (linewidth) is commonly known as *natural linewidth*. The natural linewidth, however can

not be observed without very special techniques because it is completely concealed by some other broadening effects like doppler broadening, collision induced broadening, instrumental broadening, stark broadening and time of flight broadening. The spectral lines of discrete absorption or emission spectra are, therefore, never strictly monochromatic, but have got a frequency spread and hence a spectral distribution I(ν) of intensity around the central frequency $\nu_o = (E_i - E_k)/h$, where E_i and E_k are the energies of the two states involved in the transition. The function I(ν) in the vicinity of ν_0 is called the line profile. The frequency interval $\Delta\nu = |\nu_2 - \nu_1|$ between the two frequencies ν_1 and ν_2, such that $I(\nu_1) = I(\nu_2) = I(\nu_o)/2$, is called the full width at half maximum (FWHM) of the line or often called linewidth (Γ) of the spectral line. Raman linewidth is a cumulative effect of the linewidths originating from the temperature independent vibrational dephasing and temperature dependent orientational/rotational motion. For a particular Raman linewidth, orientational/rotational motion contributes towards its wings whereas vibrational dephasing contributes towards its middle portion. In order to get an overall idea on different processes that contribute to linewidths, a brief discussion is given here on isotropic Raman line shapes and widths which provide a direct and useful probe of vibrational dephasing along with the origin of other contributions to linewidth.

The different microscopic processes affect the vibrational relaxation and energy transfer processes in systems in many ways and result in a finite correlation time for the vibrational mode. The correlation time is the time during which a well-defined phase relationship among an ensemble of identically prepared excited molecules is irreversibly

scrambled and destroyed. The primary cause of vibrational relaxation and dephasing is the interaction of forces from the environment with the cubic and quartic anharmonicities of the vibrational modes which changes its instantaneous vibrational frequency and result in loss of its phase memory [11,12]. The population and energy relaxations involve inelastic processes in which a vibration undergoes an inelastic scattering and exchanges energy with other intra-molecular and inter-molecular vibrational degrees of freedom resulting in energy dissipation as well as a loss of phase memory and correspond to the so called T_1-processes (spin-lattice relaxation). The phase relaxation involves elastic scattering of the vibration which results in the loss of phase memory without changing its quantum state. These are called T_2'-processes (pure dephasing) which contribute to the overall dephasing process T_2 (spin-spin). Although T_1 relaxation contributes to T_2, there are processes other than T_1 relaxation, which may provide a dominant mechanism for dephasing.

Vibrational dephasing is accessible to experiments primarily through two types of measurements. Spectral line shape measurements and coherent pico-second time-resolved studies. The width of a homogeneously broadened line is related to the energy (T_1) and pure dephasing (T_2') lifetimes of the excitation by the relation $2\pi\Gamma_{hom} = \frac{1}{T_1} + \frac{2}{T_2'}$. One may measure T_1 relaxation by ordinary emission experiment and an absorption experiment would give T_2 and thus we may obtain T_2', at least in principle. However, study of isotropic Raman line shapes and widths provides a direct and useful probe of vibrational dephasing. In condensed phase at room temperature, vibrational relaxation

processes are very rapid and line width data is very difficult to interpret because a large number of physical processes contribute to the observed lineshapes. The main line broadening factors include the orientational and rotational motions, vibrational population and energy relaxation, phase relaxation, isotopic splitting, hot bands, and statistical distribution of vibrational frequencies due to inhomogeneities and disorder in solids [11,12]. Under certain assumptions and suitable choice of Raman scattering geometry, it is possible to separate out the orientational contribution from other contributions from the intrinsic vibrational part.

2.6.1. High temperature cell for Raman studies of bulk samples.

In order to record the Raman spectra in bulk samples of 7.O4O.7 and 7.O5O.7, a small double walled glass cell has been used where the temperature could be easily monitored and varied while recording the Raman spectra. As shown in the Fig. 2.5a, the cell may be divided into two portions: an inner chamber and another as outer chamber. The lower part of the inner chamber was compact (solid glass) on which a groove of 2 cm depth and 1mm diameter was made to place the encapsulated sample for spectral study. The upper part of the inner chamber is hollow in order to place the temperature sensor close to the sample. Heating element is compactly wound around the inner chamber uniformly on both sides of the sample groove (leaving enough space for laser radiation to excite the sample) which gives a symmetric thermal distribution around the sample. The outer hollow chamber is especially designed for creating a vacuum around the inner chamber for maintaining temperature stability. An outlet has been provided on one side of the outer chamber for vacuum purposes with a lid protection.

Two in-built metallic leads and outlets are also made on the outer chamber for heating elements. A temperature controller (Century Model no. CT-806) was used to monitor and control the temperature by keeping its sensor in close contact with the sample. Before using the cell, the heat chamber is subjected to several stages of calibration using encapsulated samples of organic compounds of known melting points in different temperature ranges. The apparent and the actual melting point of these samples were measured and plotted graphically which is shown in the Fig.2.5b. From this figure, it is observed that the temperature gradient increases with increase in melting point of the samples. The linearity of the curve shows that this gradient is uniform. Moreover, the fluctuations in the measured temperatures were well within the experimental error of ±0.2 °C. The actual transition temperatures were extrapolated from the graph and the sample was kept at a particular temperature for at least 45 minutes before recording the spectra. The temperature rise of the sample due to laser heating was minimized by employing low laser power.

2.6.2. MEASUREMENT OF RAMAN SPECTRA

Raman spectra of the compounds 7.O4O.7 and 7.O5O.7 were recorded in 90° scattering geometry in the bulk samples. A SPEX Ramalog 1403 double monochromator equipped with an RCA 31034 photo-multiplier tube (with photon counting arrangement) and also a charge-coupled detector (CCD) was used to record the Raman spectra. The spectrometer control and data processing were accomplished with the help of a microprocessor based DM3000R series computer with the SPEX DM3000 software package. Excitation lines were obtained from a Spectra-Physics Model 165-09 Argon ion

laser. High temperature studies of the liquid crystals were done using an indigenously fabricated high temperature glass cell.

2.6.2.1. Spectra-Physics Model 165-09 Argon Ion Laser

This model consists of the laser head with a CW output and Model 265 exciter. The laser head consists of a rugged beryllium oxide (BeO) plasma tube closed at both ends by fused silica Brewster windows, a solenoid for providing necessary magnetic field and an optical resonator. The plasma tube is mounted in an optical cavity resonator formed by a spherical reflector at the output and a prism assisted by a flat mirror (to select the wavelength) at the high reflector end. The whole assembly of the resonator is held firmly against the quartz rods with springs to minimize microphonic frequency shifts. The plasma tube is supported on a kinematically adjustable mount and is adjusted in such a way that the plasma tube is exactly centered. An external thumb wheel is provided for wavelength selection and for changing the intra-cavity aperture. The plane of polarization of the output beam can be changed to the desired plane by using the polarizer for recording the polarized Raman spectra.

The Spectra-Physics Model 265 exciter is fully equipped with the necessary electronic circuits to create, sustain and regulate the ion discharge in the plasma tube and to control the output power from the laser by simultaneously regulating the solenoid current. An arrangement is provided for a desired constant output optical power when operated in the "light control" mode. The 265 Exciter is fed with a stabilized three-phase 380V (phase to phase) power supply. This unit requires cooling of the transistor pass bank in the exciter, the solenoid and the BeO plasma tube which is achieved by

circulating distilled, deionized water at 15 °C at 40 PSI from a closed cycle water chiller plant from Neslab, Model HX-500.

2.6.2.2. Spex model Ramalog 1403 double monochromator.

Raman spectra of the samples were measured with the help of the Spex model Ramalog 1403 double monochromator equipped with a RCA 31034 photo-multiplier tube and CCD. Fig. 2.6a schematically illustrates the essential parts of the instrument. The Spex 1403 double monochromator is a f/7.8 instrument with a spectral coverage from 11000 to 31000cm^{-1} with an accuracy of ±1 cm^{-1} in the 10000 cm^{-1} range. The spectral repeatability of ±0.2 cm^{-1} and a resolution of 0.15 cm^{-1} at 5791 Å (Hg line FWHM) can be achieved by this instrument. The holographic type instrument used in the instrument has 1800 grooves/mm blazed 5000Å. The gratings are mounted on a modified Czerny-Turner mount (Fig. 2.6b) using the fundamental grating equation:

$$d(\sin\alpha + \sin\beta) = n\lambda \qquad (2.6)$$

where n is the spectral order, λ is the wavelength, d is the grating spacing, and α and β are the angle of incidence and diffraction respectively. If $\alpha = \theta + \phi$ and $\beta = \theta - \phi$, where θ is the angle of rotation of the grating measured from zero as shown in the Fig. 2.6b and is a constant depending on the design of the instrument, then equation (2.6) can be written as

$$2d\sin\theta\cos\phi = n\lambda \qquad (2.7)$$

The Raman peaks are measured in terms of the frequency shifts in cm^{-1} on a linear x-axis by utilizing a cosecant drive for grating rotation with $\phi = 10^{o}$ and thus cosecϕ = 0.984 (values supplied by manufacturer). To record the Raman spectra, the laser beam is

passed through the Spex Model 1459 UVISIR illuminator after being diffracted from the Spex Model 1460 "Lasermate," which is a small unit consisting of a grating with 1200lines/mm blazed at 5000 Å and a mirror assembly to isolate and filter the spurious plasma lines. The beam is then focused on to the sample, after deflection (through 90°) by a mirror to a spot of diameter 10μm by a fused silica condensing lens. Scattered radiation from the sample is then passed through the polarization analyzer (optional), which works, on the principle of birefringence and total reflection or of dichroism. The polarization state of the observed Raman bands can be obtained by using this analyzer. The scattered radiation is then collected by an elliptical mirror (f/1.4) and focussed on to the entrance slit (S_3) of the spectrometer after reflection from the mirror (M_7) and passing through the polarization scrambler (Fig. 2.6a). The polarization scrambler converts the plane polarized scattered radiation to a randomly polarized radiation before it reaches the spectrometer and thus cancels any variation in spectrometer response that result from polarization dependent efficiencies. The polychromatic scattered radiation that is focussed on to the entrance slit gets dispersed by the 1800 lines/mm holographic gratings (G_2 and G_3). Finally, a nearly monochromatic light signal of a particular frequency selected by spectrometer control reaches the exit slit (S_7) or to the mirror (S_8) of the double monochromator. From here the beam can be either focussed on to a photomultiplier tube or a charge-coupled detector or, optionally to a third monochromator.

2.6.2.3. Spectrometer control and data processing.

The spectrometer control (frequency scanning) and data processing were accomplished using a DM-3000R series computer employing the DM3000 software package for Raman Spectroscopy. The DM3000 series of spectroscopy computers are based on an integrated comprehensive approach for controlling the spectroscopy set up and managing the obtained data with its unique combination of software and hardware. This software enables the user to manipulate the spectral data by allowing operations like background subtraction, addition, division, integration, differentiation, and frequency and intensity range expansion/reduction etc. The exceptional menu driven software package includes features that completely automate the data acquisition process. The DM3000 computers have up to 24 digital inputs /outputs to control any of the monochromator drives such as grating turrets, swing-away mirrors and other similar devices which provide a lot of flexibility and versatility to these systems. With DM3000 it is possible to acquire radiometrically corrected data in a wide variety of spectrometric units. For incremental scanning, the DM3000 allows to specify integration intervals as fast as 1 millisecond or as slow as 100 second per data point, and up to 4000 data points can be recorded in a single scan. The DM3000 has a dot-matrix graphic printer that can reproduce all the displays with comprehensive file identification.

The raw data is obtained from the output of the preamplifier. The anode of the photomultiplier tube is the input of the preamplifier, which has a gain of 400. The high voltage (1750 volts) required for operating the photomultiplier tube is also provided by the DM3000 with a stability of 0.002 % after an hour's warm up.

The photomultiplier tube Model RCA 31034 used with the experimental setup is a 2" diameter, head-on, 11-stage QUANTACON photomultiplier having a Gallium-Arsenide chip as its photocathode, an ultraviolet transmitting glass window and an in-line Copper-Beryllium dyanode structure. This tube is cooled to –30 °C by a thermoelectric cooling device and has almost absolute linear absolute response in the 3000 Å to 8500 Å wavelength range. It operates with a current gain of 10^6 with a maximum dark pulse simulation of 12CPS (counts per second).

References

1. Date, R. W., Imrie, C. T., Luckhurst, G. R. and Seddon, J. M., *Liq. Cryst.*, **12**, 203, (1992)

2. Attard, G. S., Date, R. W., Imrie, C. T., Luckhurst, G. R., Roskilly, S. J., Seddon, J. M. and Tayler, L., *Liq. Cryst*, **16**, 529, (1994)

3. Rao, N. V. S., Pisipati, V. G. K. M., Murthy, J. S. R., Bhaskara Rao, P. and Alapati, P. R., *Liq. Cryst.*, **5**, 539, (1989) and references therein.

4. Gray, G. W., *Nature*, **172**, 1137, (1953)

5. Szymanski, H, A, (ed.), "*Raman Spectroscopy*", Vol 1 (1967) and Vol 2 (1970), Plenum Press, New York.

6. Tobin, M. C., "*Laser Raman Spectroscopy*", Wiley-Inter-Science, New York, 1971.

7. Long, D. A., *Raman Spectroscopy,* McGraw Hill International Book Company, New York, 1977.

8. Placzek, G., in *Handbuch der Radiologie*, **Vol-6,** Part-2, pp-209, 1934.

9. Schrotter, H. W., and Klockner, H. W., "*Raman Spectroscopy of Glasses and Liquids;* Topics in Current Physics", (ed., Waber, A.) Springer Verlag, **Ch.4**, 1979.

10. Nester, R. J., and Lippon Coutt, E. R., *J. Raman Spectroscopy,* **1**, 309, 1973.

11. Jones, K. E., and Zewail, A. H., in *Advances in Laser Chemistry*, Ed., A.H. Zewail, Vol. 3, Springer, 1978.

12. Harris, C. B., Shelby, R. M. and Cornelius, *Phys. Rev. Lett.*, **38**, 1415, 1977.

Table 2.1. Various Phases, phase transition temperatures and transition enthalpies of liquid crystal dimers.

Compound	Phases / Parameters	K -S_F K - G*	S_F - S_C	S_F – S_A	G – I	S_C – I	S_A – I
7.O4O.7	Tr.Temperature (T° C)	111.5		165			212.8
	Enthalpy (ΔH/J mol^{-1})	24890.56		4185.75			17665.73
7.O5O.7	Tr.Temperature (T°C)	108.5		[98.8]			143
	Enthalpy (ΔH/J mol^{-1})	30815.0		9238.07			9046.68
10.O4O.10	Tr.Temperature (T° C)	104.2	165.3			205.5	
	Enthalpy (ΔH/J mol^{-1})	55167.8	14933.3			21034.81	
10.O10O.10	Tr.Temperature (T° C)	123.1		135			143.5
	Enthalpy (ΔH/J mol^{-1})	52665.45		13561.92			20515.34
10.O12O.10	Tr.Temperature (T° C)	118.2*			132		
	Enthalpy (ΔH/J mol^{-1})	50063.5*			32309.28		

[ ] indicates the monotropic transition

Plate No.2.1 Experimental set up for density study by bicapillary pyknometer

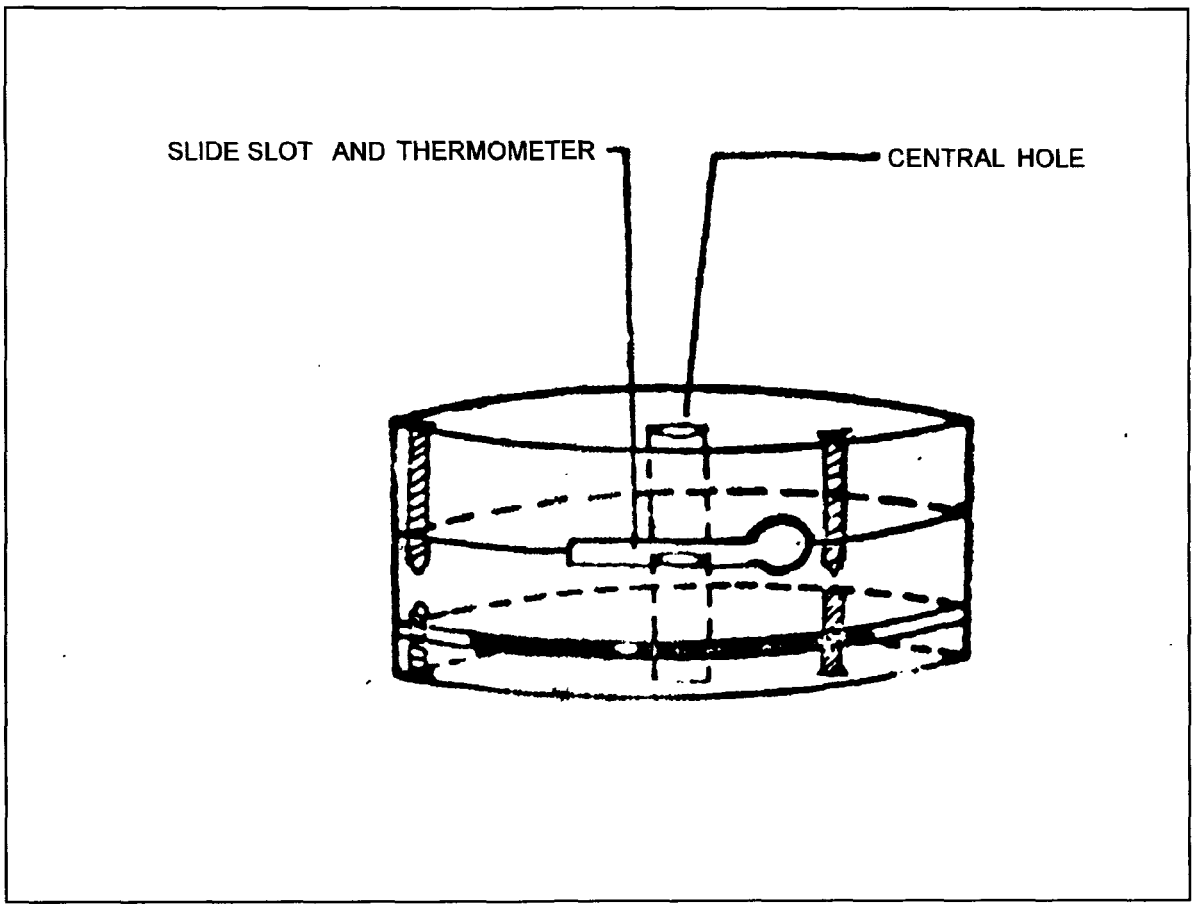

Fig 2.1 Heating Block for Polarizing Microscope

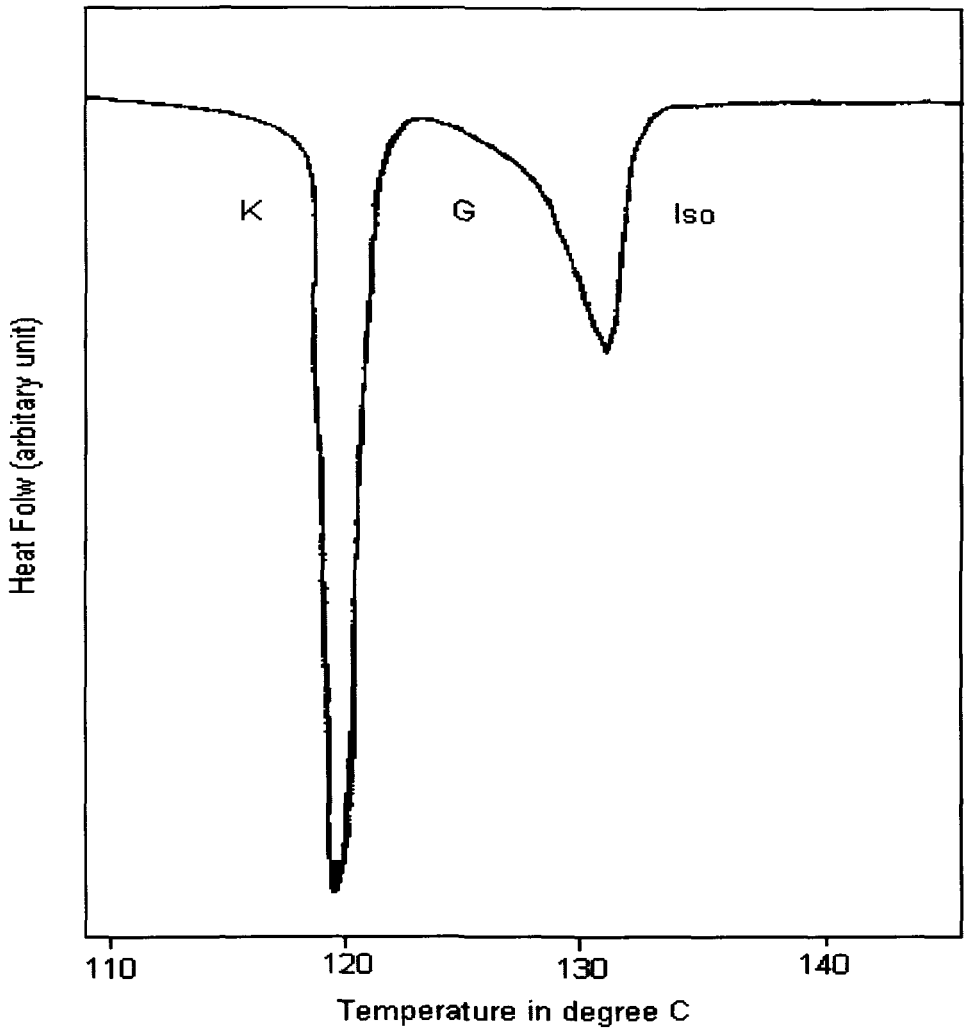

Fig. 2.2. DSC scan of liquid crystal dimer (10.O12O.10)

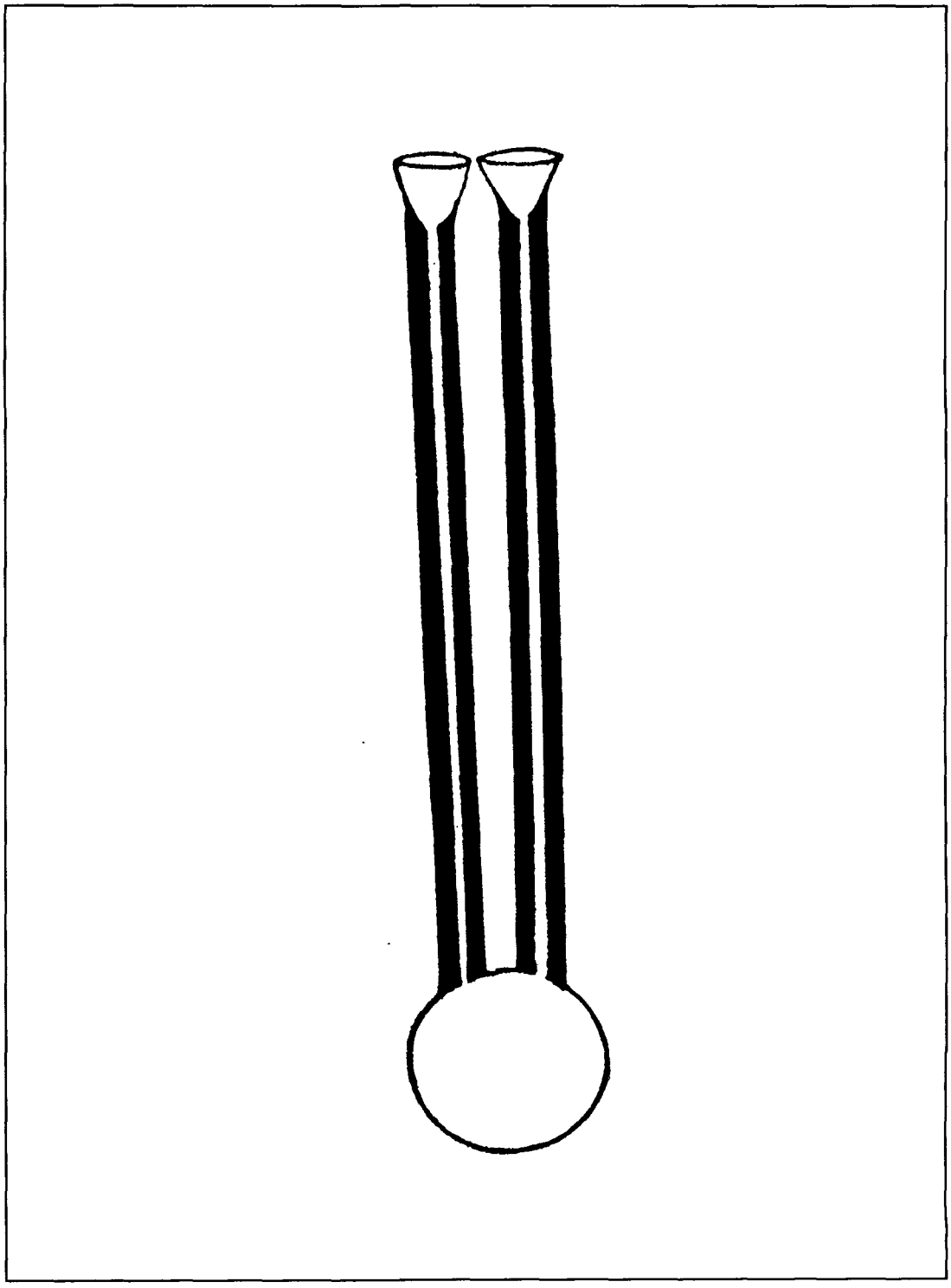

Fig. 2.3 bicapillary pyknometer

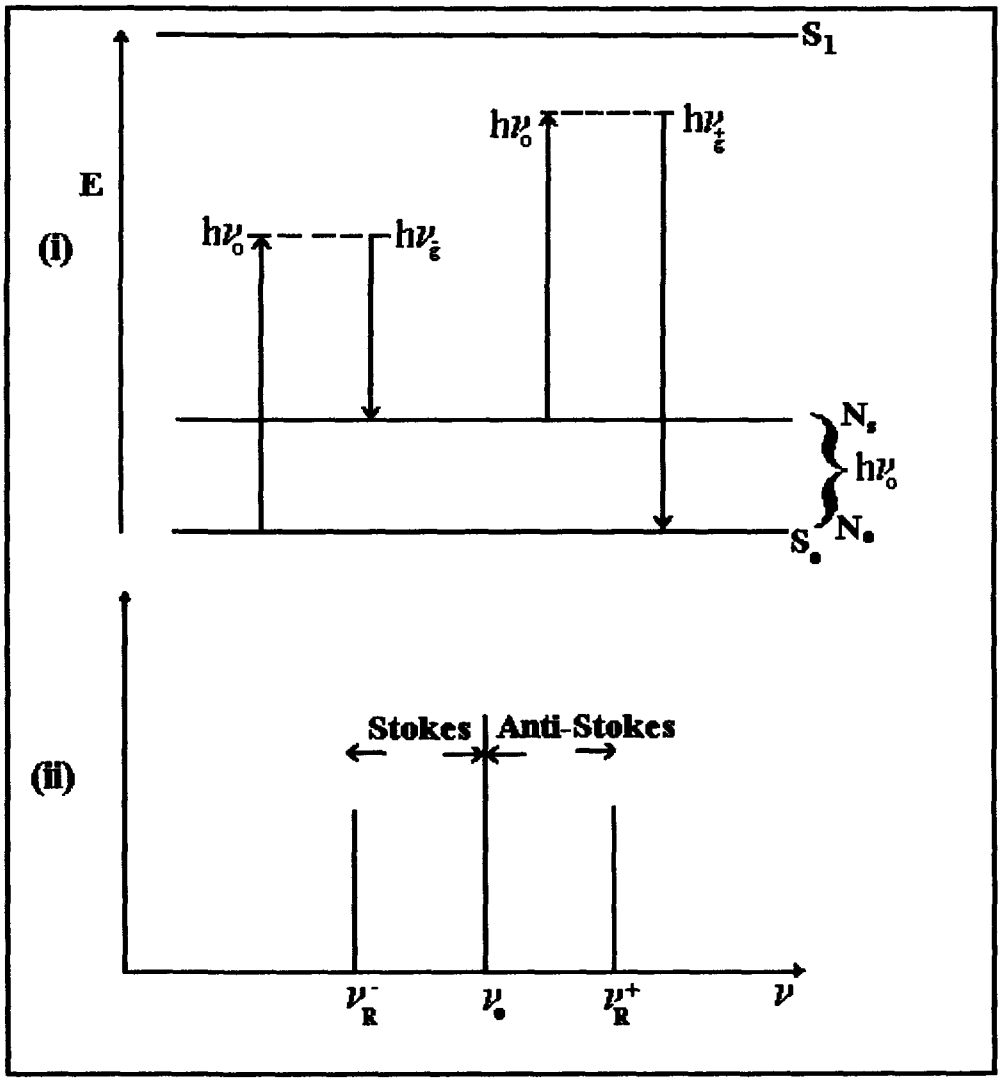

Fig 2.4. Diagrammatic representation of (i) Raman scattering process and (ii) Stokes and Anti-Stokes lines.

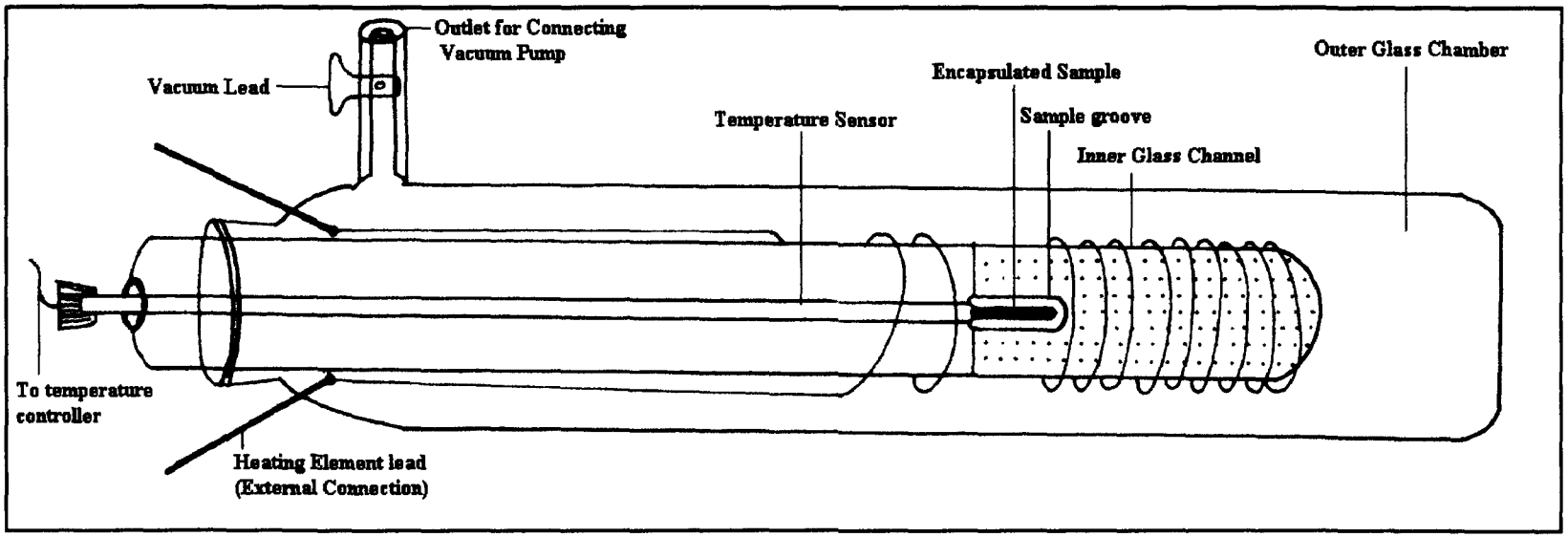

Fig 2.5a. High temperature cell for Raman studies in bulk form.

M.P. Temp. VS Observed Temp.

Calibration of the High Temperature Cell

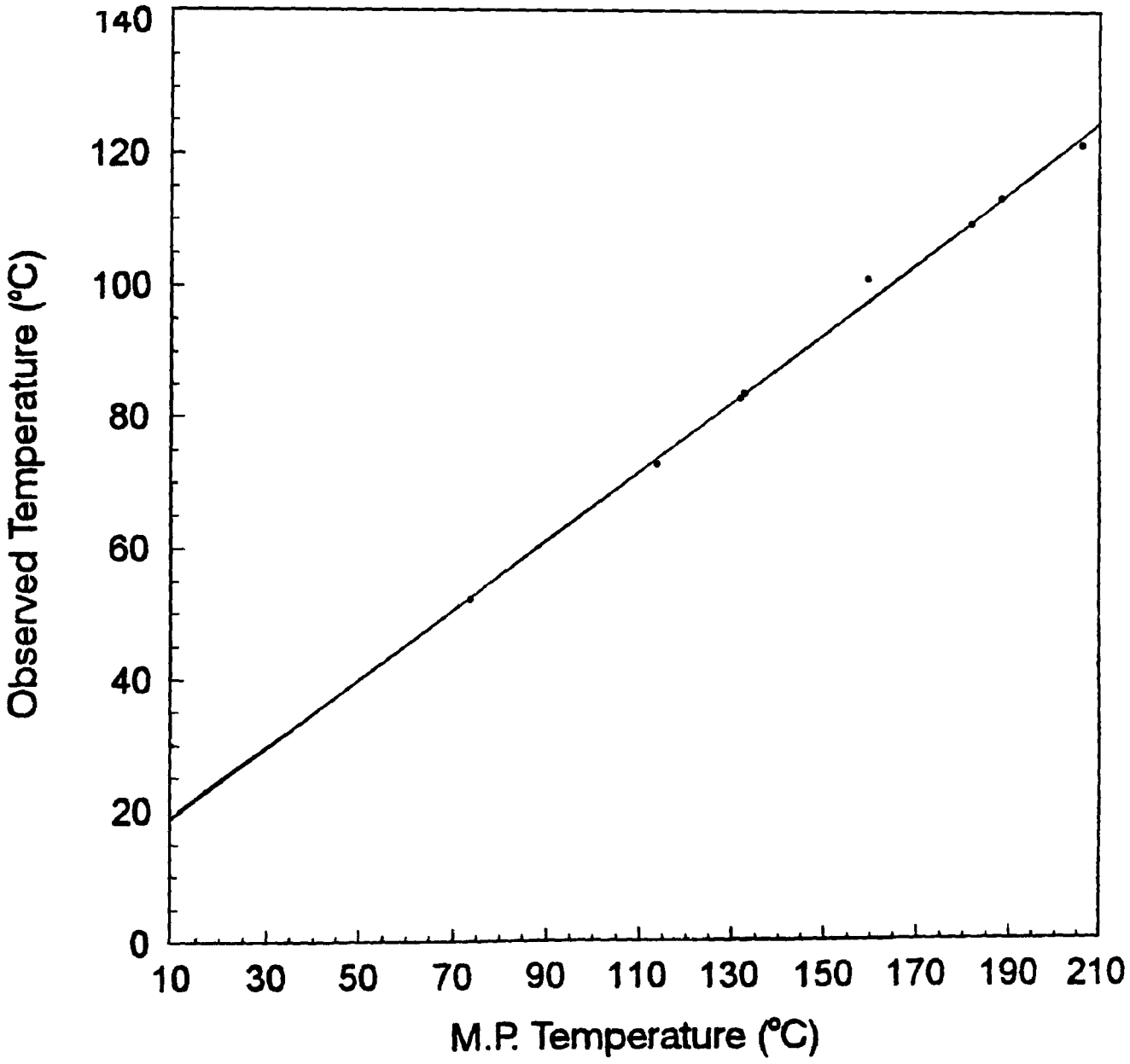

Fig 2.5b Calibration curve for the high temperature cell.

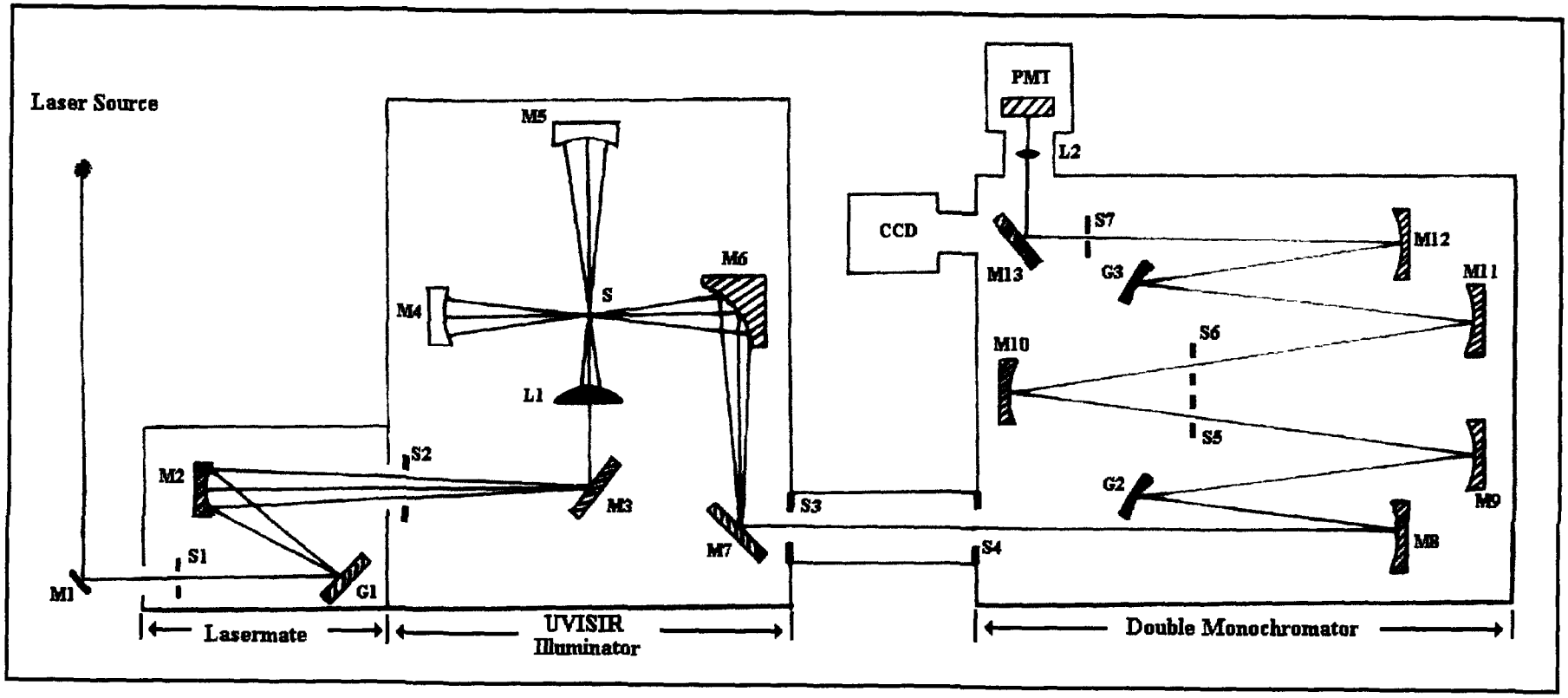

Fig. 2.6a. Optical diagram of a Spex Ramalog 1403 Spectrophotometer including the Lasermate and UVISIR illuminator. M1, M3, M7 and M13 are plane mirrors; M2, M4, M5 and M8-M12 are concave mirrors; M6 is an elliptical mirror; S1to S7 are slits; L1 is a fused silica condenser lens and L2 is a field lens; S is the sample: G1 to G3 are gratings, PMT is the photomutiplier tube and CCD is the charge couple detector.

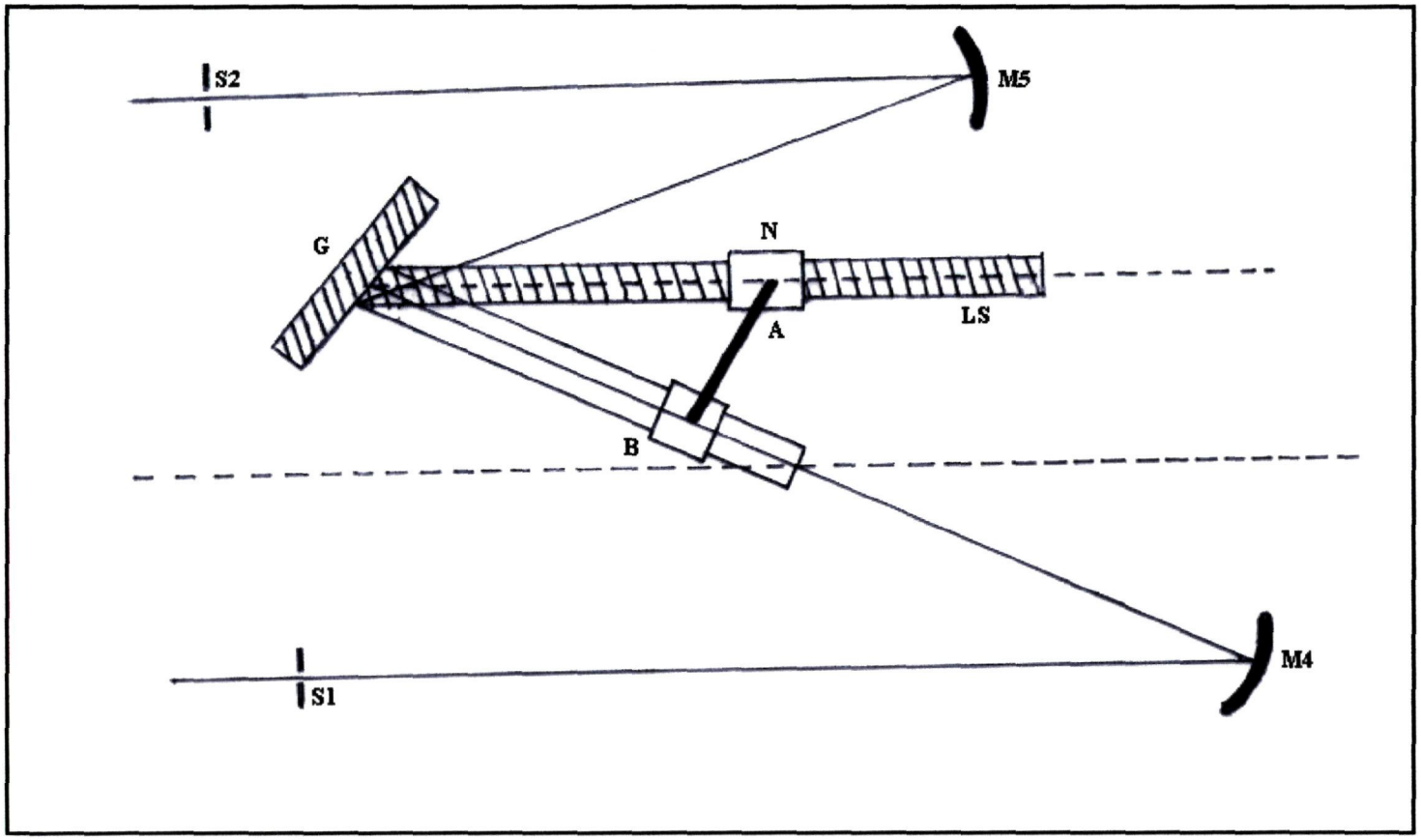

Fig. 2.6b. Mechanical cosecant drive mechanism for the Czerny-Turner mount of gratings for the SPEX Ramalog 1403 double monochromator. S1, S2 are slits, M4and M5 are mirrors, G is the grating, N is a nut, LS is the Leadscrew, B is the slide and A is the arm. The input nut N moves along leadscrew Ls while the slide B moves along a bar at right angles to the grating G. the grating rotates as the arm A moves along the bar.

CHAPTER - 3

ABSTRACT :

Schiff base symmetric liquid crystal dimers, namely α,ω-bis (4-n- alkylaniline benzylidene-4′-oxy)alkane in which two anisotropic groups are linked by a flexible spacer, exhibit a rich variety of smectic mesomorphism. The interest in this class of mesogens stems not only from their ability to act as model compounds for semi-flexible main-chain liquid crystal polymers but also from their quite different properties compared to conventional low molar mass liquid crystals (monomers). The phase transition studies on five of these schiff base liquid crystal dimers, viz. 7.O4O.7, 7.O5O.7, 10.O4O.10, 10.O10O.10 and 10.O12O.10 using the Differential Scanning Calorimetry and density measurements as a function of temperature have been discussed in light of available literature data. Present study includes the very rare phase transitions, for example smectic A – smectic F and isotropic – G transitions in addition to isotropic – smectic A, isotropic – smectic C and smectic C – smectic F phase transitions. The density jump and a peak in the thermal expansion coefficient in all the transitions confirm the first order nature of the transition but smaller jump were observed than expected in the density across certain transitions. Calculated values of pressure dependence of transition temperature and thermal expansion coefficient are also reported.

3.1. INTRODUCTION

Liquid crystal dimers are formed by linking two mesogenic groups together with a flexible spacer. They have been attracting a great deal of interest in recent years not only from their ability to act as model compounds for semi-flexible main-chain liquid crystal polymers, but also because they show quite unusual properties compared to low molar

mass liquid crystals. The liquid crystal dimers are classified into two categories: symmetric and non-symmetric. In the former class of dimers, the mesogenic groups are identical and in the latter, the mesogenic groups are not identical. The liquid crystalline properties as well as the structure of the different liquid crystal phases of these classes of compound are found to be dependent on the number of carbon atoms in the spacer [1-8]. The nematic – isotropic transition temperatures are found to exhibit a dramatic alternation as the number of carbon atoms in the alkyl spacer changes from odd to even. However, the alternation is attenuated as the spacer grows in length. In contrast, the change in the entropy of transition is essentially unchanged; at least for spacers containing up to twelve carbon atoms [9]. In addition the entropy change at the nematic – isotropic transition for dimers with odd spacers is comparable to that of monomers while for even spacers the translational entropy is typically three times larger. The behaviors of the translational entropy suggest that the orientational order for even spacers should be significantly greater than that for the odd spacer.

The present chapter includes the phase transition study by density measurement as a function of temperature on some symmetric liquid crystal dimers at various phase transitions. The symmetric liquid crystal dimer,α,ω-bis(4-n-alkylanilinebenzylidene-4′-oxy)alkane, popularly known as m.OnO.m homologues series of compounds show a rich smectic mesomorphism [1]. In addition to commonly observed Sm A, Sm C, Sm B phases, the uncommon Sm F phase is also present in a number of long terminal alkyl chain length homologues. Many of the transitional properties of these dimers depend strongly on the length and parity of the spacer. In addition to different transitional

properties, these compounds exhibit quite interesting structural features. The x-ray diffraction studies have shown an unusual feature in the diffraction pattern for the Sm F phases exhibited by odd-membered compounds [1]. This feature is an unresolved shoulder on the peak in the wide-angle region, which has not been previously reported and may arise from a distortion of the hexagonal lattice due to the difficulties in packing of bent molecules. Further, it is interesting to note that the smectic phase formation for these dimers involve, microphase separation into three regions viz., mesogenic groups, terminal chains and spacers each constituting a microphase in contrast to monomers, where only two regions, mesogenic groups and terminal chains are present.

Density studies across some rare phase transitions, such as Sm A – Sm F, Isotropic – G transitions in addition to commonly observed Isotropic – Sm A, Isotropic – Sm C, Sm C - Sm F in five symmetric liquid crystal dimers viz. 7.O4O.7, 7.O5O.7, 10.O4O.10, 10.O10O.10, 10O.12O.10 are presented in this chapter.

3.2. EXPERIMENTAL DETAILS

The general molecular structure of the m.OnO.m homologous series of compounds is given below.

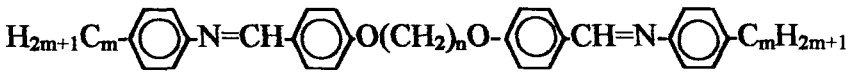

m = 7;	7.OnO.7;	n = 4,5
m = 10;	10.OnO.10;	n = 4,10,12

The compounds were synthesized following a standard procedure as discussed in chapter 2. The crude product was repeatedly recrystallized from ethyl acetate until the

transition temperatures were constant and reproducible. The Differential Scanning Calorimetry (DSC) studies were carried out on Perkin Elmer DSC – 7. Various phases exhibited by the compounds were characterized by observing their textures under a polarizing microscope attached with an indigenously built hot stage. The temperature resolution of the microscope was ± 0.1° C. The density measurement was carried out with a bicapillary pyknometer. The diameter of the capillary of the pyknometer was about 0.35 mm and the accuracy in the density measurements was ±0.1Kg m^{-3}. The permitted cooling rate was 2° C hr^{-1} and temperature accuracy was ±0.1°C.

The compounds 7.O4O.7, 7.O5O.7 and 10.O10O.10 exhibit Isotropic - Sm A, Sm A – Sm F phase transitions while the compounds 10.O4O.10 exhibits Isotropic – Sm C and Sm C – Sm F whereas 10.O12O.10 exhibits Isotropic – G phase transitions.

Representative DSC scans of two liquid crystal dimers (7.O4O.7 and 10.O4O.10) are shown in Figs. 3.1a and 3.1b respectively. The DSC scans of all the compounds show sharp melting transition, which is an indication of the purity of compounds. The transition temperature and entropy changes at different transitions are in good agreement with the reported literature values and shown in Table 3.1. It is observed that the entropy values at different phase transitions for the dimeric compounds are larger than that of other monomeric compounds. It may be noted that the entropy change at isotropic – Sm A phase transition for the even spacer dimer is twice that of monomeric compounds. Further, the entropy value of even spacer dimer (7.O4O.7) at the Isotropic – Sm A transition is nearly double compared to the odd dimer (7.O5O.7). These very large entropy values suggest that, both the orientational and translational ordering in the

smectic A phase are high for even spacers and also reflect the alternation of entropies in varying the flexible spacer for any given length of terminal chain.

The variation of density as a function of temperature in the entire mesophase region and the variation of estimated thermal expansion coefficient (α = dlnV/dT, where V is molar volume) with temperature for all the compounds are shown in Figs. 3.2a, 3.2b, 3.2c, 3.2d, 3.2e, 3.2f, 3.2g, 3.2h, 3.2j, and 3.2k. In all the compounds, the density increases as the temperature decreases, except in the vicinity of the phase transitions. It is found that the increment of molar volume per methylene unit is 15.50 x 10^{-6} m^3 mol^{-1}, for all the compounds, which is in excellent agreement with the available literature data.

An estimate of the pressure dependence of transition temperatures can be obtained using Clausius-Clapeyron equation.

$$\frac{dT_t}{dP} = T_t\left(\frac{\Delta V}{\Delta H}\right)$$

Where T_t - Transition temperature

ΔV – Molar volume change associated with the transition

ΔH – Heat of transition

3.3.1. Isotropic to Smectic A Transition (7.O4O.7, 7.O5O.7 and 10.O10O.10)

The isotropic to smectic A phase transition is confirmed by the development of characteristic optical textures of smectic A phase under the crossed polarizers. Smectic A phase has been assigned from the focal-conic fan and homeotropic textures and indicate the Isotropic to smectic A phase transition.

The Isotropic – Sm A phase transition in all the compounds (7.O4O.7, 7.O5O.7 and 10.O10O.10) is confirmed as a first order transition with a significant jump in density as well as by a peak in thermal expansion coefficient at the transition. Besides the higher slope of the density value in the Sm A phase compared to the isotropic phase indicates the dense packing and higher structural ordering in Sm A phase than in the isotropic phase. Further, co-existence of isotropic and smectic A phases (which suggest the simultaneous growth of orientational and translational order) is observed for a temperature range of 0.6°C in 7.O4O.7, 0.9°C in both 7.O5O.7 and 10.O10O.10, but large part of density jump is completed within 0.2°C in 7.O4O.7 and 10.O10O.10 whereas within 0.3°C in 7.O5O.7. The observed density jump ($\Delta\rho/\rho$) across I –Sm A transition is 1.57% in 7.O4O.7, 0.95% in 7.O5O.7 and 2.26% in 10.O10O.10. The minimum and maximum density jump reported so far across the I – Sm A transitions are 0.35% and 2% respectively. These density jumps and thermal expansion coefficient peak values of 428 x 10^{-04} $°C^{-1}$ for 7.O4O.7 and 182 x 10^{-04} $°C^{-1}$ and 486 x10^{-04} $°C^{-1}$ for 10.O10O.10 confirmed the I – Sm A transition to be first order. However, the density jumps at the I – Sm A transitions of these compounds are significantly smaller than that for the transition exhibited by monomers [10]. This is quite unexpected since the entropy change at I – Sm A transition is much higher in these dimers compared to that of monomers.

In compounds exhibiting two-phase transitions separated by a narrow temperature range, large density jumps are observed in some compounds at the phase transition on the high temperature side. Analogous results are observed at Nematic – Smectic A transition

also in the compounds exhibiting narrow nematic phase. In the present study, presumably, large smectic A phase thermal range of 46.8 °C in 7.O4O.7 and 44.2°C in 7.O5O.7 is responsible for smaller density jumps at the I – Sm A transition although the enthalpy change at the transition is significantly higher.

The estimated values of pressure dependence of transition temperatures are found to be 29.08 K/k bar for 7.O4O.7, 30.07 K/k bar for 7.O5O.7 and 39.71 K/k bar for 10.O10O.10 and these values are in good agreement with the literature data [11]. A comparison of density jump, transition enthalpy and pressure dependence of transition temperature of some compounds at isotropic – smectic A transition is shown in Table 3.2.

3.3.2. Isotropic to Smectic C Transition (10.O4O.10)

The isotropic phase to smectic C phase transition is confirmed by the development of characteristic optical textures of smectic C phase from isotropic phase viewed under the crossed polarizers. Smectic C phase has been identified from the broken focal-conic fan and schlieren textures.

The Isotropic – Smectic C (I – Sm C) transition is accompanied by a large jump in density. Further, the co-existence of isotropic and smectic C phases is observed in the temperature range of 0.9°C. However, the significant jump in density at the transition is completed within 0.4°C. The observed density jump of 2.09% and a thermal expansion coefficient maxima, 451 x 10^{-04}°C^{-1} confirm the transition to be first order transition. The slope of the density plot (calculated away from the phase transition i.e., in the thermally stable linear region) is found to attain a higher value with the growth of the relatively densely packed smectic C phase. The observed density jump is found to be comparable to

that of the other compounds and largest across the I – Sm C transition reported so far to the best of our knowledge. The estimated value of the pressure dependence of transition temperature from our results is 36.67 K/k bar and is in reasonable agreement with the reported values for this transition. However, the estimated values of the dT_t/dP for 4,4'-di-n-octadecyloxy benzene (27.1 K/k bar) [12] and di-n-hexadecyl4,4'-azoxy 2 methyl cinnamate (30 K/k bar) at the I – Sm C transition are found to be lower than the present results. The contribution of true latent heat and pretransitional heat of transition to enthalpy may lead to the estimated dT_t/dP values to be lower than the experimental values.

The observed density jumps across the I – Sm C transition are found to be higher than those across I – Sm A transition and lower than that across I – Sm F ($\Delta\rho/\rho$ =2.14% in 10O.14) phase transitions. It is due to the growth of characteristic intermediate Sm C molecular order (in between structural orders that grow across I – Sm A and I – Sm F transitions) from the isotropic liquid. A comparison of density jump and pressure dependence of transition temperature of some compounds at isotropic – smectic C transition is given in Table 3.3.

3.3.3. Isotropic to G Transition (10.O12O.10)

The isotropic to G transition is a very rare kind of phase transition and is an example of a transition between a completely disordered liquid phase to a well-defined three-dimensional structure in smectic phase. Moreover, at this transition, the infinite rotational symmetry of isotropic phase is broken with the growth of a three dimensional positional correlation of bond orientational order. The Isotropic – G transition in

10.O12O.10 is accompanied by a large density jump of 1.57% and a peak in thermal expansion coefficient (α = 101 x 10^{-04} $°C^{-1}$) indicating the transition to be first order transition. In our study, it is observed that the density jump is much less than what would have been expected for a transition of entropy change ($\Delta S/R$) of 9.60. However, this density jump is found to be smaller compared to the isotropic to smectic A transition and the isotropic to smectic C phase transition in the same series of the dimer (10.O4O.10, 10.O10O.10) [19] but comparable to that of isotropic to smectic A transition in 7.O4O.7 [20]. It may be due to the dimensionality and crystal structural order change which is different at the isotropic to G transition. Also, it could be due to the terminal chain length. This value is different from the values at the onset of Smectic A, C and F directly from isotropic liquid. It is noticed that the dimensionality and the crystal structural change are different (from Smectic A, C and F) at the isotropic to G transition resulting in a larger density jump. This decreasing trend of the density jump with the increase of the flexible spacer length irrespective to type of transition is in agreement with that reported [21] in the case of TBNA and 12O.m series [22] where this type of behavior was reported for increasing terminal chain length. As the terminal chain length (here the spacer length) increases, the total volume occupied per methylene unit is comparatively smaller than volume required per methylene unit with smaller terminal chains. That is, the volume swept by methylene unit in the compound possessing small alkyl terminal chain is larger while the close packing of alkyl terminal chains results in smaller volume variation at the transition [23]. However, the above trend is more pronounced in the case of alkoxy chain

rather than alkyl chain. The calculated pressure dependence of transition temperature is found to be 18.25 K/k bar.

3.3.4. Smectic A to Smectic F Transition (7.O4O.7, 7.O5O.7 and 10.O10O.10)

The optical texture observed under crossed polarizers for the Sm F phase formed on cooling Sm A phase consists of finely arced focal-conic fans and poorly colored mosaic platelets with sharply defined boundaries which develop from the homeotropic regions of Sm A phase and indicate the Sm A – Sm F transition.

The Sm A – Sm F transition is inferred by a large jump in density in all the three compounds. The observed density jump is 0.55% in 7.O4O.7, 0.62% in 7.O5O.7 and 1.80% in 10.O10O.10. These density jumps along with a large thermal expansion coefficient peak values of 165 x 10^{-04} $°C^{-1}$ for 7.O4O.7, 160 x 10^{-04} $°C^{-1}$ for 7.O5O.7 and 450 x 10^{-04} $°C^{-1}$ for 10.O10O.10 at the transition confirm Sm A- Sm F transition as the first order transition. The Sm A – Sm F transition is an example of a transition from disordered orthogonal structure in Sm A to the ordered Sm F phase in which the molecules are packed in layers with a pseudo-hexagonal arrangement with a two dimensional structure of the positional order and long axis tilted (direction of tilt is towards an edge of hexagon) with respect to the layer planes (i.e., with uncorrelated layers but long range bond orientational order) is expected to be a first order transition. This transition is observed very rarely. The only other compound reported so far for which density studies were reported across the Sm A – Sm F transition is N-(4-n-nonyloxybenzylidene)-4′-n-butylaniline (9O.4) in which the observed density jump was 1.42%. The density jump observed for 10.O10O.10 at the Sm A – Sm F transition is

higher than that reported so far for other compounds. The estimated pressure dependence of the transition temperature is found to be 37.25 K/k bar for 7.O4O.7, 16.82 K/k bar for 7.O5O.7 and 45.76 K/k bar for 10.O10O.10 [19,20]. However, these values are significantly smaller than those reported for 9O.4,for which it is 48 K/k bar [10].

3.3.5. Smectic C to Smectic F Transition (10.O4O.10)

On cooling the Sm C phase, the break in focal-conic fans became well defined changing into black patches while the mosaic schlieren texture developed from the regions of schlieren texture. These textural changes under the crossed polarizers indicate transition to be a Sm C to Sm F transition.

A large density jump of 1.83% and a thermal expansion peak value of 370 x 10^{-04} $°C^{-1}$ characterize the Sm C – Sm F transition to be a first order transition. This is also consistence with the large entropy change ($\Delta S/R$ = 4.10) observed at the transition in the DSC studies. It may be noted that the large thermal range of (39°C) smectic C phase in 10.O4O.10 is expected [20] to unlock the high temperature two-fold biaxial mode from the exponentially growing six-fold hexatic continuous symmetry resulting into a second order transition (against the observed first order Sm C – Sm F transitions in the case of two-dimensional melting crystals). The existence of Sm C – Sm F tricritical point, where the order of transition changes from second order to first order was discussed in a study of TBPA [24]. The estimated pressure dependence of transition temperature of Sm C – Sm F transition is found to be 39.66 K/k bar. This value is found to be comparable with that of 5O.5 (42.5 K/k bar) and TBOA (43 K/k bar) and lower than that reported for 9O.6 and 9O.8 [25].

3.4. CONCLUSIONS

The important conclusions of this chapter are that the entropy values of different phase transitions of the dimers are larger than that of other monomeric compounds (twice that of monomeric compounds). Further, the entropy value of even spacer dimer (7.O4O.7) at the Isotropic – Sm A transition is nearly double compared to the odd spacer dimer (7.O5O.7). These very large entropy values suggest that, both the orientational and translational ordering in the smectic A phase are high for even spacers and also reflect the alternation of entropies in varying the flexible spacer for any given length of terminal chain. Also, unlike the I – Sm A, I – Sm C and Sm C – Sm F phase transitions, the very rare phase transitions Sm A – Sm F and I – G are found to be of first order in nature. However, the density jumps across the certain phase transitions viz. Sm A – Sm F and Sm C - Sm F are found to be smaller than expected.

References

1. Date, R.W., Imrie, C.T., Luckhurst, G.R., and Seddon, J.M., *Liq. Cryst.*, **12**, 203 (1992)

2. Heeks, S.K., and Luckhurst, G.R., *J. Chem. Soc., Faraday Trans.*, **89**, 3289 (1993)

3. Attard, G.S., Date, R.W., Imrie, C.T., Luckhurst, G.R., Roskilly, S.J., Seddon, J.M., and Taylor, L., *Liq. Cryst.*, **16**, 529 (1994)

4. Date, R.W., Luckhurst, G.R., Shuman, M., and Seddon, J.M., *J. de Physique II*, **5** 587 (1995)

5. Fletcher, I.D., and Luckhurst, G.R., *Liq. Cryst.*, **18**, 175 (1995)

6. Le Masurier, P.J., and Luckhurst, G. R., *Liq. Cryst.*, **25**, 63 (1998)

7. Blatch, A. E., Fletcher, I. D., and Luckhurst, G. R., *J. Mater. Chem.*, **7**, (1997)

8. Barnes, P.J., Douglas, A.G., Heeks, S.K., and Luckhurst, G.R., *Liq. Cryst.*, **13**, 603 (1993)

9. Ferrarini, A., Luckhurst, G. R., Nordio, P. L., and Roskilly, S. J., *Chem. Phys. Lett.*, **214**, 3 (1993).

10. Alapati, P.R., Saran, D, and Raman, S.V., *Mol. Cryst. Liq. Cryst.*, **287**, 239 (1996) and references therein.

11. Alapati, P. R., Ph. D. Thesis Nagarjuna University, (1987)

12. Demus, D., and Rurainski, R., *Z. Phys. Chem.(Leipzrg)*, **255**, 53 (1973)

13. Pisiapti, V.G.K.M., Rao, N.V.S., Gouri Sankar, Y., and Murthy, J.S.R., *Acustica*, **60**, 163 (1986)

14. Rao, N.V.S., and Pisipati, V.G.K.M., *Phase Trans.*, **3**, 171 (1983)

15. Alapati, P.R., Potukuchi, D.M., Rao, N.V.S., Pisipati, V.G.K.M., and Saran, D., *Mol. Cryst. Liq. Cryst.*, **146**, 111 (1987) and references therein.

16. Rao, N.V.S., Pisipati, V.G.K.M., Gouri Sankar, Y., *Mol. Cryst. Liq. Cryst.*, **131**, 237 (1985)

17. Rao, N.V.S., Pisipati, V.G.K.M., Alapati, P.R., and Potukuchi, D.M., *Mol. Cryst. Liq. Cryst.*, **162B**, 119 (1998)

18. Narayan,S.L., Prabhu, C.R., Potukuchi, D.M., Rao, N.V.S., and Pisipati, V.G.K.M., *Liq. Cryst.*, **20**, 177 (1996)

19. Gogoi, B., Arulsankar, A., and Alapati, P.R., *Mol. Cryst. Liq. Cryst.* **366**, 69 (2001)

20. Gogoi, B., Arulsankar, A, Ghosh, T.K., and Alapati, P.R., *Mol. Cryst.Liq. Cryst.*, **365**, 561 (2001)

21. Lakhminarayana, S., Prabhu,C.R., Potukuchi, D.M., Rao, N.V.S., and Pisipati, V.G.K.M., *Liq. Cryst.*, **20** , 117(1993)

22. Srinivasulu, M., Potukuchi, D.M., and Pisipati, V.G.K.M., *Z. Naturforsch.*, **52a**, 713 (1997)

23. Jitendra Nadh, M., Rama Rao, C. G., Srinivasulu, M., Potukuchi, D.M., and Pisipati, V.G.K.M., *Mol. Cryst. Liq. Cryst.*, **366**, 457 (2001)

24. Noh, D.Y., Brock, J.D., Litster, I.D., Birgeneau, R.J., and Googby, J.W., *Phys. Rev. B*, **40**, 4920 (1989)

25. Rao, N.V.S., Potukuchi, D.M., Sankar Rao, P.V., Pisipati, V.G.K.M., *Liq. Cryst.*, **12**,127, (1992)

Table 3.1. Various Phases and phase transition temperatures, transition entropy, enthalpy and density jumps of liquid crystal dimers.

Compound	Phases / Parameters	K -S_F K – G#	S_F - S_C	S_F – S_A	G – I	S_C – I	S_A – I
7.O4O.7	Tr.Temperature ((T° C) Entropy (ΔS/R) Enthalpy (ΔH/J mol^{-1}) Density Jump (Δρ/ρ)	111.5 7.79 24890.56		165 1.15 4185.75 0.55%			212.8 4.38 17665.73 1.57%
7.O5O.7	Tr.Temperature (T° C) Entropy (ΔS/R) Enthalpy (ΔH/J mol^{-1}) Density Jump (Δρ/ρ)	108.5 9.72 30815.0		[98.8] 2.99 9238.07 0.62%			143 2.62 9046.68 0.95%
10.O4O.10	Tr.Temperature (T° C) Entropy (ΔS/R) Enthalpy (ΔH/J mol^{-1}) Density Jump (Δρ/ρ)	104.2 17.6 55167.8	165.3 4.10 14933.3 1.83%			205.5 5.29 21034.81 2.09%	
10.O10O.10	Tr.Temperature (T° C) Entropy (ΔS/R) Enthalpy (ΔH/J mol^{-1}) Density Jump (Δρ/ρ)	123.1 16.0 52665.45		135 4.0 13561.92 1.80%			143.5 5.93 20515.34 2.26%
10.O12O.10	Tr.Temperature (T° C) Entropy (ΔS/R) Enthalpy (ΔH/J mol^{-1}) Density Jump (Δρ/ρ)	118.2# 15.2# 50063.5#			132 9.60 32309.28 1.57%		

[ ] indicates the monotropic transition

Table 3.2 Comparison of density jump ($\Delta\rho/\rho$ %), transition enthalpy (ΔH/J mol^{-1}) and pressure dependence of transition temperature (dT_t/dP K/k bar) of some liquid crystal compounds at isotropic – smectic A phase transition.

COMPOUND	$\Delta\rho/\rho$ %	ΔH/J mol^{-1}	dT_t/dP K/k bar	REFERENCE
7.O4O.7	1.57	17665.73	29.08	Present work
7.O5O.7	0.95	9046.68	30.07	- do -
10.O10O.10	2.26	20515.34	39.71	- do -
Di-n-hexadecyl 4,4′-azoxy cinnamate	0.40	4764	26.70	12
Di-n-undecyl 4,4′-azoxy-α-methyl cinnamate	1.21	8565	18.90	12
n-amyl-4(4-n-dodecyloxybenzy lidene amino) cinnamate	1.28	8414	33.70	12
N-(4-n-Heptyloxybenzylidene)4′-n-octylaniline	1.04	5870	27.30	13
N-(4-n-octyloxybenzylidene)4′-n-butylaniline	1.11	5680	26.50	14
Terephthalylidene-bis-p-n-decyl aniline	1.82	7080	72.20	15
Terephthalylidene-bis-p-n-octyl aniline	0.96	5670	42.0	16

Table 3.3. Comparison of density jump ($\Delta\rho/\rho$ %), and pressure dependence of transition temperature (dT_t/dP K/k bar) of some liquid crystal compounds at isotropic – smectic C phase transition.

COMPOUND	$\Delta\rho/\rho$ %	dT_t/dP K/k bar	REFERENCE
10.O4O.10	2.09	36.67	Present work
Terephthalylidene-bis-p-n-dodecyl aniline	1.13	36.30	17
Terephthalylidene-bis-p-n-tetra decyl aniline	1.20	33.03	18
Terephthalylidene-bis-p-n-hexa decyl aniline	0.75	29.99	18

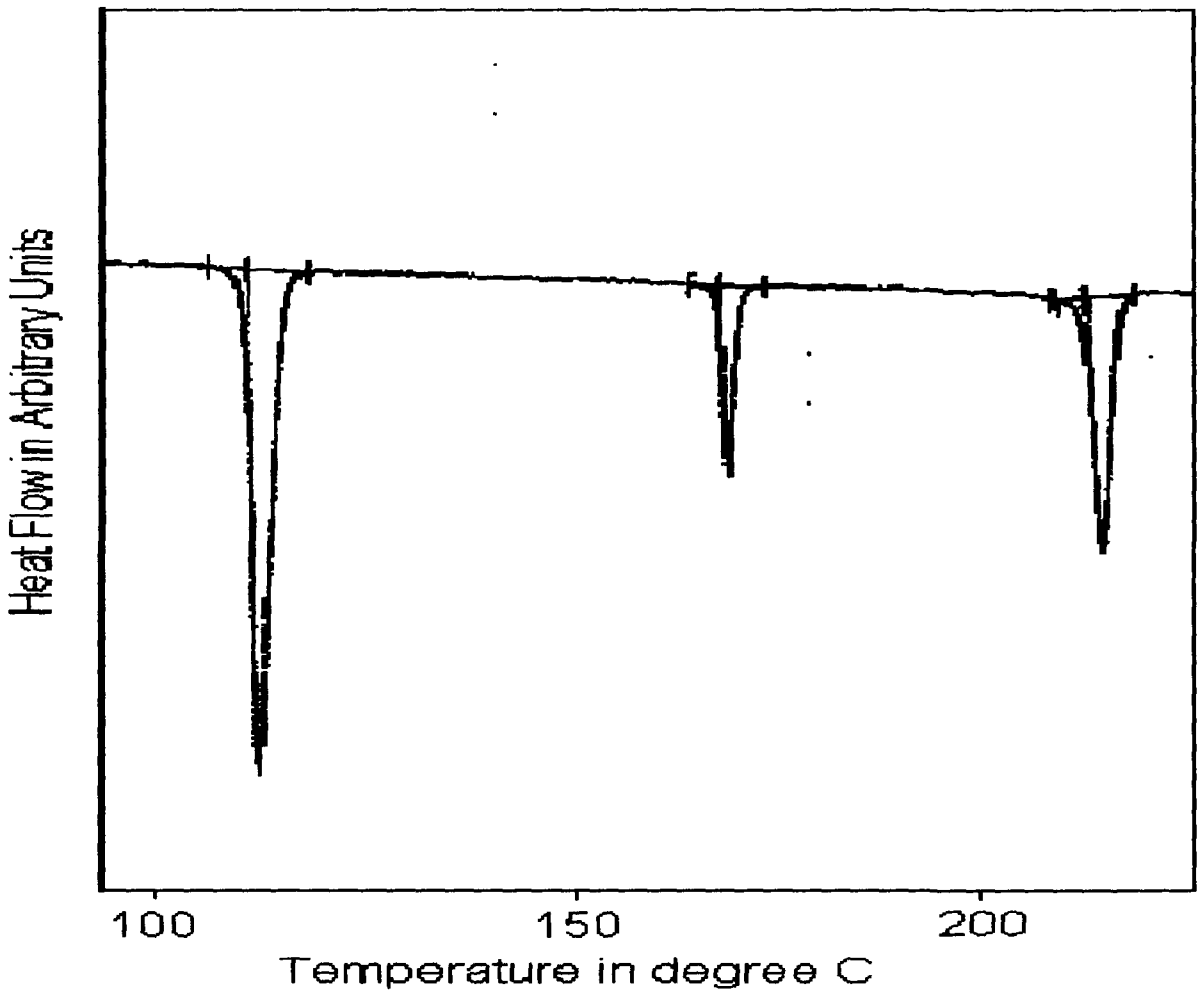

Fig 3.1(a) DSC Scan of 7.040.7

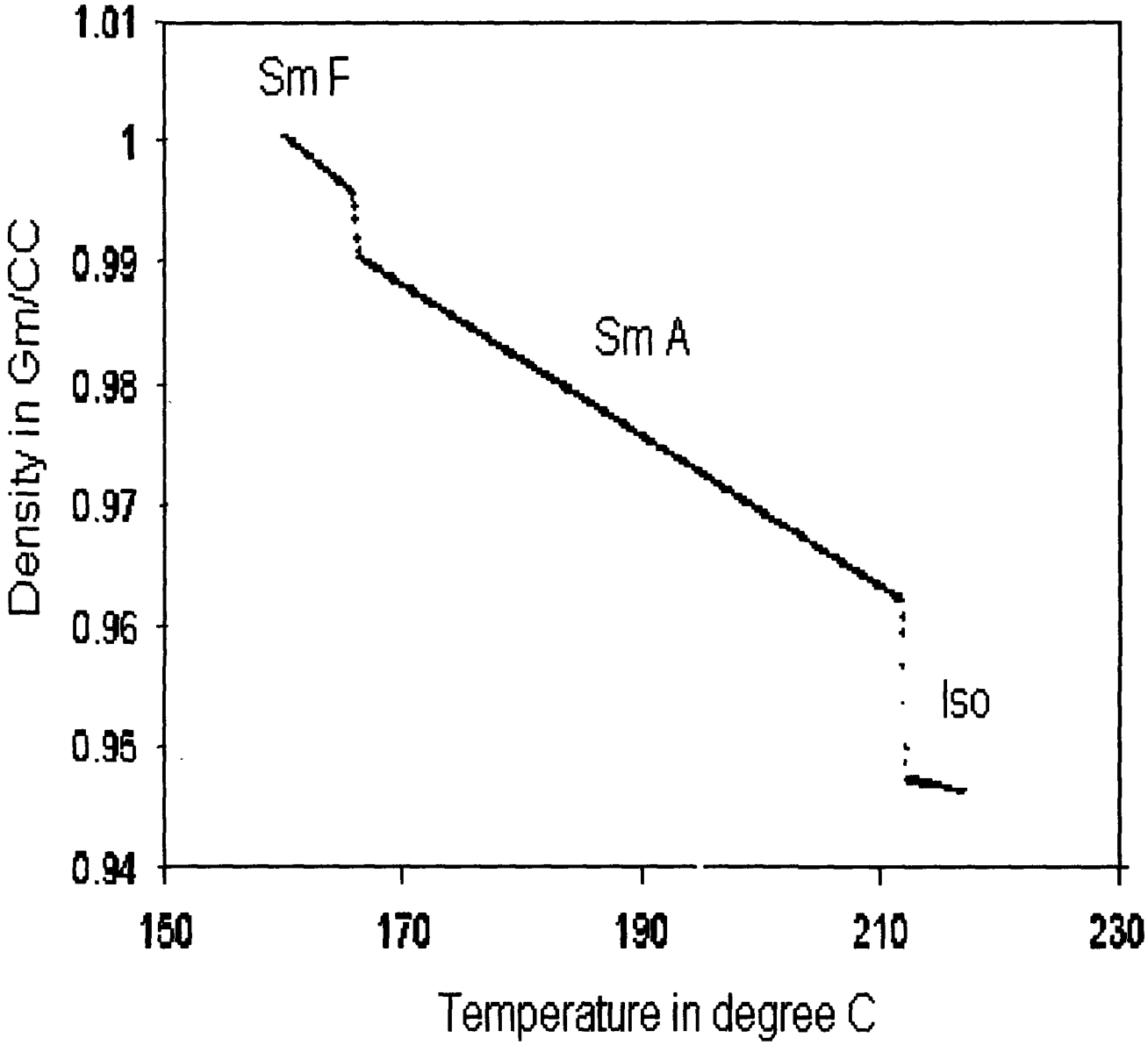

Fig. 3.2a. Variation of density with temperature in Isotropic, Sm A and Sm F phases for 7.O4O.7

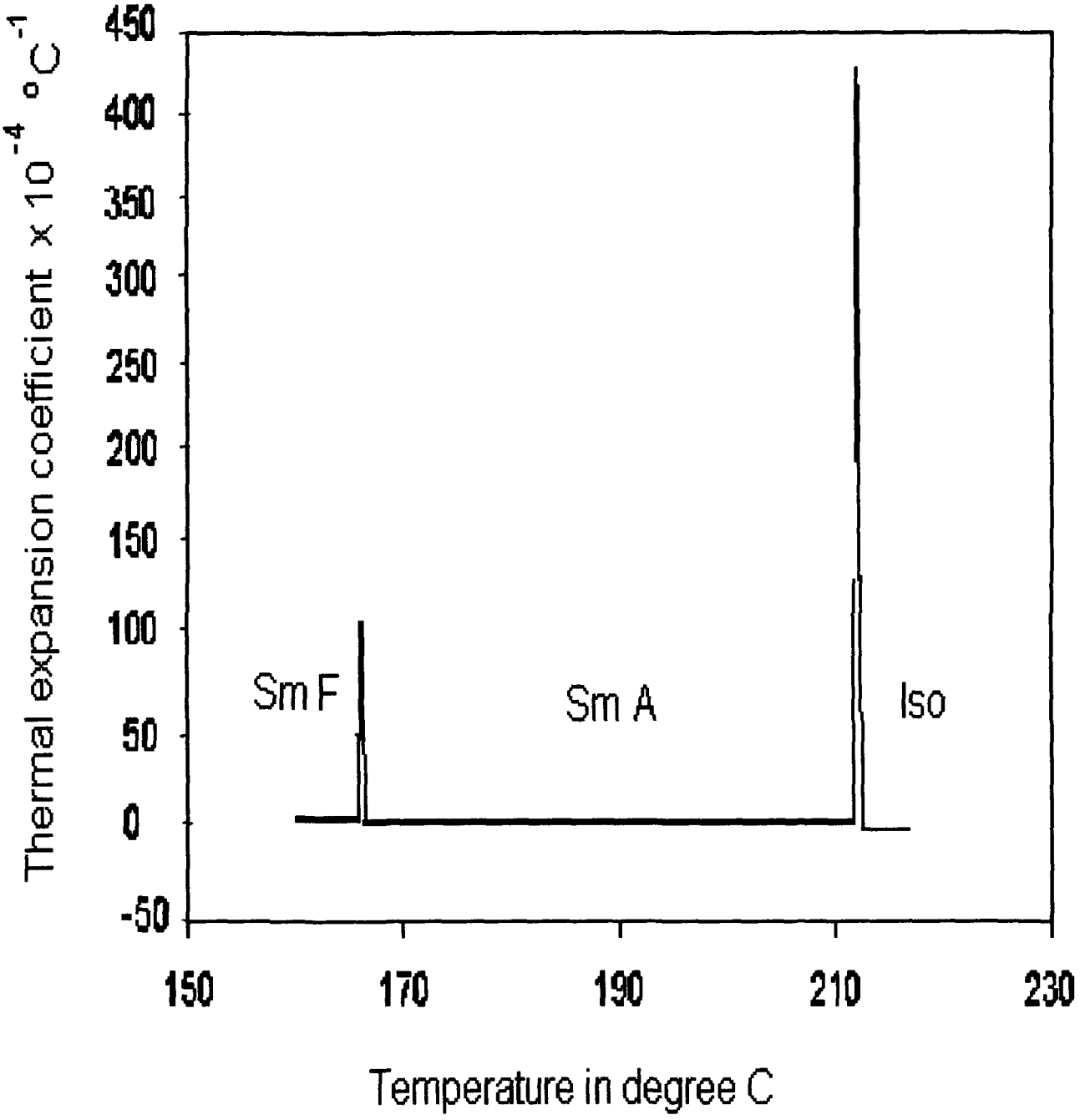

Fig. 3.2b Variation of thermal expansion coefficient with temperature in isotropic, Sm A and Sm F phases of 7.O4O.7

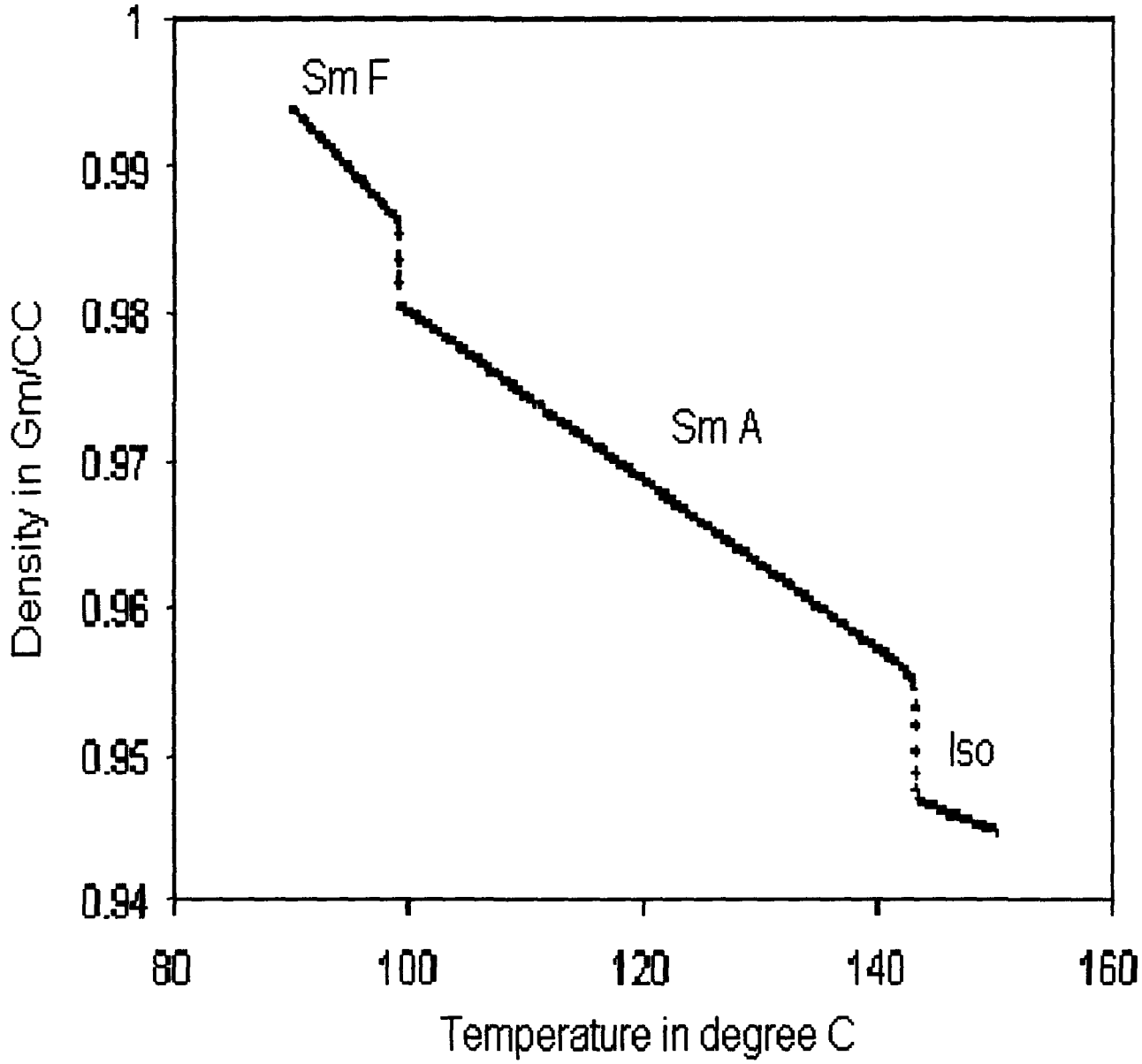

Fig 3.2c. Variation of density with temperature in Isotropic, Sm A and Sm F phases for 7.O5O.7

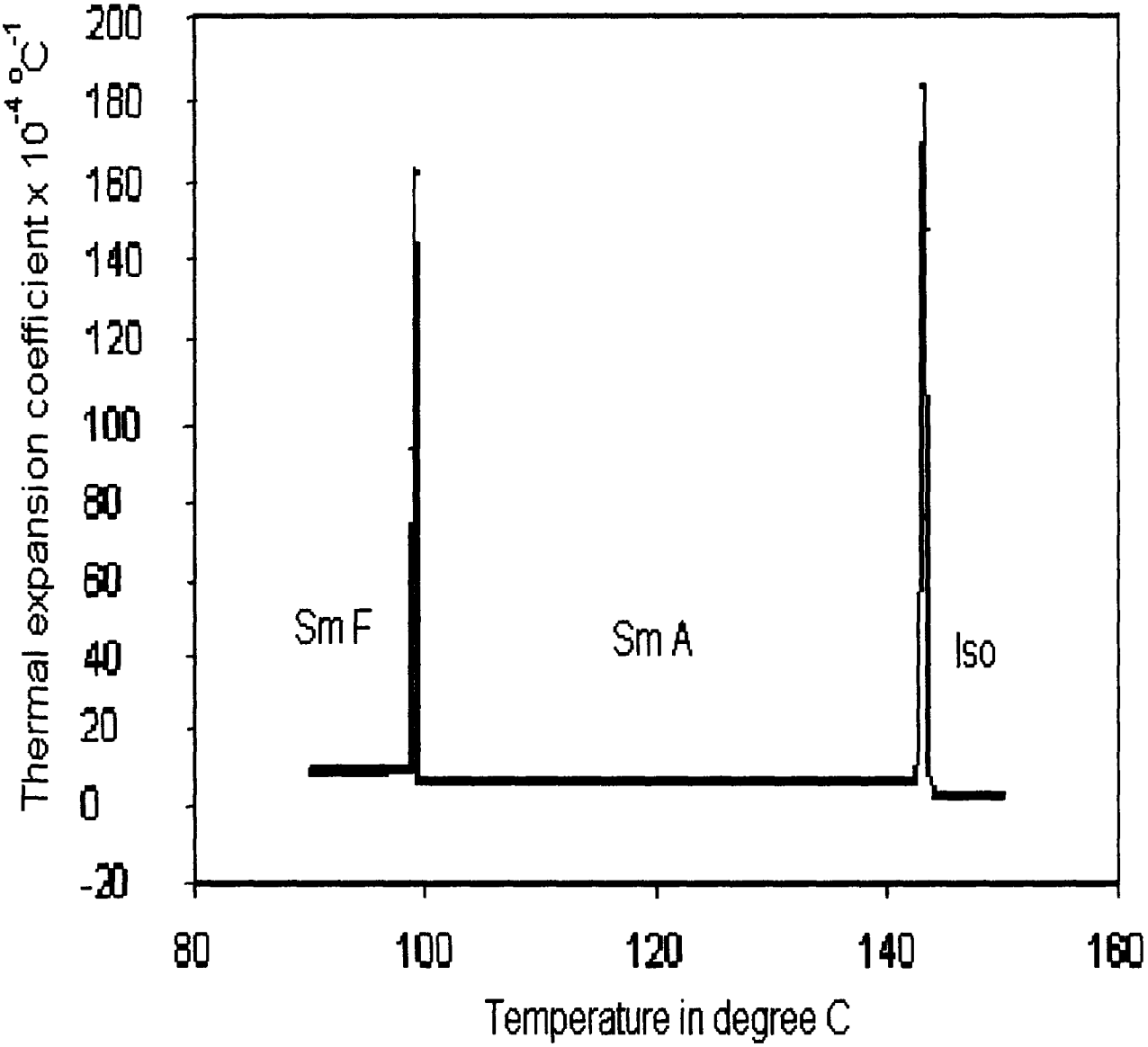

Fig. 3.2d. Variation of thermal expansion coefficient with temperature in isotropic, Sm A and Sm F phases for 7.O5O.7.

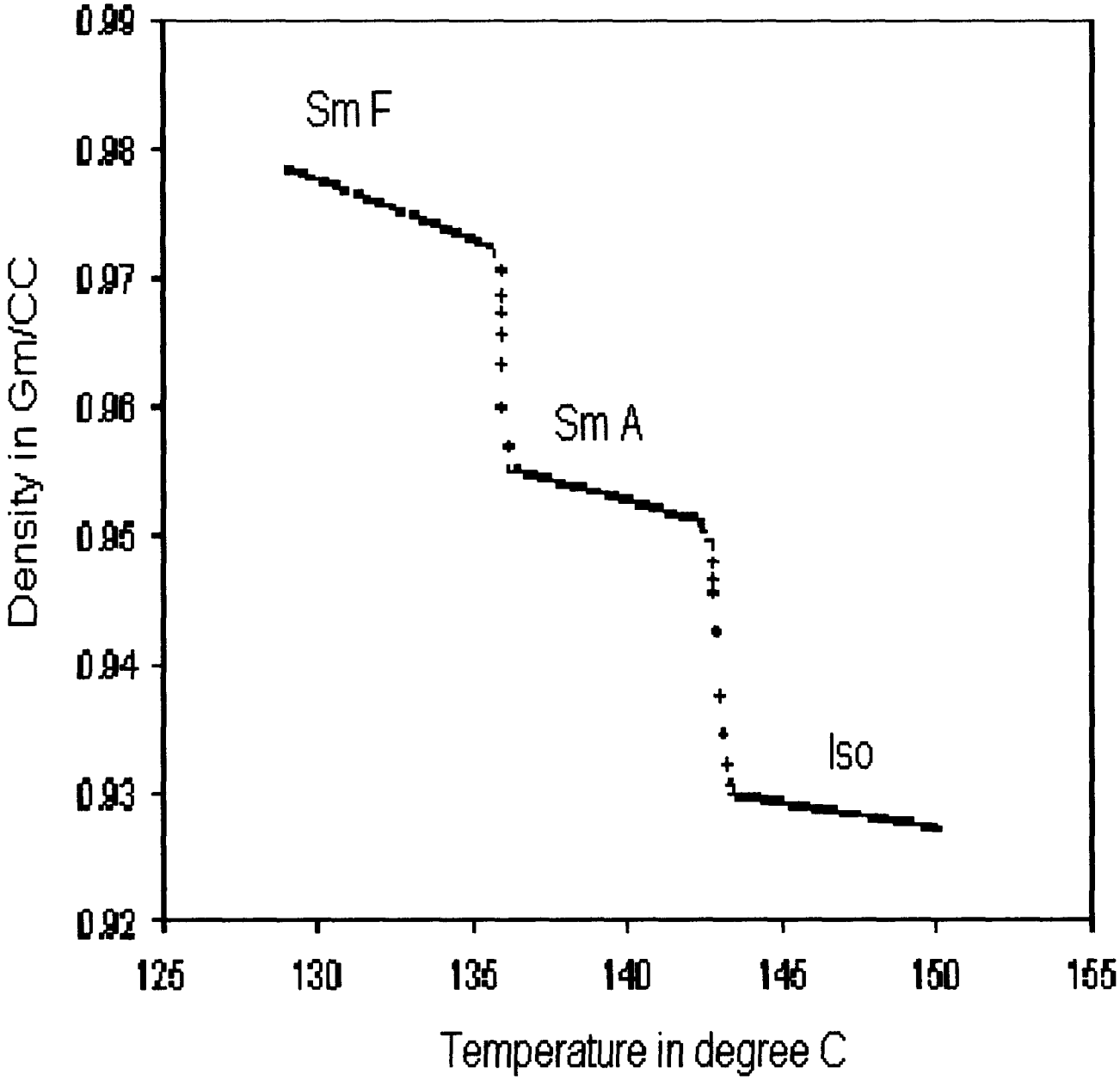

Fig 3.2e. Variation of density with temperature in isotropic, Sm A and Sm F phases for 10.O10O.10.

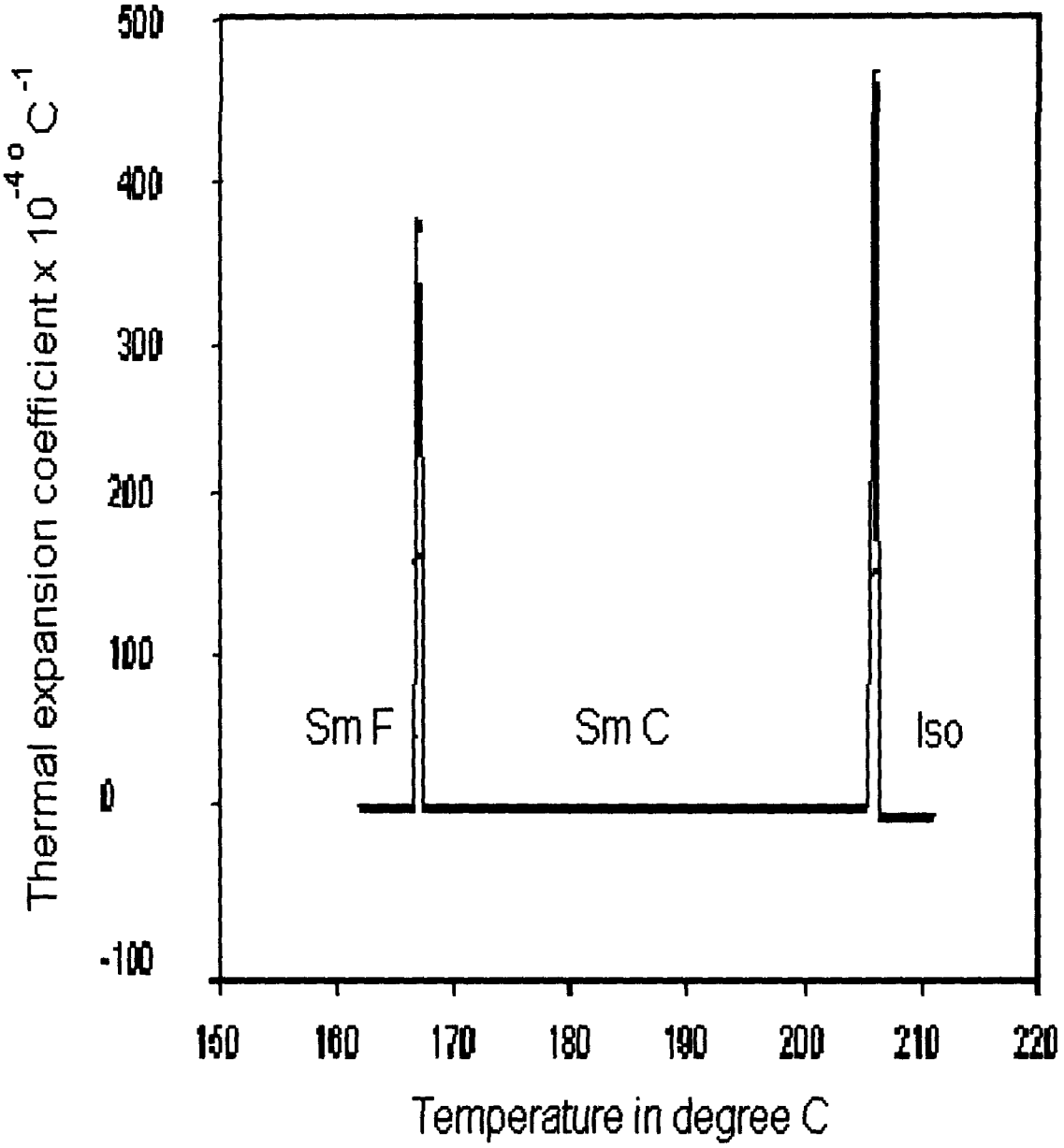

Fig 3.2f. Variation of thermal expansion coefficient with temperature in isotropic, Sm C and Sm F phases for 10.O4O.10.

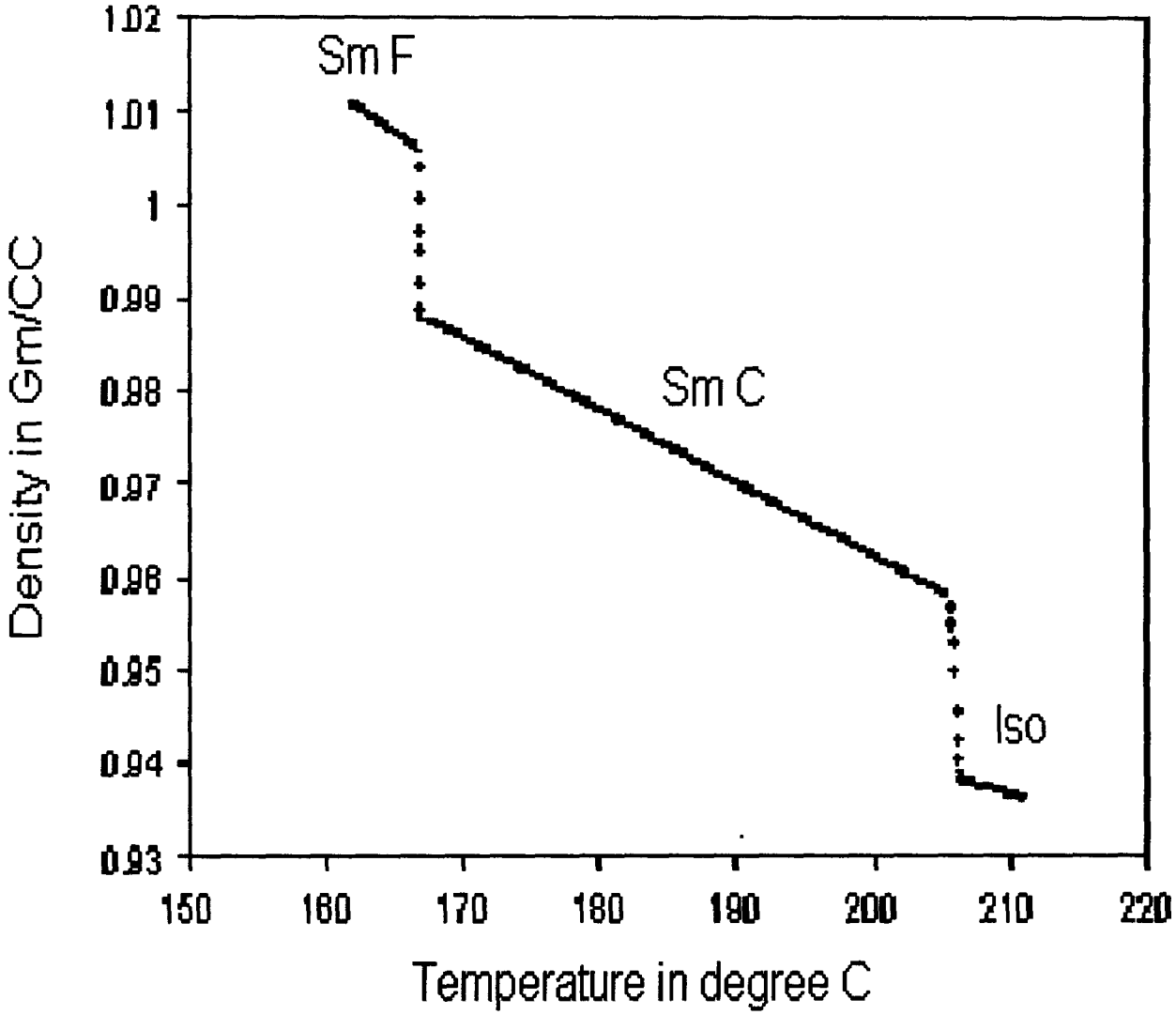

Fig 3.2g. Variation of density with temperature in isotropic, Sm C and Sm F phases for10.O4O.10.

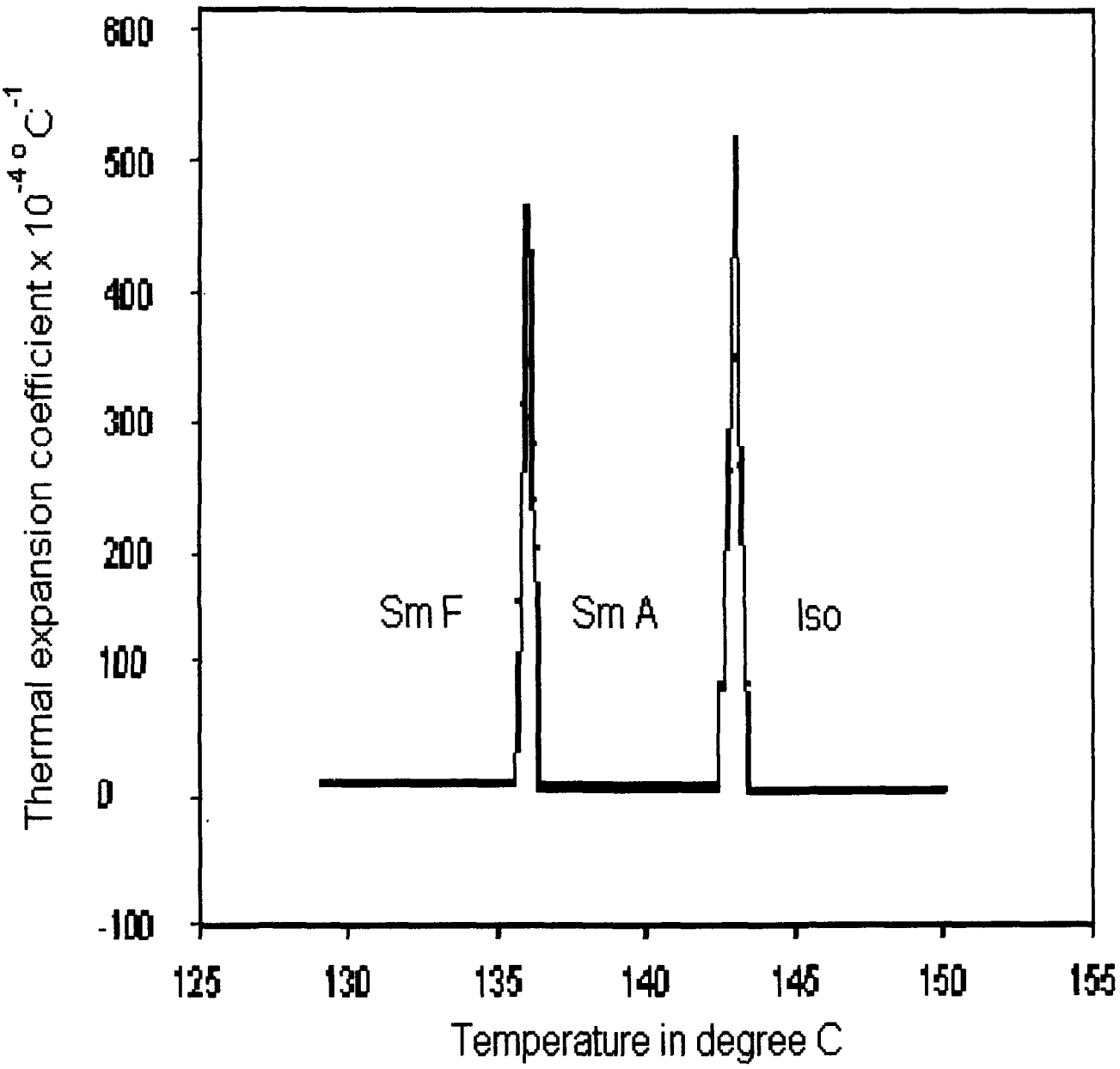

Fig 3.2h. Variation of thermal expansion coefficient with temperature in isotropic, Sm A and Sm F phases for 10.O10O.10.

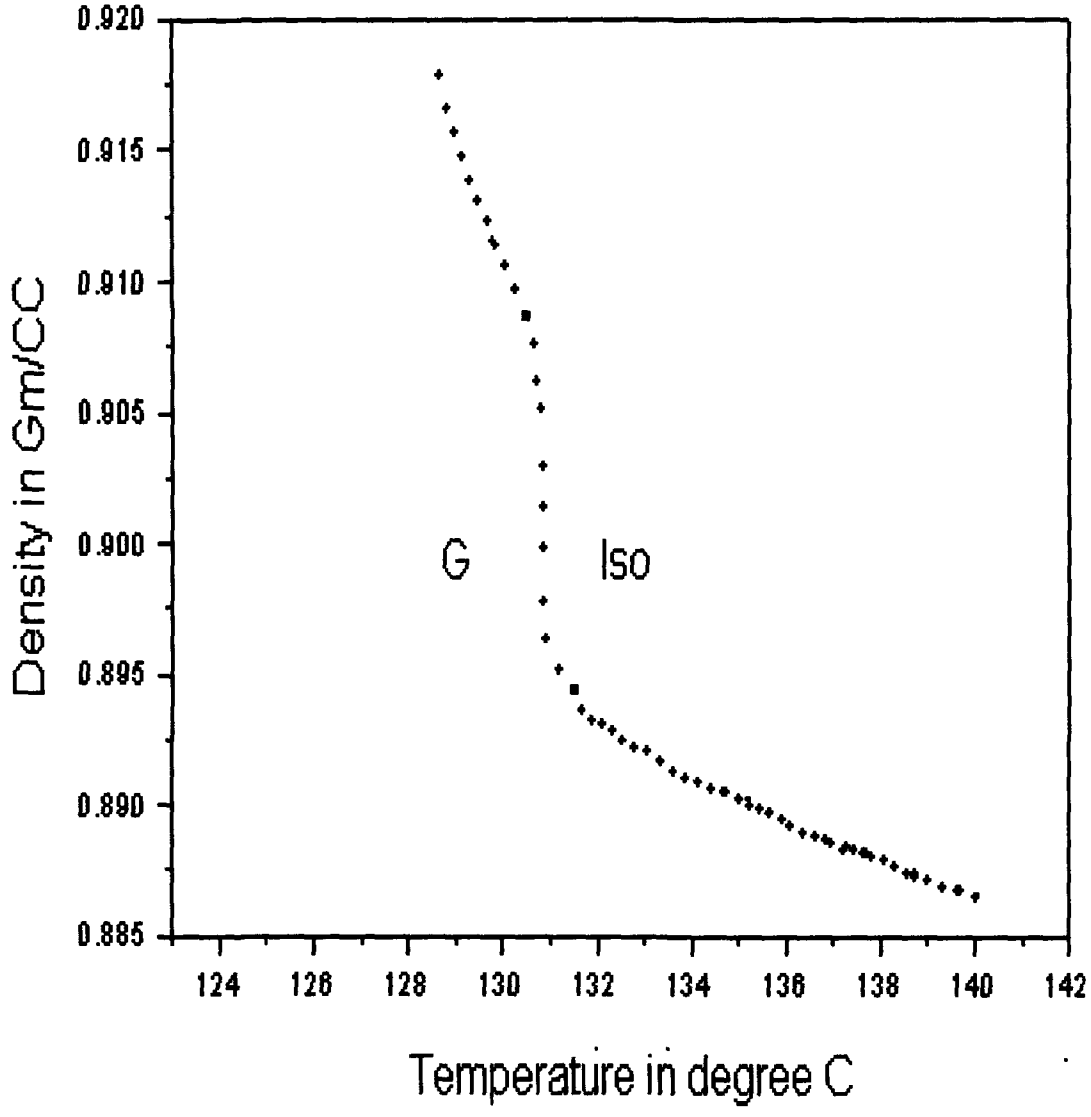

Fig. 3.2j Variation of density with temperature from isotropic to G phase in 10.O12O.10

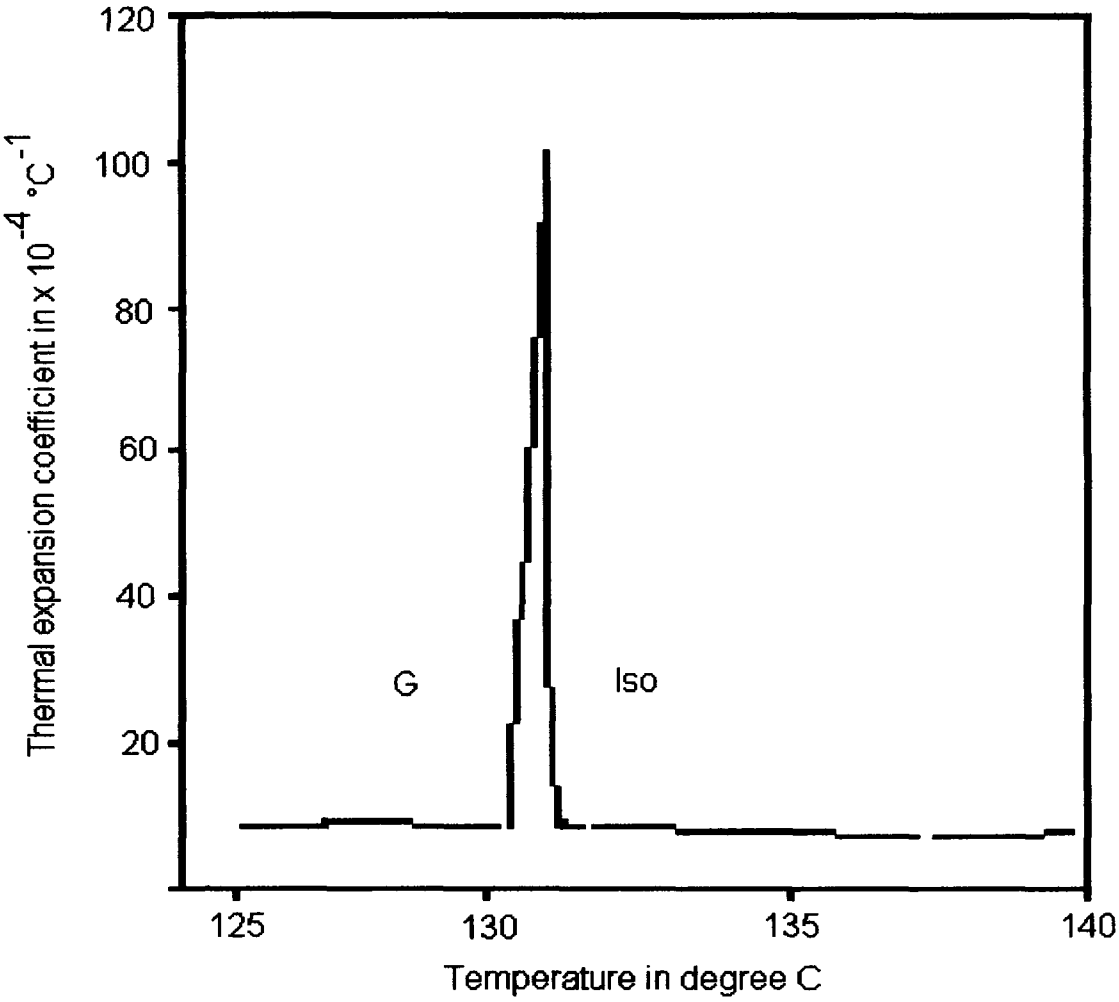

Fig. 3.2k. Variation of thermal expansion coefficient with temperature in isotropic to G phases of 10.O12O.10

CHAPTER - 4

ABSTRACT :

Laser Raman studies on two compounds of the α,ω-bis(4-alkylaniline benzylidene -4′-oxy)alkane series were carried out in the spectral regions of 1140 – 1220 cm $^{-1}$ and 1550 – 1650 cm $^{-1}$ as a function of temperature. Compounds, 7.O4O.7 and 7.O5O.7, exhibit Sm A and Sm F phases. The structural differences of these liquid crystal dimers having odd and even number of carbon atoms in the spacer have been remarkably exhibited in the room temperature Raman spectra. The results are explained on the basis of the bending dynamics of these compounds, and its manifestation in the odd – even effect at the molecular level by assuming a semi-rigid core region of the dimeric molecule and it is found that the odd spacer dimer (7.O5O.7) satisfies the molecular model, whereas the even spacer dimer (7.O4O.7) is established to behave like monomeric compounds such as nO.m. In both the cases, the dynamical changes around the C = N bond have a profound effect on the molecular shape in different phases and phase behaviour.

4.1. INTRODUCTION

Dimeric liquid crystals are formed by linking two mesogenic groups by an alkyl chain (spacer). The liquid crystal dimers have attracted a great deal of interest in recent years, both theoretically and experimentally, due to their unusual properties as compared to the low molar mass liquid crystals. They serve as model compounds for semi -flexible main - chain liquid crystal polymers [1-8]. These dimers are classified into two categories : symmetric dimers and non – symmetric dimers. In the former class of dimers, both of

the mesogenic groups are identical whereas in the later, the mesogenic groups are different. The nematic – isotropic phase transition temperature in these dimeric compounds exhibit a marked alternation as the number of carbon atoms in the alkyl spacer changes from odd to even. However, these changes decrease as the spacer grows in length. In contrast, the variation of entropy of the nematic – isotropic phase transition is essentially unattenuated, at least for spacers containing upto twelve carbon atoms [9]. In addition, the entropy changes at the nematic – isotropic phase transition for dimers with odd chain length spacers is comparable to that of monomers while for compounds containing even chain length spacers, the translational entropy suggests that the orientational order for even spacers should be significantly greater than that for odd spacer dimers.

Although, detailed studies on dimeric liquid crystals have been conducted using various techniques such as XRD, NMR, ESR and Dilatometry [1-12], a thorough investigation to understand the origin of the interesting behaviour at molecular level has not been reported so far to the best of our knowledge.

Raman spectroscopy has proved to be a very powerful technique in the investigation of the dynamics of liquid crystalline compounds, because in this technique not only does one obtain information that is bond specific, but the changes at the microscopic level are also observed as measurable quantities [13 -15]. The spectra – structure correlation as well as the connection between structural changes at the phase transition and the corresponding changes in Raman spectra are of particular interest. These correlations have been very effectively used to obtain information on the liquid

crystals at the molecular level such as molecular orientation/rotation, intra and inter molecular interactions etc.

In the present chapter, a systematic study using Raman spectroscopy on two liquid crystal dimers of the homologues series α-ω-bis(4-alkylanilinebenzylidene -4'-oxy)alkane (hereafter referred to as m.OnO.m) as a function of temperature has been carried out. The compounds 7.O4O.7 and 7.O5O.7 were selected for our study as both of these compounds exhibit a very rare Sm F – Sm A phase transition. Further, as these compounds differ only by a CH_2 spacer group, we hope to obtain evidence of odd – even effect at molecular level in these dimers.

Our studies reveal that these dimeric liquid crystalline compounds are very different in their properties when compared to those of the monomers. The Raman spectra of these compounds at the room temperature remarkably highlight the odd – even effect. From temperature dependent studies we have explained the very rare Sm F – Sm A phase transition in terms of orientational/rotational changes of the various segments of the molecule. We have also made an effort to understand the bending dynamics of these compounds, and its manifestation in the odd – even effect at the molecular level.

4.2. EXPERIMENTAL DETAILS

The compounds were synthesized following a standard procedure as discussed in literature [1]. The crude product was repeatedly recrystallized from ethyl acetate until the transition temperatures were found to be constant and reproducible. The differential scanning calorimetric studies (DSC) were carried out on a Perkin – Elmer DSC – 7.

Various phases exhibited by these compounds were characterized by observing their optical textures under a polarizing microscope attached with an indigenously fabricated hot stage. The temperature resolution in these microscopic studies was 0.1°C. The transition temperatures and entropy change at different phase transitions are found to be in excellent agreement with literature values [1].

The Raman spectra of the samples were recorded at different temperatures on a Spex Ramalog 1403 double monochromator equipped with a RCA – 30134 photomultiplier tube and a CCD detector in the 1140 – 1220 cm^{-1} and 1550 – 1650 cm^{-1} regions. The spectra were recorded over a wide range of temperature starting from 25 °C (crystalline phase) to 212 °C (isotropic phase) for 7.O4O.7 and 145 °C for 7.O5O.7 at an interval of 0.3°C near phase transitions and at 2°C intervals elsewhere. For recording the temperature dependent Raman spectra of the samples, two different thermal set- ups were used. In the first set-up, the sample was placed in a small well of 2 mm diameter and depth of 1mm which was drilled in a square glass slide. This slide was mounted on the FP82 hot stage of the Metler FP900 thermo system. The temperature stability in this system was maintained to an accuracy of ±0.1 °C. However, this sample was found to be sensitive to laser heating, the experiments were also repeated by confining the sample in a 0.8 mm diameter quartz capillary sealed at both ends in an inert atmosphere and then placed in an indigenously fabricated high temperature glass cell. The temperature of this cell could be maintained to an accuracy of ±0.2°C and a copper-constantan thermocouple was placed in close contact with the sample to continuously monitor the temperature. The excitation source used was the 488.0 nm Ar^{+} laser. In order to avoid the laser heating of

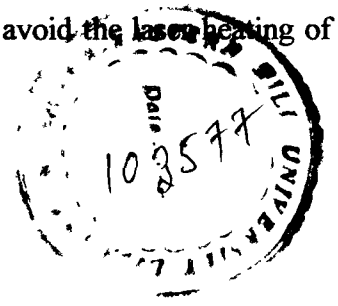

the sample, very low laser power (20 –30 mW) was employed. A scanning increment of 0.3 cm^{-1} with an integration time of 1 second were found suitable to record the spectra with a reasonably good signal to noise ratio with a slit combination of 200 – 400 – 400 – 200 μm. Our data had a very high reproducibility with the uncertainty in peak positions being within ±0.20 cm^{-1} for sharp peaks while the band areas and linewidth (FWHM) being accurate within ±2%. The spectra obtained from both the temperature control set-ups were found to be highly consistent with respect to each other. As the spectral parameters, viz., peak positions, linewidths and integrated intensity were required to be precisely measured, the laser plasma lines were recorded at the same slit setting as used for recording Raman spectra to eliminate the slit width effects. A small attachment called 'lasermate' was used to eliminate the spurious plasma lines from the spectra. In order to calculate the slit function, a few spectra were re-recorded without the lasermate. The slit function, S = 2.62 cm^{-1} was calculated as the full width at half maxima (FWHM) of the plasma line recorded at 1576.60 cm^{-1} from the Ar^{+} laser. In an ideal case, the plasma line should be very close to the position of the Raman band of interest. To approach the bands under study as closely as possible, two more plasma lines at 1138.8 cm^{-1} and 1172.5 cm^{-1} from the Ar^{+} laser were recorded. The FWHM of these two lines were also found equal to 2.62 cm^{-1}. This value of the slit function was used in fitting the curves and determining their linewidths. The curve fitting, deconvolutions of the various spectral parameters were carried out using the GRAMS software.

4.3. RESULTS AND DISCUSSION

The molecular structures of 7.O4O.7 and 7.O5O.7, their phase sequences and transition temperatures are shown in Fig. 1. The molecule can be broadly divided into three parts. There are two mesogenic groups, M and M′ where benzene rings are connected by a flexible spacer, S. Earlier studies have considered the region of MSM′ as a semi-rigid core [1,9]. Both of the 7.O4O.7 and 7.O5O.7 molecules also contain C_7H_{15} terminal alkyl chains, (T and T′) which are attached to the two ends of the mesogenic segments M and M′.

As we are interested in investigating the effects of increased spacer length on the mesogenic region, we concentrated on spectral measurements in two regions, viz., 1140 – 1220 cm^{-1} and 1550 – 1650 cm^{-1} in which Raman bands from the functional groups of spacer are expected. Another reason for selecting these spectral regions is the fact that the bands in these regions are comparatively strong and isolated. Bands in the other regions, like the 2800 – 3200 cm^{-1} due to the alkyl chain modes were extremely weak. Moreover, as these alkyl chains are present in both the spacer as well as the tail regions of the molecules, only average information would be obtained from measurements in this region.

4.3.1. Comparison of Room Temperature spectra of 7.O4O.7 and 7.O5O.7

The Raman spectra of 7.O4O.7 and 7.O5O.7 at room temperature in the 1140 –1220 and 1550 – 1650 cm^{-1} spectral region are shown in Figs. 2(a) and 2(b), respectively. The band assignment along with dichroic ratios (ratio of intensity of the bands with the parallel and perpendicular polarizations) are shown in Table 1. Peak

positions, linewidths and integrated intensities for the 7.O4O.7 and 7.O5O.7 systems in the crystalline state are given in Table 2. The dichroic ratio for all the bands under study are greater than one suggesting some disorder in the individual segments of the molecules. Radical differences are observed between the room temperature spectra of 7.O4O.7 and 7.O5O.7, though the only difference between the two compounds is an extra CH_2 group in the spacer region of 7.O5O.7 molecule. In the Raman spectra of 7.O4O.7, two distinct peaks appear at 1165 and 1172 cm^{-1} whereas in the case of 7.O5O.7, one peak is clearly observed at 1167 cm^{-1} with an overlapped region at 1163 cm^{-1}. Changes are also observed in the 1570 – 1580 and 1590 – 1600 cm^{-1} regions of the spectra. The quadrant stretching modes related to the phenyl rings which appear at 1595 and 1601 cm^{-1} in 7.O4O.7 show an upward shift of few wave numbers and appear at 1597 and 1602 cm^{-1} respectively in case of 7.O5O.7. The band at 1577 cm^{-1} in 7.O4O.7 due to the quadrant stretching mode of the benzene ring splits into two parts in case of 7.O5O.7 with components at 1572 cm^{-1} and 1577 cm^{-1}. The band at 1201 cm^{-1} due to C – N stretching mode for 7.O4O.7 appears at 1195 cm^{-1}, showing a downward shift of 7 cm^{-1} in case of 7.O5O.7. The band due to C = N stretching mode shows a downward shift of 5 cm^{-1} from 1627 cm^{-1} to 1622 cm^{-1} for 7.O4O.7 compared to 7.O5O.7.

To understand these changes, we compare our results with some previous experimental results and theoretical calculations on similar type of dimeric liquid crystalline compounds [1,9]. These studies have shown that the experimentally observed molecular length is less than the calculated all trans molecular length. This has been explained by assuming a bent shape of the molecule about the flexible spacer region.

Also in the model, it is expected that the molecules of the dimeric liquid crystals possess different shapes depending on whether the spacers are odd or even as shown in Fig. 3. Our observations from Raman spectroscopy provide independent support for similar conclusions. The upward shift of the peak position for the phenyl ring related modes indicate an increase in the energy of the various bonds in 7.O5O.7, which suggests that due to change in bending shape, the 7.O5O.7 molecule is capable of attaining energetically favorable arrangement. As regards to the C = N linkage mode, in the case of 7.O4O.7, it appears at 1627 cm^{-1} which is the same position as that in the monomers of nO.m series [16 -17]. It has been experimentally observed that the schiff base monomers of the nO.m series, which are precursors to these dimers, crystalline in a c – centered monoclinic lattice with a two-fold axis along the b- axis. A visual comparison of the X-ray diffraction patterns of 7.O4O.7 and 7.O5O.7 dimers with that of the monomers confirmed the existence of a monoclinic lattice in both 7.O4O.7 and 7.O5O.7. Considering the bent shape structure of 7.O4O.7 and 7.O5O.7 in Fig. 3, we see that the structure of 7.O4O.7 is more or less very similar to the structure of the monomeric compounds of the nO.m series and it shows band positions similar to those of the monomers. In case of bow-like structure of 7.O5O.7 and also given the constraints of the monoclinic lattice, it is possible that either the different segments of the molecule twist along the single bonds or there is some distortion in specific regions resulting in weakening of the bonds. Twisting of the molecule along any of the single bonds such as C – O, Φ - O or Φ - N (Φ = phenyl ring) would have greater impact on the bending shape. This is possible due to the constraints of the monoclinic lattice, the 7.O5O.7

molecule tend to attain a less bent shape and in doing so the C = N and C – N linkages are severely effected. In such cases the peak position of the Raman bands related to these modes are expected to be lowered. This is exactly what is observed in our studies where the C = N stretching mode appears at 1622 cm^{-1} instead of 1627 cm^{-1}. We also see that C = N linkage plays significant role in the bent shape of the spacer. This is also supported by the changes that are observed in linewidths and integrated intensities of the various bands. For the band related to the C – N linkage, a large change in linewidth is observed from 6.65 to 11.7 cm^{-1} while the integrated intensity shows only a small change. For the C = N stretching mode at 1627 cm^{-1}, the linewidth shows a small increase but a drastic decrease is observed in the integrated intensity. This decrease in integrated intensity is accompanied by an increase of integrated intensity for one of the C – H in plane bending and one pair of quadrant stretching modes of the benzene ring. This clearly shows that there is a redistribution of the electron cloud from the C = N linkage towards one of the aromatic rings. This further substantiates our conclusion that the bent shape is affected by the C = N linkage. Therefore, in addition to the semi-rigid nature of MSM′ core region, the C = N linkage plays a major role in the bent shape of the spacer.

4.3.2. Crystal – Smectic F Transition

Comparison of Raman spectra of 7.O4O.7 and 7.O5O.7 in the crystalline, Sm F and Sm A phases are shown in Figs. 4 and 5 respectively. The peak positions, linewidths and integrated intensities of different bands in crystal, Sm F and Sm A phases of 7.O4O.7 and 7.O5O.7 are given in Tables 3 (a) and 3 (b) respectively. The crystalline to smectic F (K – Sm F) phase transition in 7.O4O.7 is marked by definite changes in all the spectral

parameters of the system. The nature of the changes in all the spectral parameters, i.e., peak positions, linewidths and integrated intensities occur abruptly indicating a first order nature of this transition. The crystalline phase is characterized by a proper monoclinic lattice. The Sm F phase, on the other hand, is characterized by a hexagonal clusterization of the molecules with a short range ordering. The major difference between these two phases is the hexagonal packing order of the molecules within the layered structure in the Sm F and the crystalline phases. The most significant spectral changes observed at the transition are the appearance of two spectral bands at 1573 and 1576 cm^{-1} in the Sm F phase in contrast to a single peak at 1577 cm^{-1} in case of the crystalline phase. Another major change observed in the Sm F phase is a drastic shift of the peak position of the band associated with the C – N mode from 1201 cm^{-1} in crystalline phase to 1191 cm^{-1} in the Sm F phase. The band associated with the C – O stretching mode at 1172 cm^{-1} also exhibits a shift towards the lower wave number side by 5 cm^{-1}, shifting from 1172 cm^{-1} in the crystalline phase to 1166 cm^{-1} in the Sm F phase. The C – H in plane bending mode of the aromatic ring as also the quadrant stretching modes show small changes in peak position towards the lower wave number region in the crystalline state, which appear as overlapped region in the Sm F phase. The changes in integrated intensity during this phase transition are also large. In general, line widths of almost all the bands show an increase, but the integrated intensities show quite irregular changes. The relative intensity of the band at 1162 cm^{-1} shows a major change when compared to 1166 cm^{-1} band in case of Sm F phase. All these changes when correlated suggest that due to the relaxation of the lattice constraints of the crystalline solid phase and attainment of the layered structure,

some deformations occur in the molecule along the C – N and C – O single bond regions of the molecule. Also, the molecule can be considered to have a double mesogenic core, the short range ordering in the Sm F phase results in rotation along the said single bond regions which, in turn, causes change in the peak position of the C = N stretching mode. The changes in the molecule suggest a shape which is more or less similar to that of the monomeric liquid crystals.

The crystalline – Sm F phase transition in 7.O5O.7 occurs while cooling the sample through 88°C from the Sm F phase (monotropic Sm F Phase). In this case, the major changes in the peak position are observed for the 1167 cm^{-1} phenyl ring in plane C – H stretching and the four quadrant stretching modes at 1572, 1577, 1597 and 1602 cm^{-1}. For the C – N mode at 1195 cm^{-1}, a downward shift is observed in the Sm F phase where it appears at 1192 cm^{-1}. Simultaneously, the C = N stretching mode at 1622 cm^{-1} in the crystalline phase appears at 1625 cm^{-1} in the Sm F phase exhibiting an upward shift of 3 cm^{-1} (Table 3). The C – O stretching mode, on the other hand, shows minimal changes. However, the changes in integrated intensity and linewidths show large changes in all the bands. All the changes observed at the crystalline - Sm F phase transition of 7.O5O.7 show that the semi rigid bow like shape is possible for this molecule, but still there are changes in the C = N linkage regions which tend to straighten the molecule.

4.3.3. Sm F – Sm A phase transition

The Sm F – Sm A phase transition in 7.O4O.7 is marked by an abrupt change in peak positions, integrated intensities and linewidths of the different bands in the spectra

indicating the first order nature of the transition. The Sm F phase has a c – centered monoclinic lattice with strong in-plane short-range positional correlation and almost negligible interlayer positional correlation. The molecules in this phase are tilted with respect to the layer planes and are packed in pseudo-hexagonal clusters. The Sm A phase is characterized by a one-dimensional density wave whose wave vector is along the molecular director. It has a layered structure and maintains translational invariance within the smectic layer planes. The Sm A phase is disordered and possesses only short range ordering between the molecules without existence of any packing order. The Sm F – Sm A phase transition is marked by changes in peak position of all the bands. As is clear from the Table 3a, the peak position of the Raman bands associated with the selected modes show a shift towards the higher side by 2 to 3 cm^{-1} accompanied by the changes in the linewidths and integrated intensities. The increase in the peak positions at the Sm F – Sm A transition is an indication of the increase in the freedom of the individual molecules in the clusters in the Sm A phase. The changes in integrated intensity and linewidth point towards small changes in inter-molecular positional/orientational ordering. Hence, we can conclude that the Sm F – Sm A transition in 7.O4O.7 is a manifestation of a transition between ordered Sm F phase to a disordered Sm A phase. Also, in this transition, it is observed that not only the individual segments, but the molecule as a whole is affected.

The only difference between the 7.O4O.7 and 7.O5O.7 compounds is an extra methylene unit in the spacer region of the molecule. This extra methylene unit has a profound effect on the molecular behavior. Unlike 7.O4O.7, the 7.O5O.7 exhibits

monotropic Sm F phase with a lower transition temperature (only in cooling cycle at 99°C) for the Sm F – Sm A phase transition. The Sm F – Sm A phase transition in 7.O5O.7 is marked by upward shift of peak position by about 2 cm^{-1} when one moves from Sm F to the Sm A phase. However, the position of the band due to the C – O mode remains unchanged in this transition. One of the quadrant-stretching modes of the aromatic ring at 1570 cm^{-1}, however, shows a downward shift to 1569 cm^{-1}. The lower peak position of the different modes in the Sm F phase as compared to the Sm A phase is understood by the hexagonal clusterization and short range ordering in the Sm F phase. The changes in linewidths and integrated intensities are similar to those in 7.O4O.7, which again indicates small changes in the intermolecular orientational ordering. One major difference observed is that the band due to the C – O mode in 7.O5O.7 does not show any change in position suggesting that in the Sm F phase due to hexagonal close clustering and the rigidity of the C – O portion, the bow-like structure of the molecule has become more curved. This acuteness of the bow-like structure of the molecule would result in the individual mesogenic parts to behave in a peculiar way. One can only visualize that the tilting of the bow would result in one mesogenic segment being acutely tilted while the other mesogenic segments will be almost orthogonal due to the rigidity of the C – O region. This would lead to an unusual feature in the Sm F phase, which is neither tilted nor orthogonal. This is exactly what has been found [1,18] in the X-ray diffraction studies where the odd member of this dimer exhibits unusual feature in the diffraction pattern for the Sm F phases.

Spectra in the isotropic phase could not be obtained with consistency and reproducibility as the sample spread very thinly and became susceptible to laser heating and degeneration.

4.4. CONCLUSIONS

This chapter can be concluded by emphasizing that the two members of m.OnO.m homologous series viz. 7.O4O.7 and 7.O5O.7 have a structural dissimilarity in their vibrational Raman spectra though only a methylene unit is the difference in the spacer region of the two compounds. In order to understand the difference in their vibrational Raman spectra, the results have been explained on the basis of the bending dynamics of these compounds, and its manifestation in the odd – even effect at the molecular level by assuming a semi-rigid core region of the dimeric molecule and it is found that the odd spacer dimer (7.O5O.7) satisfy bending structure of the molecular model, whereas in the even spacer dimer (7.O4O.7) the molecular shape is linear. Also, it is found in both the cases that the dynamical changes around the C = N bond have a profound effect on the molecular shape in different phases and phase behaviour.

References

1. Date, R.W., Imrie,C.T., Luckhurst, G. R., and Seddon J.M., 1992, *Liq. Cryst.*, **12,** 203.

2. Heeks, S.K., and Luckhurst, G.R., 1993, *J. Chem. Soc., Faraday Trans.*, **89,** 3289.

3. Attard, G.S., Date, R.W., Imrie, C.T., Luckhurst, G.R., Roskilly, S.J., Seddon J.M.,and Taylor L., 1994, *Liq. Cryst.*, **16,** 529.

4. Date, R.W., Luckhurst, G.R., Shuman, M., and Seddon, J.M., 1995, *J. de Physique II,* **5,** 587.

5. Fletcher, I.D., and Luckhurst, G.R., 1995, *Liq. Cryst.*, **18,** 175.

6. Le Masurier, P.J., and Luckhurst, G. R., 1998, *Liq. Cryst.*, **25,** 63.

7. Blatch, A. E., Fletcher, I. D., and Luckhurst, G. R., 1997, *J. Mater. Chem.*, 7
Blatch, A. E., and Luckhurst, G. R., 2000, *Liq. Cryst.*, **27,** 775.

8. Barnes, P.J., Douglas, A.G., Heeks, S.K., and Luckhurst, G.R., 1993, *Liq. Cryst.*, **13,** 603.

9. Ferrarini, A., Luckhurst, G. R., Nordio, P. L., and Roskilly, S. J., 1993, *Chem. Phys. Lett.*, **214,** 3.

10. Alapati, P. R., and Luckhurst, G. R. (unpublished results)

11. Gogoi, B., Arulsankar, A., and Alapati, P. R., 2001, *Mol. Cryst. Liq. Cryst.*, **366,** 69.

12. Gogoi, B., Arulsankar, A., Ghosh, T. K., and Alapati, P. R., 2001, *Mol. Cryst. Liq. Cryst.* **365,** 561.

13. Fontana, M., and Binni, S., 1976, *Phys. Rev. A.*, **14,** 1555.

14. Dash, S. K., Singh, R. K., Alapati, P. R., and Verma, A. L., 1998, *Liq. Cryst.*, **25,** 459.

15. Dash, S. K., Singh, R. K., Alapati, P. R., and Verma, A. L., 1999, *Liq. Cryst.*, **26,** 1479.

16. Bhattacharjee, A., Alapati, P. R., and Verma, A. L., 2001, *Liq. Cryst.*, **28,** 1315.

17. Bhattacharjee, A., Alapati, P. R., and Verma. A. L., 2002, *Liq. Cryst.*, **29**, 725.

18. Gogoi, B., and Alapati, P. R., (unpublished results)

Table 4.1 Band assignment and dichroic ratio for the different Raman bands of 7.O4O.7 and 7.O5O.7 liquid crystals.

7.O4O.7			7.O5O.7	
Band position	Dichroic Ratio	Band Assignment	Band position	Dichroic Ratio
1165	1.50	Aromatic C – H in plane bending mode	1167	1.19
1172	1.61	C – O Stretch	1172	1.37
1201	1.41	Aromatic C – N stretching mode	1195	1.17
		Quadrant stretching mode of the Aromatic ring	1572	1.19
1577	1.87	- do -	1577	1.22
1595	1.63	- do -	1597	1.13
1602	1.21	- do -	1602	1.14
1627	1.40	- do -	1622	1.31

Table 4.2 The peak positions, linewidths and integrated intensities of selected Raman bands for 7.O4O.7 and 7.O5O.7 at room temperature (crystalline phase)

7.O4O.7	PP	1165	1172	1201	-	1577	1595	1601	1627
	LW	3.95	5.74	6.65	-	6.85	7.41	7.08	7.01
	I I	28.33	36.39	35.28	-	9.28	11.43	49.96	29.33
7.O5O.7	PP	1167	1172	1195	1572	1577	1597	1602	1622
	LW	7.05	3.91	11.73	7.99	3.90	7.87	9.92	9.22
	I I	50.64	14.40	34.94	20.60	12.92	20.28	25.23	20.97

PP – Peak Position; LW – Line Width; I I – Integrated Intensity

Table 4.3a The peak positions, linewidths and integrated intensities of selected Raman bands for 7.O4O.7 at Crystalline, Sm F and Sm A phases.

Crystalline Phase (K)			Sm F Phase			Sm A Phase		
PP	LW	I I	PP	LW	I I	PP	LW	I I
1165	3.95	28.33	1162	10.07	44.89	1163	8.7	36.75
1172	5.74	36.39	1166	6.71	28.31	1168	7.46	34.32
1201	6.65	35.29	1191	10.24	26.79	1193	10.24	28.93
-	-	-	1573	10.43	10.53	1576	8.56	7.54
1577	6.85	9.28	1576	5.76	6.19	1578	4.45	4.98
1595	7.41	11.43	1594	11.20	31.82	1596	9.31	30.36
1602	7.08	49.96	1598	10.57	28.00	1600	10.38	29.35
1627	7.01	29.33	1625	12.05	23.46	1627	10.27	27.28

PP - Peak position; LW – Line Width; I I – Integrated Intensity

Table 4.3b The peak positions, linewidths and integrated intensities of selected Raman bands for 7.O5O.7 at Crystalline, Sm F and Sm A phases.

Crystalline Phase			Sm F Phase			Sm A Phase		
PP	LW	I I	PP	LW	I I	PP	LW	I I
1167	7.05	50.64	1163	9.22	25.31	1165	8.39	45.29
1172	3.91	14.40	1171	5.59	45.79	1172	6.45	28.21
1195	11.73	34.94	1192	7.65	28.89	1193	9.15	26.50
1572	7.99	20.60	1570	7.83	11.20	1569	7.09	9.30
1577	3.90	12.92	1575	4.07	5.15	1576	4.73	5.26
1597	7.87	20.28	1594	5.86	25.09	1595	9.48	28.29
1602	9.92	25.23	1598	10.15	35.00	1600	9.64	28.41
1622	9.22	20.97	1625	11.4	33.36	1627	11.05	28.74

PP - Peak position; LW – Line Width; I I – Integrated Intensity

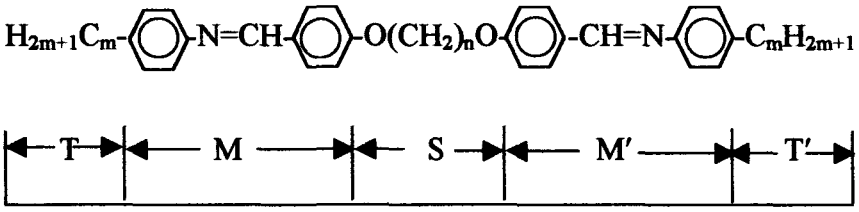

m = 7
n = 4 for 7.O4O.7
n = 5 for 7.O5O.7

Phase and Phase Transition Temperature

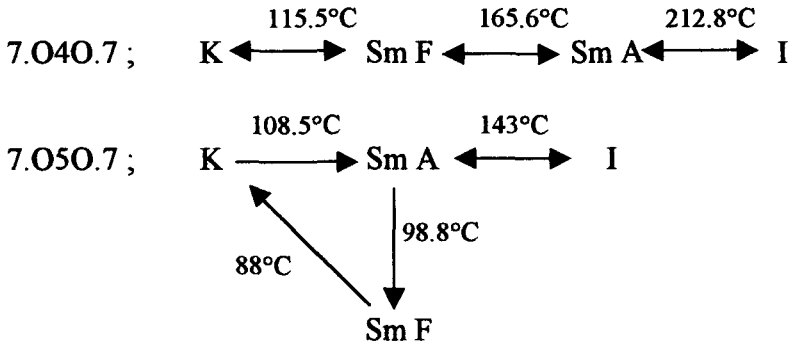

Fig. 4.1 General molecular structure of liquid crystal dimer and phase transition temperatures of 7.O4O.7 and 7.O5O.7

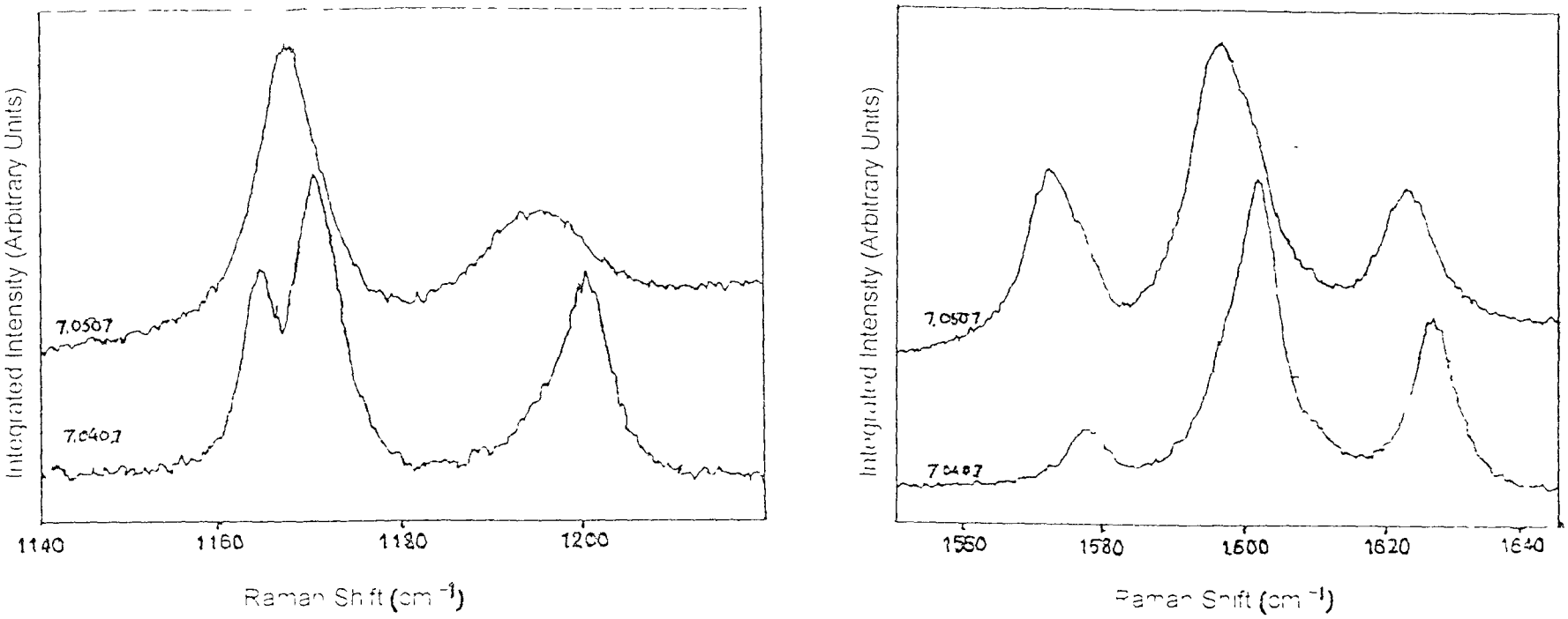

Fig 4.2 Comparison of Raman spectra of 7.040.7 and 7.050.7 in crystalline phase at room temperature in two spectral regions

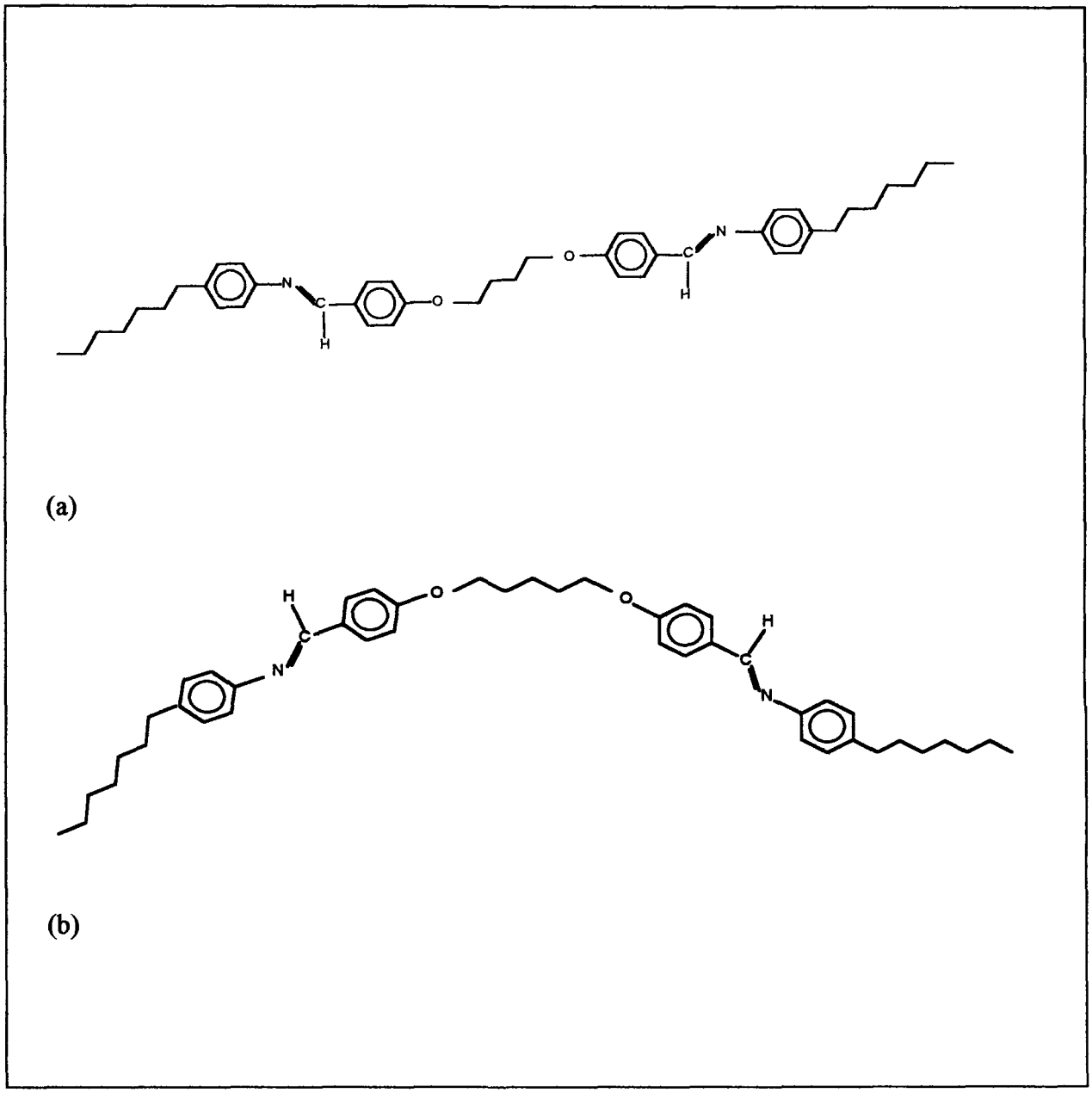

Fig. 4.3. Molecular shape of (a) 7.O4O.7 and (b) 7.O5O.7

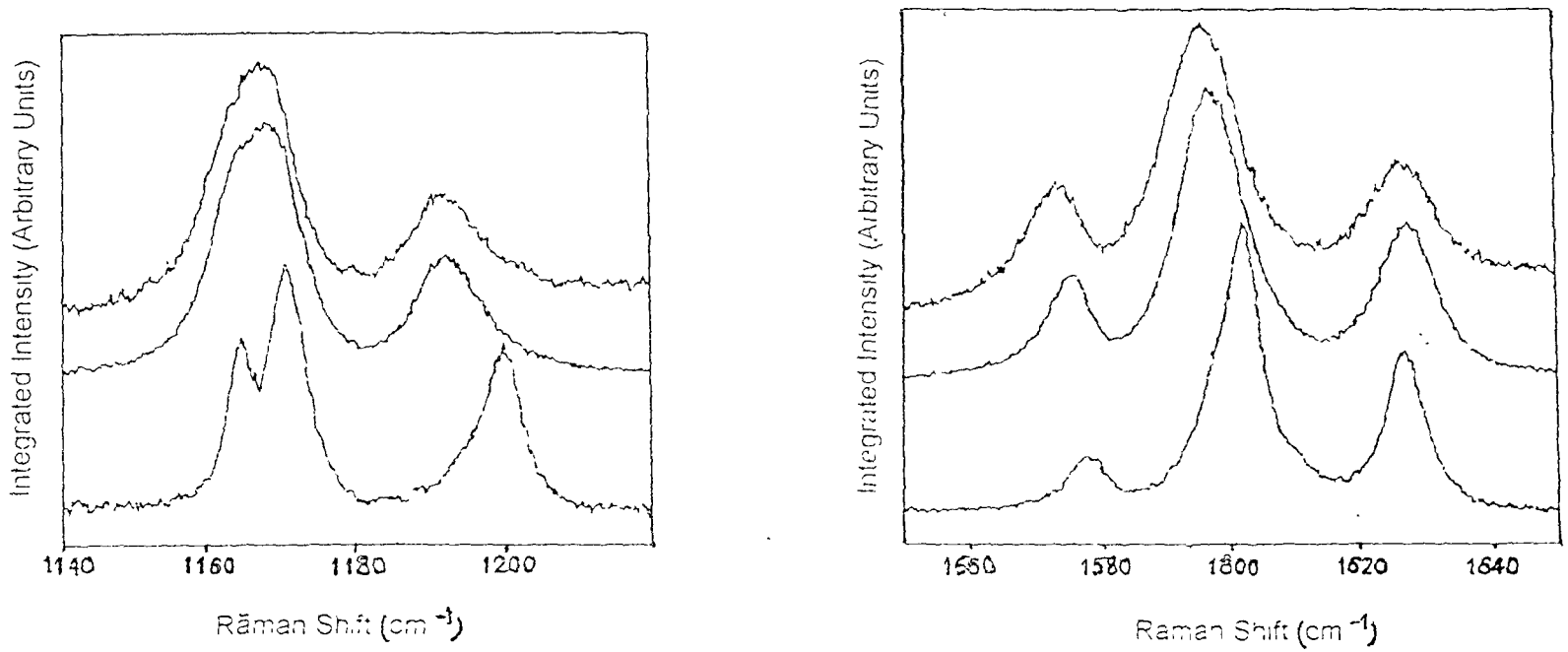

Fig 4 4 Comparison of Raman spectra of 7 C4O 7 in crystalline Sm A and Sm F phases in two spectral regions

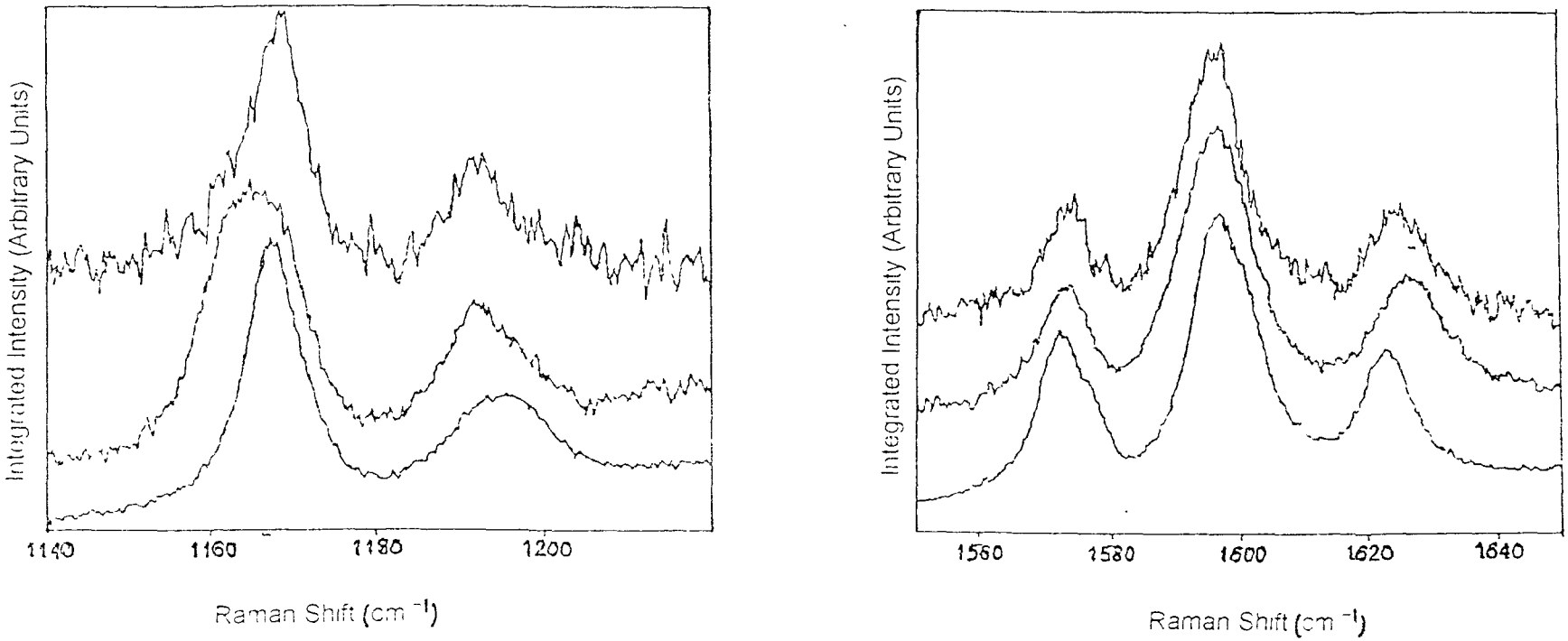

Fig. 4.5 Comparison of Raman spectra of 7 O5O 7 in crystalline Sm A and Sm F phases in two spectral regions

CHAPTER - 5

ABSTRACT:

Terepthalylidene-bis-p-n-alkylanine, popularly known as TBAA homologues series is one of the well-known and interesting series of schiff base liquid crystalline compounds for its rich variety of polymesomorphism with wide thermal ranges. One of the many interesting aspects of these series of compounds is the existence of two or three second order phase transitions (Sm A – Sm C, Sm I - Sm F, Sm F - Sm G) in addition to the first order transitions (I - Sm A, Sm C - Sm I, Sm G - K) in a single compound. However, the TBNA and TBDA, higher homologues of the TBAA series, are the only examples of non-ferroelectric thermotropic liquid crystals which exhibit a weakly first order Sm A – Sm C phase transition, whereas the TBBA, the lower homologue exhibits a clear second order Sm A – Sm C phase transition within the series. These findings imply the existence of a tricritical point, where a first order transition becomes second order transition. In order to investigate the tricritical point (TCP) of Sm A – Sm C phase transition, binary mixtures of TBBA and TBDA of different weight percent of few compositions have been studied with the variation of density as tricritical point is approached using DSC and density measurements as a function of temperature.

5.1. INTRODUCTION

The smectic A to smectic C phase transition has received considerable attention in both theoretically and experimentally for last the few decades. The Sm A and Sm C phases may be simply described as orientationally ordered fluids with the existence of one dimensional mass-density wave [1]. The wave may be either along (Sm A) or at an

angle (Sm C) with respect to the molecular director. The Sm A – Sm C phase transition involves the growth of a tilted ordering of molecules in the Sm A layered structure resulting in a biaxial Sm C phase. In general, the Sm A – Sm C phase transition is found to be a second order transition in almost all the non-ferroelectric thermotropic liquid crystals. De Gennes [1] proposed a simple model which places this transition in the universality class of superfluid helium, but, subsequent studies [2-8] have clearly shown that the Sm A - Sm C (or Sm A – Sm C^*) transition is mean-field like with a sixth-order term in Landau free energy expansion describing the Sm C order parameter. As first pointed out by Huang and Viner [8], the presence of sixth order term implies that the mean-field like Sm A- Sm C transition is always close to a mean-field tricritical point with a concomitant existence of a "cross over" behavior from a mean-field like region to tricritical- like region. However, the existence of a first order as well as second order Sm A – Sm C transition has been reported recently [9-12] in both ferroelectric and non-ferroelectric thermotropic liquid crystals. The Sm A – Sm C tricritical points have also been reported [13-19] either as fluctuations mediated weak first order Sm A – Sm C transitions or weakly first order transitions due to the strong coupling between the chiral group to the orientational order, or due to the narrow Sm A range and also in the vicinity of N - Sm A - Sm C multicritical points.

The tricritical behavior of phase transitions, where a particular phase transition goes over from first order to second order, has been studied extensively in various systems, viz. metamagnet [20], He^3 – He^4 mixtures [20 - 21], superconductors [22] and liquid crystals. So far, in the liquid crystal systems, the tricritical point of N – Sm A and

Sm F – Sm I phase transition has been extensively studied by changing the length of the alkyl end chains [15, 23], varying the concentration in binary mixture [24] and increasing the pressure [25] etc. However, we have selected Sm A – Sm C tricritical point studies and observed the tricritical point by varying the concentration of binary mixtures of compounds: one exhibiting a first order Sm A – Sm C transition and the other exhibiting a second order transition. Higher homologues of TBAA series of compounds, viz. TBDA and TBNA exhibit first order/weakly first order Sm A – Sm C transition [11-12] while TBHA (H indicates heptyl) and TBBA exhibit a second order transition. We present here the systematic study of Sm A – Sm C tricritical point (TCP) of the binary mixtures of TBDA and TBBA at different weight percent using Differential Scanning Calorimetry (DSC) and density studies. The only other study of the Sm A – Sm C tricritical point in TBAA homologues series was reported by Prasad et al [14] using x-ray diffraction studies on binary mixtures of TBDA and TBOA where they have observed a second order Sm A – Sm C transition in TBOA. However, density studies reported earlier confirm this to be a weakly first order transition in TBOA [15]. For this reason we have chosen to study binary mixtures of TBBA and TBDA, where TBBA has been well established to exhibit a second order Sm A – Sm C phase transition

The present chapter describes and emphasizes to find out the TCP from the phase diagrams of Sm A – Sm C transition using Polarizing thermal microscopy and DSC, entropy change at the transition and Navard – cox parameter as a function of weight percent of TBDA in TBBA. Secondly, study of the density as a function of temperature at

different weight percent of TBDA and TBBA mixtures for determining the tricritical point at Sm A – Sm C phase transition was also carried out.

5.2. EXPERIMENTAL DETAILS

The molecular structure of the compounds, TBBA and TBDA is given below.

(TBBA)

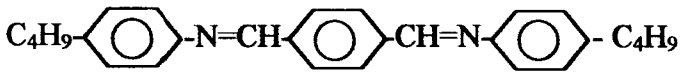

(TBDA)

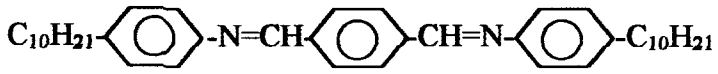

The compounds, TBBA and TBDA were synthesized following the standard procedure as discussed in chapter 2. The different mole percent for TBDA and TBBA was accurately weighted and combined together and refluxed with ethanol-benzene mixture as a solvent. The solvent was fully removed under vacuum using a rotary evaporator. The transition temperatures and transition entropies were determined by using Perkin-Elmer DSC-7. Various phases exhibited by the mixtures were identified by observing their textures under a polarizing microscope attached with an indigenous hot stage. The temperature resolution of the hot stage attached with the microscope was 0.1° C. The density measurement was carried out with a bicapillary pyknometer. The diameter of the capillary of the pyknometer was about 0.35 mm and the accuracy in the

density measurement was ±0.1Kg m^{-3}. The permitted cooling rate was 2 °C hr^{-1} and temperature accuracy was ±0.1°C.

DSC scans for the pure TBBA and TBDA compounds are shown in Fig. 5.1. The compound TBBA exhibit enantiotropic Sm G, Sm C, Sm A, N phases and TBDA exhibits Sm H, Sm G, Sm F, Sm I, Sm C, Sm A phases. As we are interested in studying the tricritical point of Sm A – Sm C transition, the phase diagram of the binary mixtures of TBBA + TBDA was studied involving the transition from isotropic liquid to Sm A – Sm C transition. The compositions of TBBA + TBDA for this purpose include on both sides of the TCP observed. Lower temperature part of the phase diagram has not been studied in detail. The phase diagram studied is shown in Fig. 5.2. The isotropic – Sm A and Sm A – Sm C phase transition temperatures and entropy change (ΔS/R) at these transitions in seven compositions of mole percent of TBDA in TBBA are presented in Table 5.1

5.3. DSC STUDIES

The DSC studies indicate a small but noticeable transition entropy for few mixtures of TBDA (100%, 93.55%, 85.15% and 82.80%) in TBBA and no entropy change for the rest of the compositions. However, the smooth variation of entropy change at the Sm A – Sm C transition in different mixtures indicates the existence of Tricritical point near 81% of TBDA in TBBA. The variation of entropy change as a function of weight percent of TBDA in TBBA is shown in Fig. 5.3. The variation of entropy change (ΔS/R) at Sm A – Sm C transition as a function of scaled parameter, T_{AC}/T_{IA} (where T_{AC} is the Sm A – Sm C and T_{IA} is the I – Sm A transition temperature) similar to Mc Millan

parameter for N – Sm A transition is shown in Fig. 5.4. It appears that the cross over of the first order to second order transition takes place at a T_{AC}/T_{IA} value of 0.960. The Navard-cox parameter, $N = h_2/h_1$, where h_1 and h_2 are the height of the DSC transition peaks obtained at the Sm A – Sm C transition with two different temperature scanning rates: one (h_2) being twice the other (h_1) keeping the weight of the compounds constant are $1 \leq N \leq \sqrt{2}$ for an isothermal first order transition, equals 2 for a second order transition [25]. The variation of N ($=h_2/h_1$) as a function of weight percent of TBDA is shown in Fig. 5.5. A constant value of N = 2 for mixtures lower than 80.05% TBDA indicates that the transition is second order whereas the smooth decrease of N value from 2 at 80.05% TBDA to 1.34 at 100% TBDA indicates that the transition becomes weakly first order in mixtures above 80.05% of TBDA. Therefore, the existence of TCP for Sm A – Sm C transition is established in 80.05% TBDA in TBBA at a T_{AC}/T_{IA} value of 0.959. The values of T_{AC}/T_{IA} for other compositions of TBDA+TBBA are shown in Table 5.2.

5.4. DENSITY MEASUREMENT STUDIES

The variation of density as a function of temperature in six binary mixtures of TBDA and TBBA, viz. 93.55%, 85.15%, 82.80%, 81.06%, 80.05% and 75.39% of TBDA in TBBA are shown in Figs. 5.6 [a, b, c, d, e and f respectively]. A small but noticeable density jumps ($\Delta\rho/\rho\%$) of 0.21% for the mixture 93.55% TBDA, 0.12% for the 85.15% TBDA and 0.08% for 82.8% are observed at the Sm A – Sm C transitions indicating that the transition weakens further from TBDA as the percent of TBBA is increased. Further, a small co-existence region of Sm A and Sm C phases was observed

at the transition in these mixtures. These values are in good comparison with the density jump ($\Delta\rho/\rho\%$) at Sm A – Sm C transition in pure TBDA and TBNA, where it was 0.39% and 0.13% respectively [11-12]. No density jump was observed at the transition for the remaining mixtures studied indicating that the transition is second order. However, the transition is indicated by a very small change in slope of the density curve at the Sm A – Sm C transitions.

The results of the above studies envisage the decisive role played by Sm A thermal range in determining the nature of Sm A – Sm C transition and governing the TCP, since the transition becomes weakly first order as the thermal range of Sm A decreases. The TCP for TBOA was reported at the thermal range of 9.4°C [15], which is much lower than that of our TBDA+TBBA mixture (present study) where the Sm A thermal range is about 17°C.

5.5. CONCLUSIONS

In conclusion, the binary mixtures of TBBA and TBDA of different weight percent of few compositions have been studied as tricritical point (TCP) is approached. The results of these studies clearly suggest the decisive role played by the Sm A thermal range in determining the nature of the Sm A – Sm C transition that the transition becomes weakly first order as the thermal range of Sm A decreases. The existence of TCP in the binary mixtures of TBBA + TBDA is established at 80.05% weight percent of TBDA in TBBA at a T_{AC}/T_{IA} value of 0.959.

References

1. de Gennes, P. G., "The Physics of Liquid Crystals" Clarendon, Oxford, 1974
   Litster, J. D. and Birgeneau, R. J., *Phys. Today*, **35**, 26, (1982)

2. Safinya, C. R., Kaplan, M., Als-Nielsen, J., Birgeneau, R. J., Davidov, D., Litster, J. D., Johnson, D. L. and Neubert, M., *Phys. Rev. B*, **21**, 4149, (1980)

3. Huang, C. C. and Lien, S. C., *Phys. Rev. Lett.*, **47**, 1917, (1981)

4. Huang, C. C. and Viner, J. M., *Phys. Rev. A*, **25**, 3385, (1982)

5. Birgeneau, R. J., Garland, C. W., Kortan, A. R., Litster, J. D., Meichle, M., Ocko, B. M., Rosenblatt, C., Yu, L. J. and Goodby, J. W., *Phys. Rev. A*, **27**, 1251, (1983)

6. Meichle, M. and Garland, C. W., *Phys. Rev. A*, **27**, 2624, (1983)

7. Dumrongrattana, S., Nounesis, G. and Huang, C. C., *Phys. Rev. A*, **33**, 2181, (1986)

8. Huang, C. C. and Viner, J. M., in "Liquid Crystals and Ordered Fluids" edited by A. C. Griffin and J. F. Johnson (Plenum, New York, 1984), Vol. – 4, pp-643

9. Bahr, Ch. And Fliegner, D., *Phys. Rev. A*, **46**, 7657, (1992)

10. Ratna, B. R., Shashidhar, R., Nair, G. G., Krishna Prasad, S., Bahr, Ch. And Heppke, G., *Phys. Rev. A*, **37**, 1824, (1988)

11. Alapati, P. R., Potukuchi, D. M., Rao, N. V. S., Pisipati, V. G. K. M. and Saran, D., *Mol. Cryst. Liq. Cryst.*, **146**, 111, (1987) and references therein

12. Rao, N. V. S., Pisipati, V. G. K. M., Murthy, J. S. R., Rao, P. B. and Alapati. P. R., *Liq. Cryst.*, **5**, 539, (1989)

13. Shashidhar, R., Ratna, B. R., Nair,G. G., Krishna Prasad, S, Bahr, Ch and Heppke,G., *Phys. Rev. lett.*, **61**, 547 (1988) and references therein.

14. Prasad, S., Raja, K. V. N., Rao,D. S., Nair, G. G. and Neubert, M. E., *Phys. Rev. A*, **4**, 2479 (1990)

15. Rao, N.V.S., Pisipati, V.G.K.M., and Gouri Sankar, Y., *Mol. Cryst. Liq. Cryst.*, **131**, 237, (1985) and references therein

16. Bahr, Ch. and Heppke, G., *Phys. Rev. A*, **41**, 4335 (1990)

17. Goates, J. B., Garland C. W., and Shashidhar, R., *Phys. Rev. A*, **41**, 3192 (1990)

18. Bahr, Ch. and Heppke, G., *Mol. Cryst. Liq. Cryst.*, **150B**, 313 (1988)

19. Liu, H. Y., Huang, C. C., Bahr. Ch and Heppke, G., *Phys. Rev. lett.*, **61**, 345 (1988)

20. Reatto, L., *Phys. Rev. B*, **5**, 204, (1972)

21. Griffiths, R. B., *Phys. Rev. Lett.*, **24**, 715, (1970)

22. de Gennes, P. G., *Solid State. Commun.*, **10**, 753, (1972)
Halperin, B. I., and Lubensky, T. C., *Solid State Commun.* **14**, 997, (1974)

23. Doane, J. W., Parker, R. S., Cvikl, B., Johnson, D. L. and Fishel, D. L., *Phys. Rev. Lett.*, **28**, 1694, (1972)

24. Johnson, D. L., Maze, C., Oppenheim, E. and Reynolds, R., *Phys. Rev. Lett.*, **34**, 1143, (1975)

25. McKee, T. J. and Mc Coll, J. R., *Phys. Rev. Lett.*, **34**, 1076, (1975)

26. Navard, P. and Hauding,J. M., *J. Thermal Analysis*, **29**, 405 (1984)
Mol. Cryst. Liq. Cryst., Letters, **101**, 261 (1984)
Mol. Cryst. Liq. Cryst., Letters, **102**, 265 (1984)

Table 5.1. I-S_A and S_A-S_C phase transition temperatures and entropy change ($\Delta S/R$) at the transitions in different compositions of weight percent of TBDA in TBBA.

% TBDA	Transition Temperature/°C		Sm A Thermal Range/°C	Entropy change ($\Delta S/R$)	
	I-S_A	S_A-S_C		I-S_A	S_A-S_C
100	190.90	189.02	1.88	1.81	0.152
93.55	193.00	187.20	5.80	1.79	0.098
85.15	198.60	184.70	13.90	1.67	0.048
82.80	197.60	181.60	16.00	1.68	0.028
81.06	197.17	181.10	16.07	1.62	-
80.26	198.93	181.00	17.93	1.63	-
80.05	199.20	180.9	18.30	1.56	-
75.39	200.87	177.4	23.47	1.59	-

Table 5.2. Density jumps, pressure dependence of Sm A – Sm C transition temperatures and Sm A thermal range.

Compound	$\Delta\rho/\rho\%$	T_{AC}/T_{IA}	Sm A Thermal Range (°C)
93.55% TBDA	0.21	0.988	5.80
85.15% TBDA	0.12	0.971	13.90
82.80% TBDA	0.08	0.966	16.00
TBDA	0.39	0.996	1.90
TBNA	0.13	-	6.40
TBOA	-	-	9.40

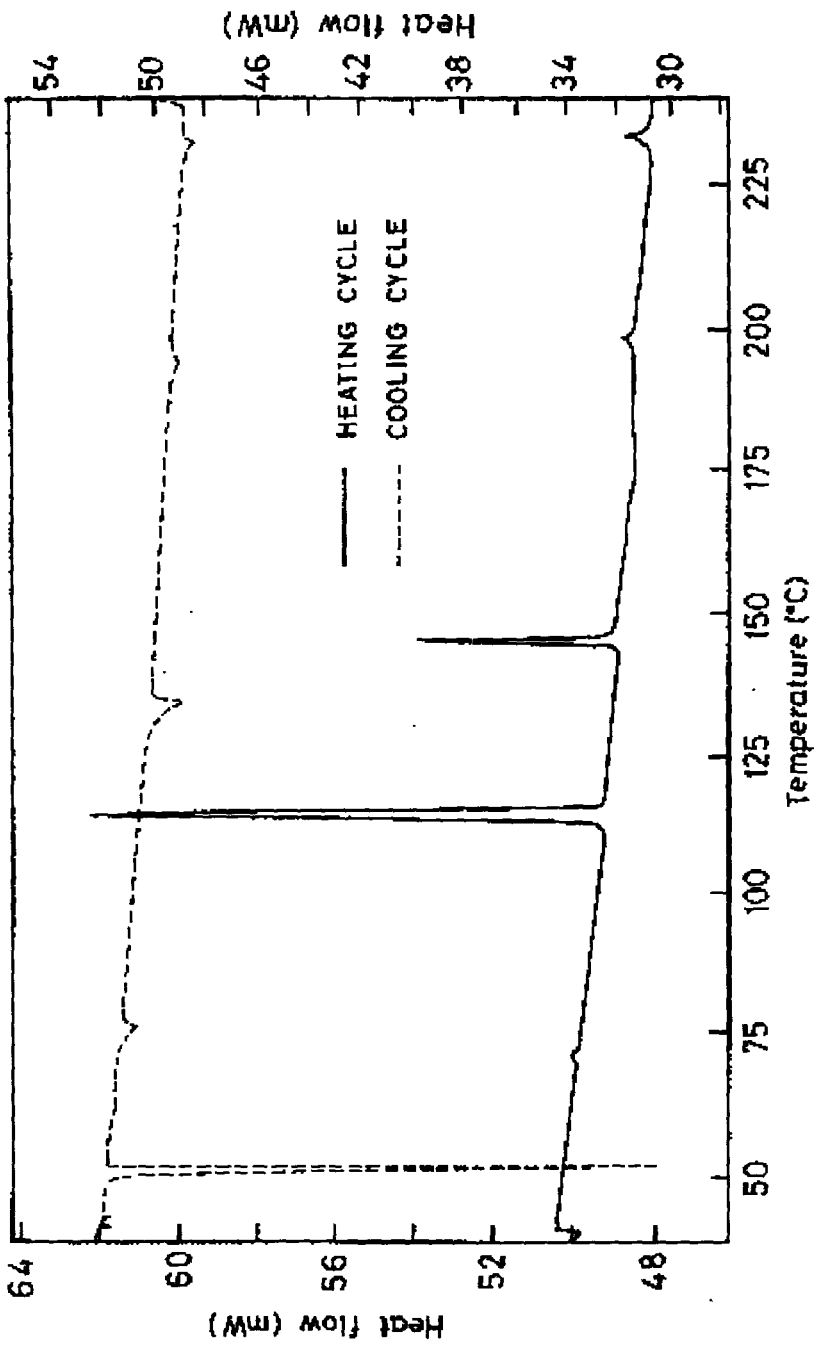

Fig. 5.1a DSC Scan of TBBA

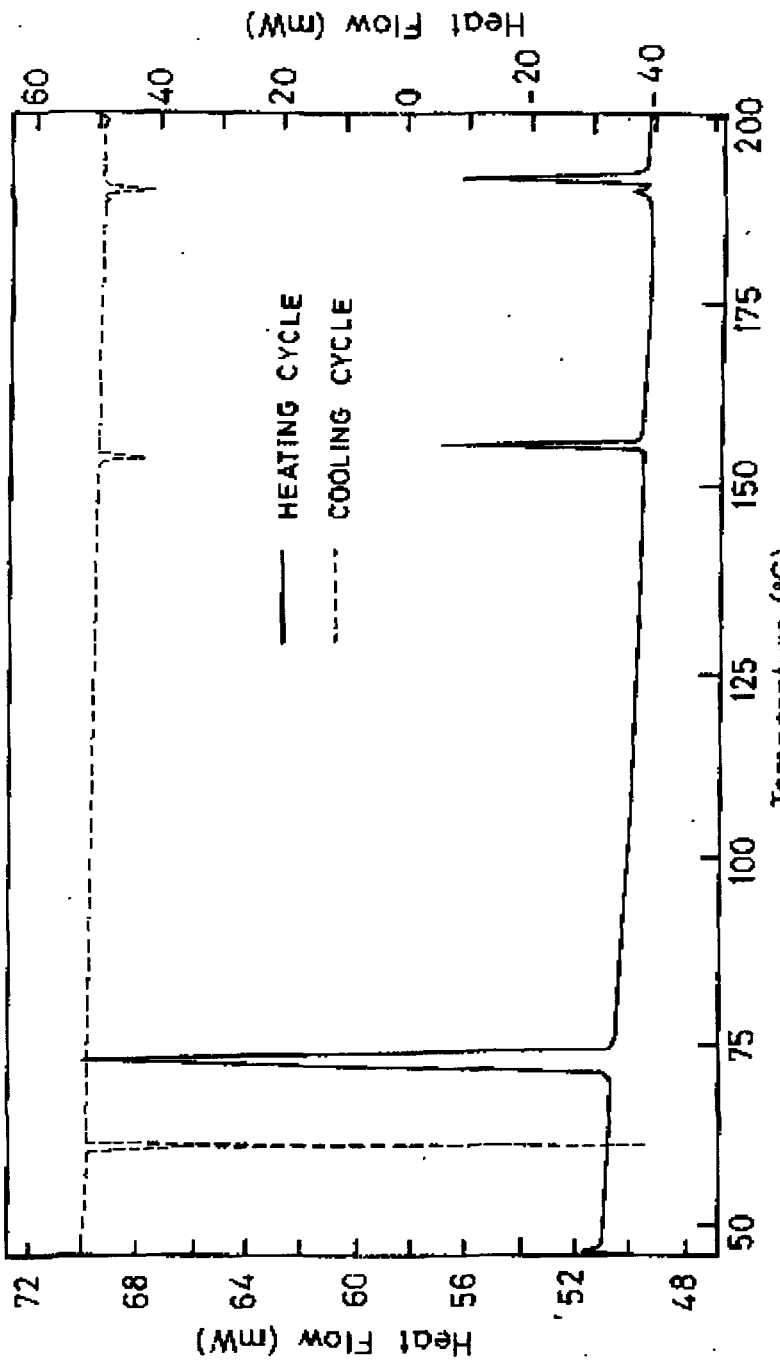

Fig. 5.1b. DSC scan of TBDA

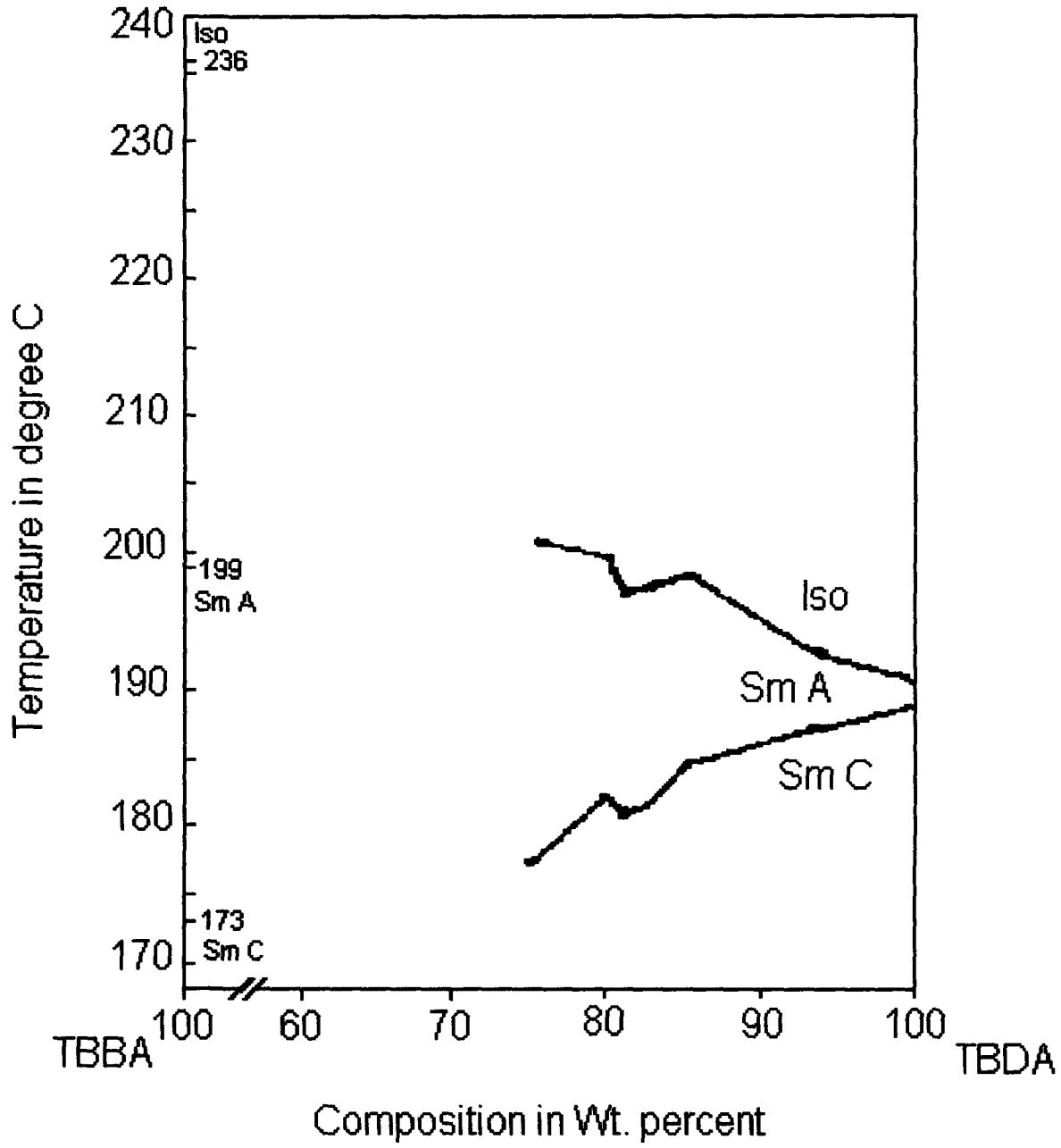

Fig. 5.2. Phase diagram of binary mixtures of TBBA and TBDA at different wt. percent at isotropic – smectic A and smectic A – smectic C phases.

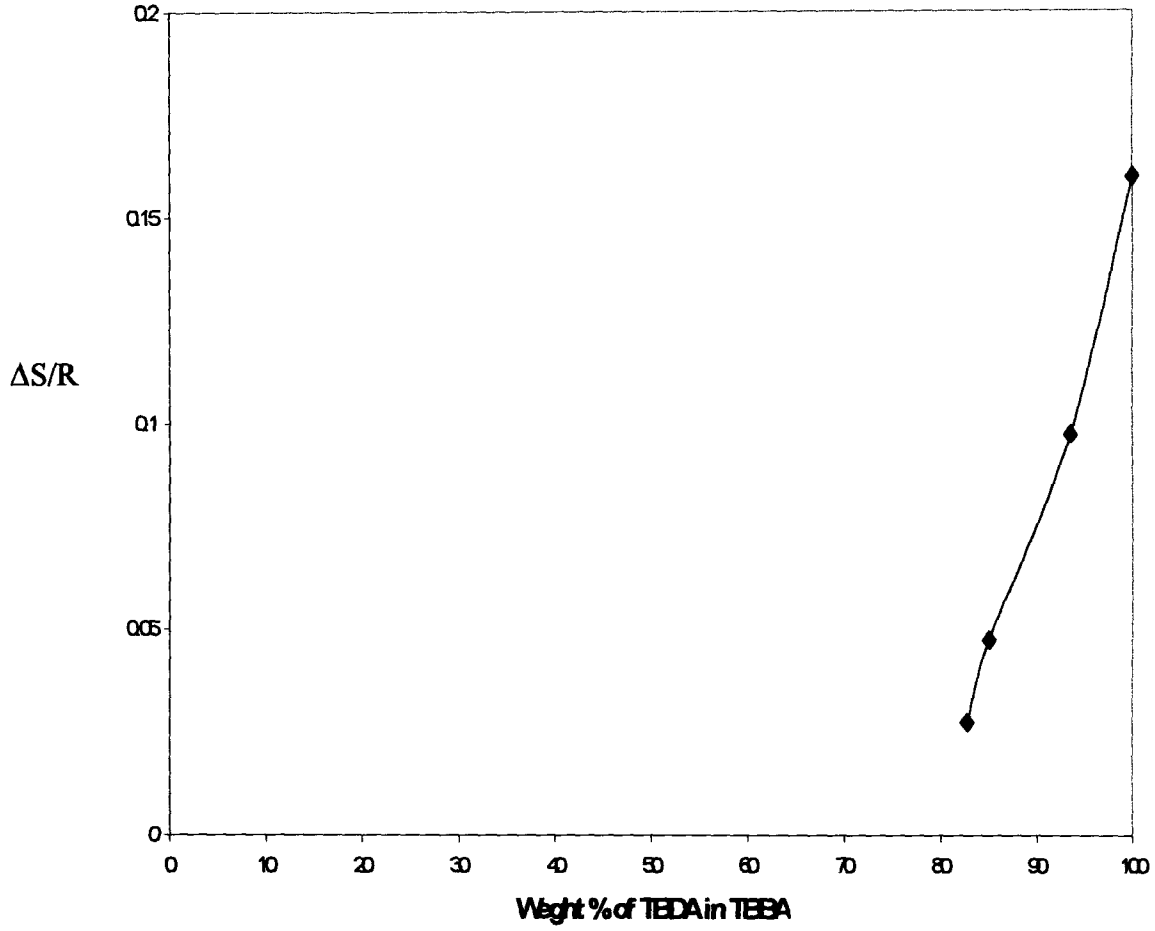

Fig.5.3. Variation of entropy change as a function of weight percent of TBDA in TBBA.

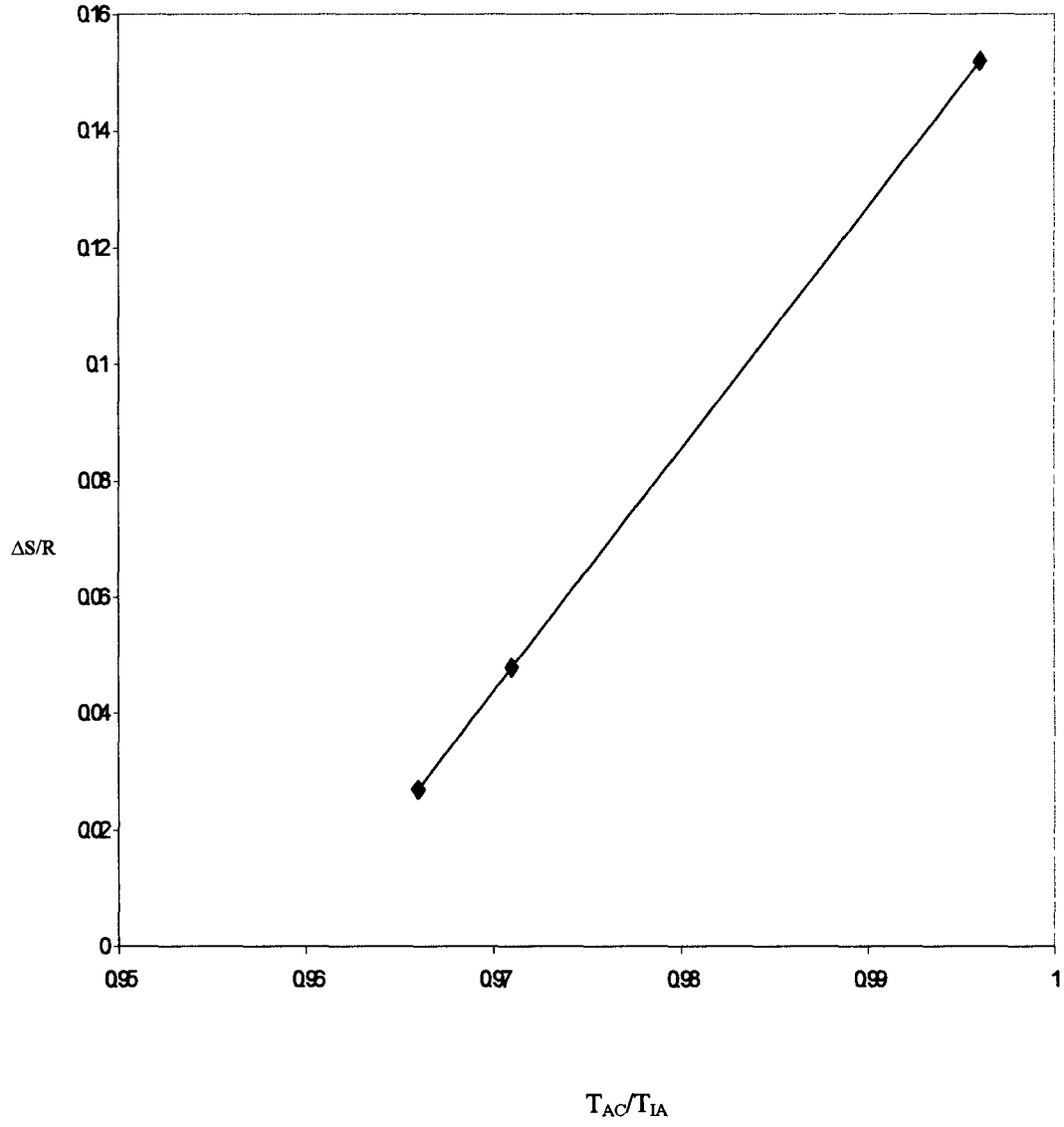

Fig. 5.4. Variation of entropy change ($\Delta S/R$) as a function of scaled parameter T_{AC}/T_{IA}

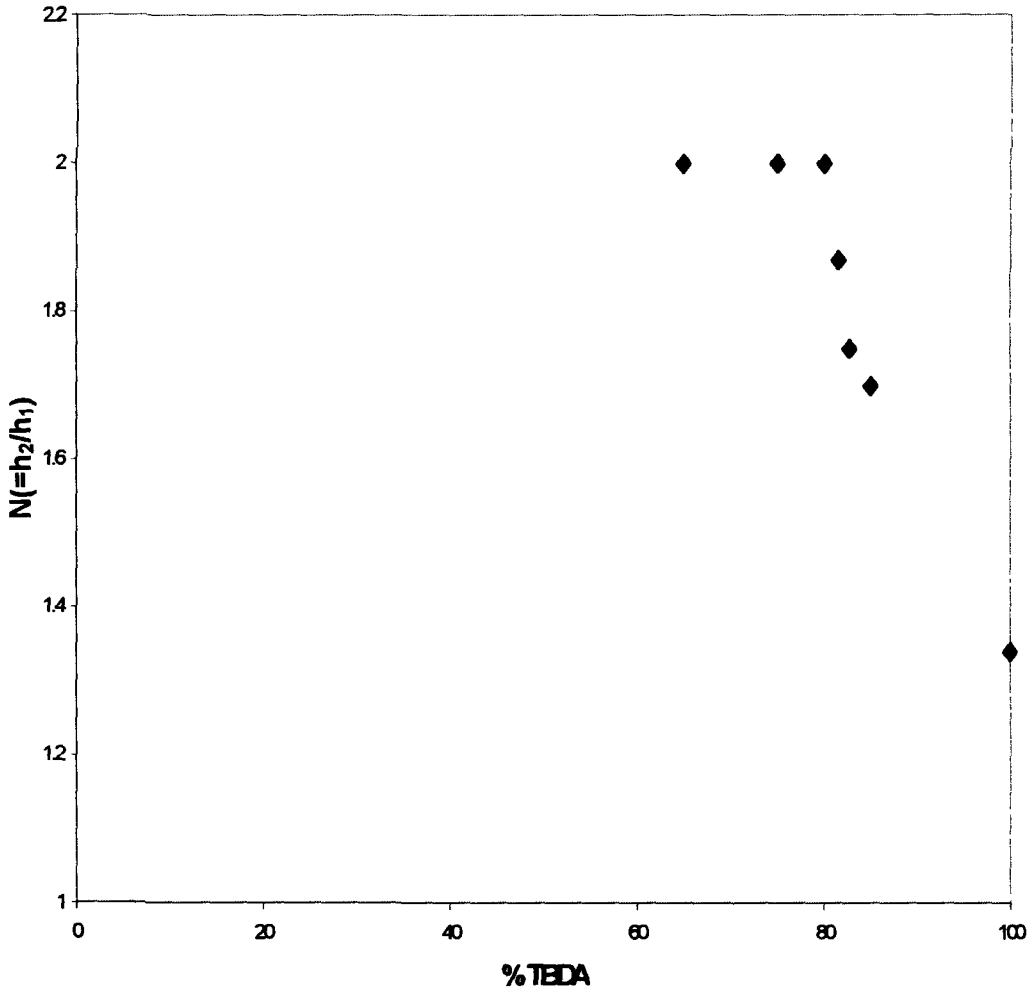

Fig. 5.5. Ratio of heights of DSC peaks at double scan rates ($N = h_2/h_1$)as a function of weight % of TBDA

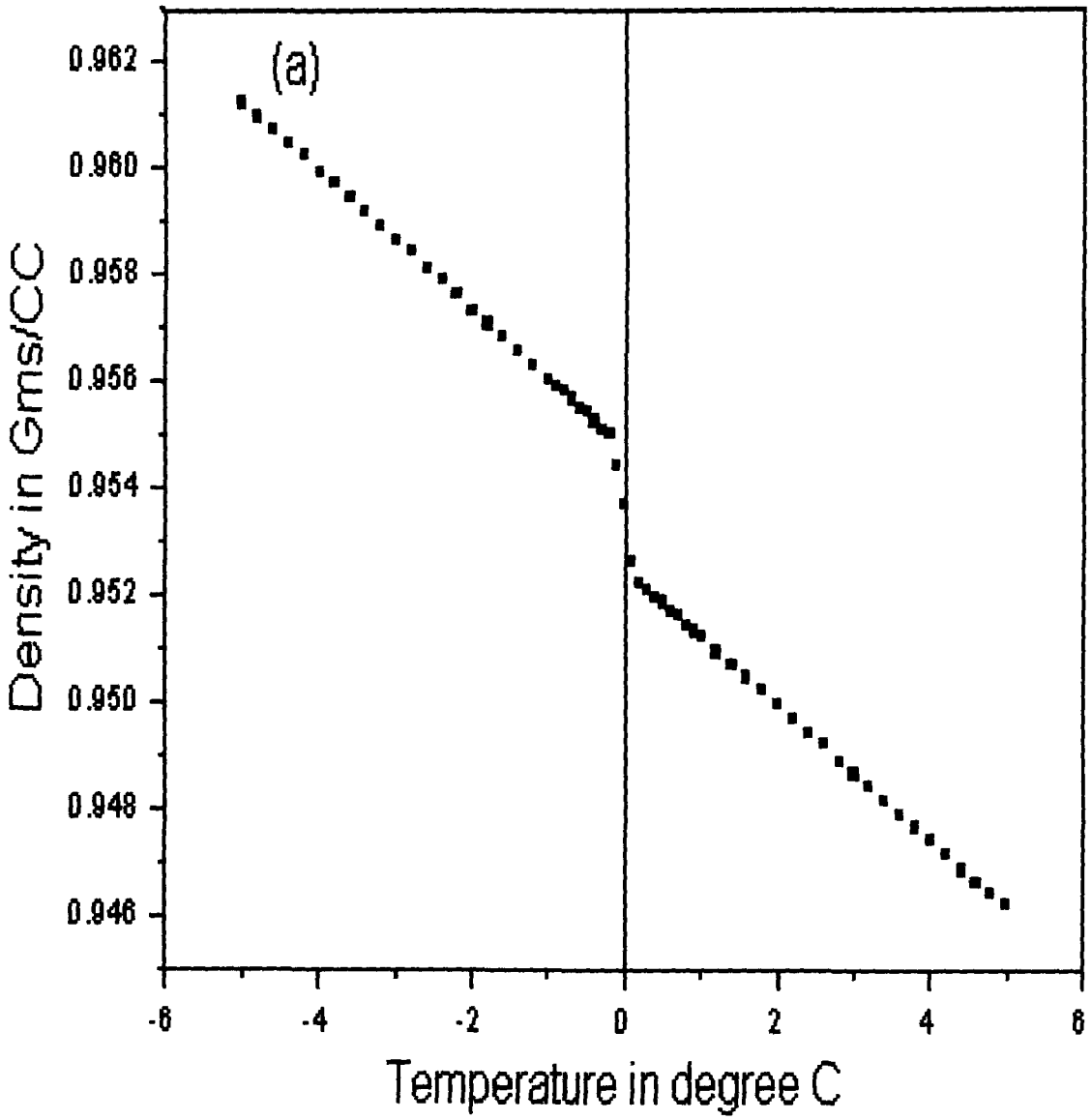

Fig. 5.6a Variation of density as a function of temperature in the binary mixtures of TBDA + TBBA: (a) 93.55% TBDA

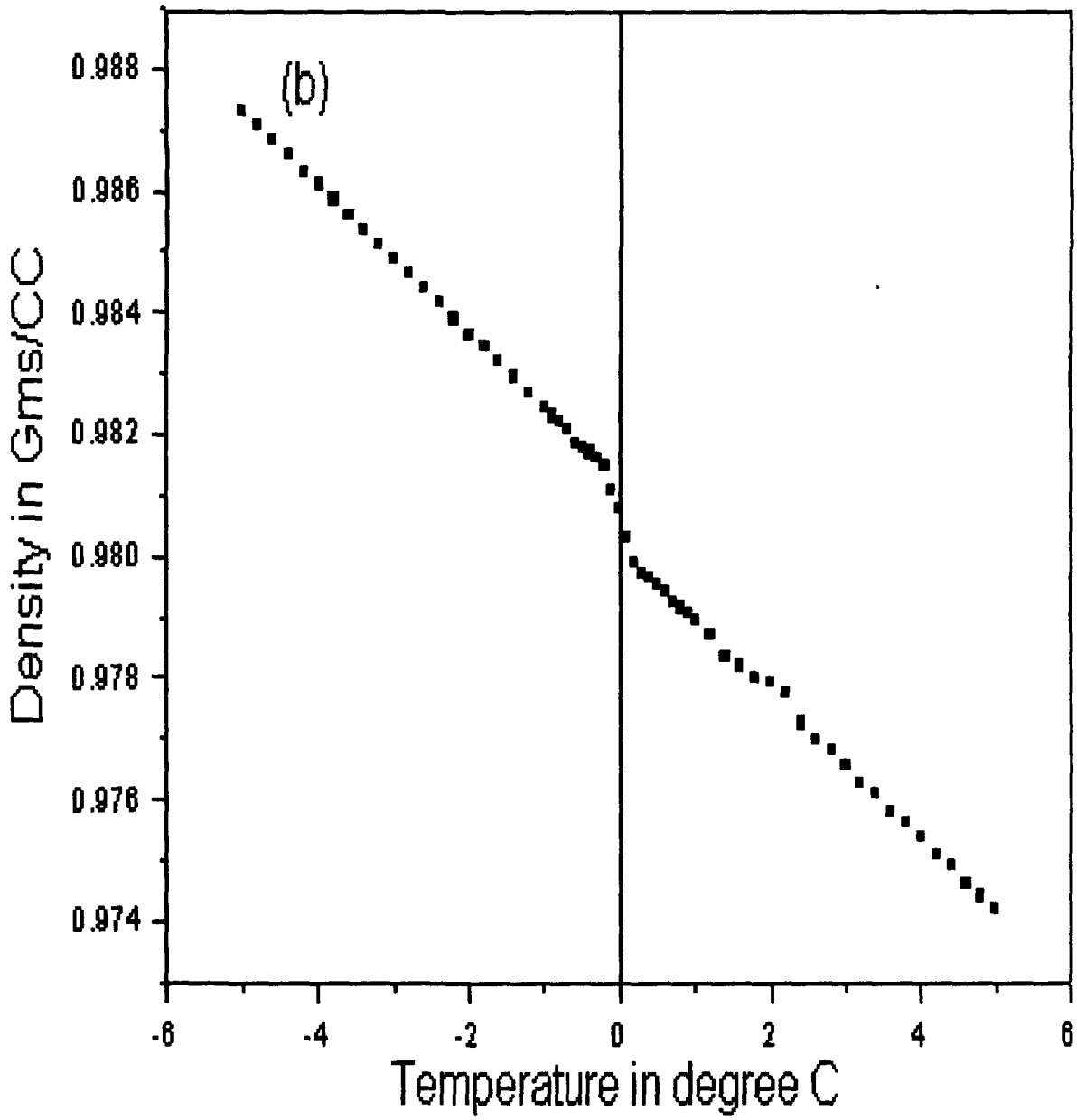

Fig 5.6b Variation of density as a function of temperature in the binary mixtures of TBDA + TBBA: (b) 85.15% TBDA

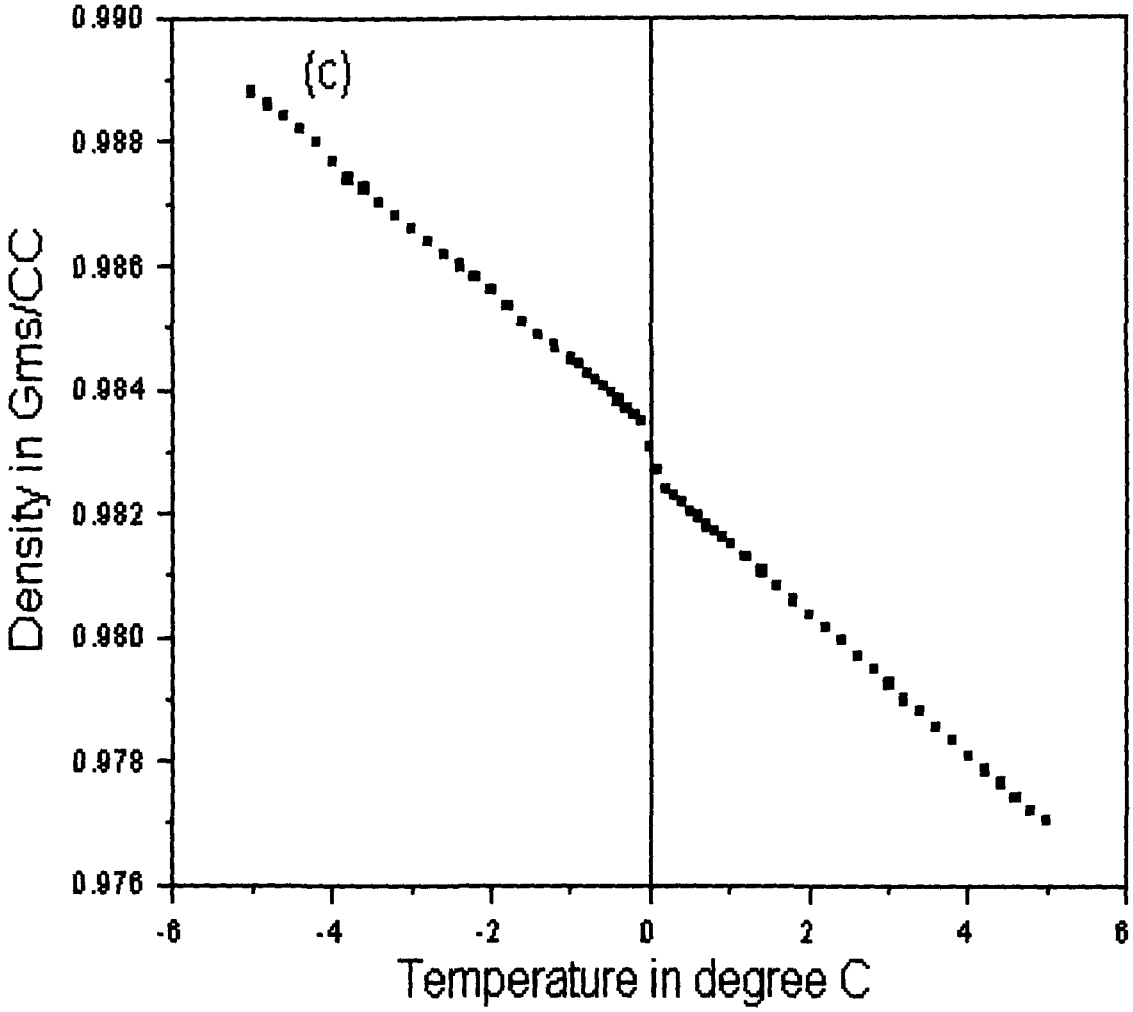

Fig 5.6c. Variation of density as a function of temperature in the binary mixtures of TBDA + TBBA: (c) 82.80%TBDA

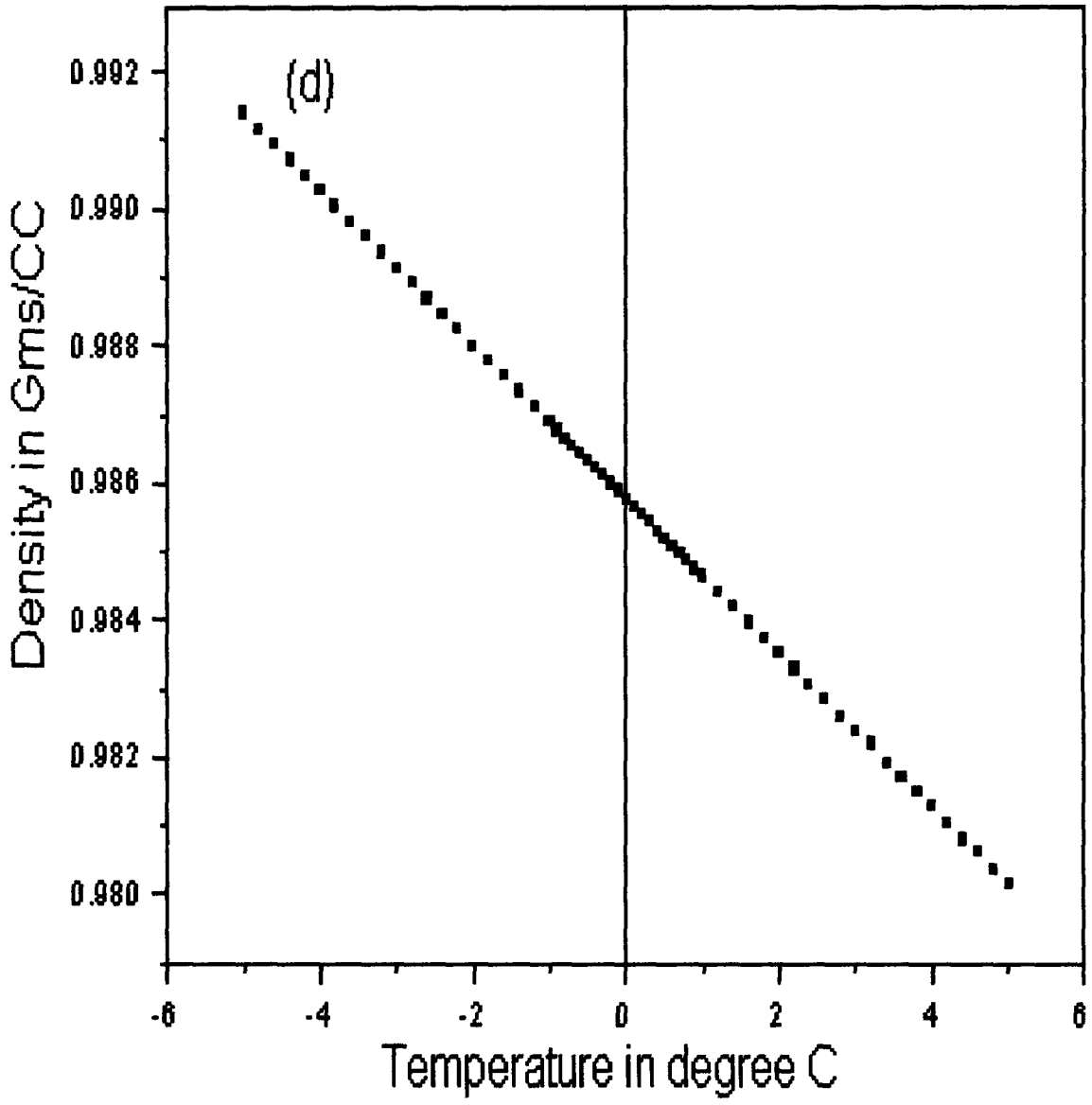

Fig. 5.6d Variation of density as a function of temperature in the binary mixtures of TBDA + TBBA: (d) 81.06%TBDA

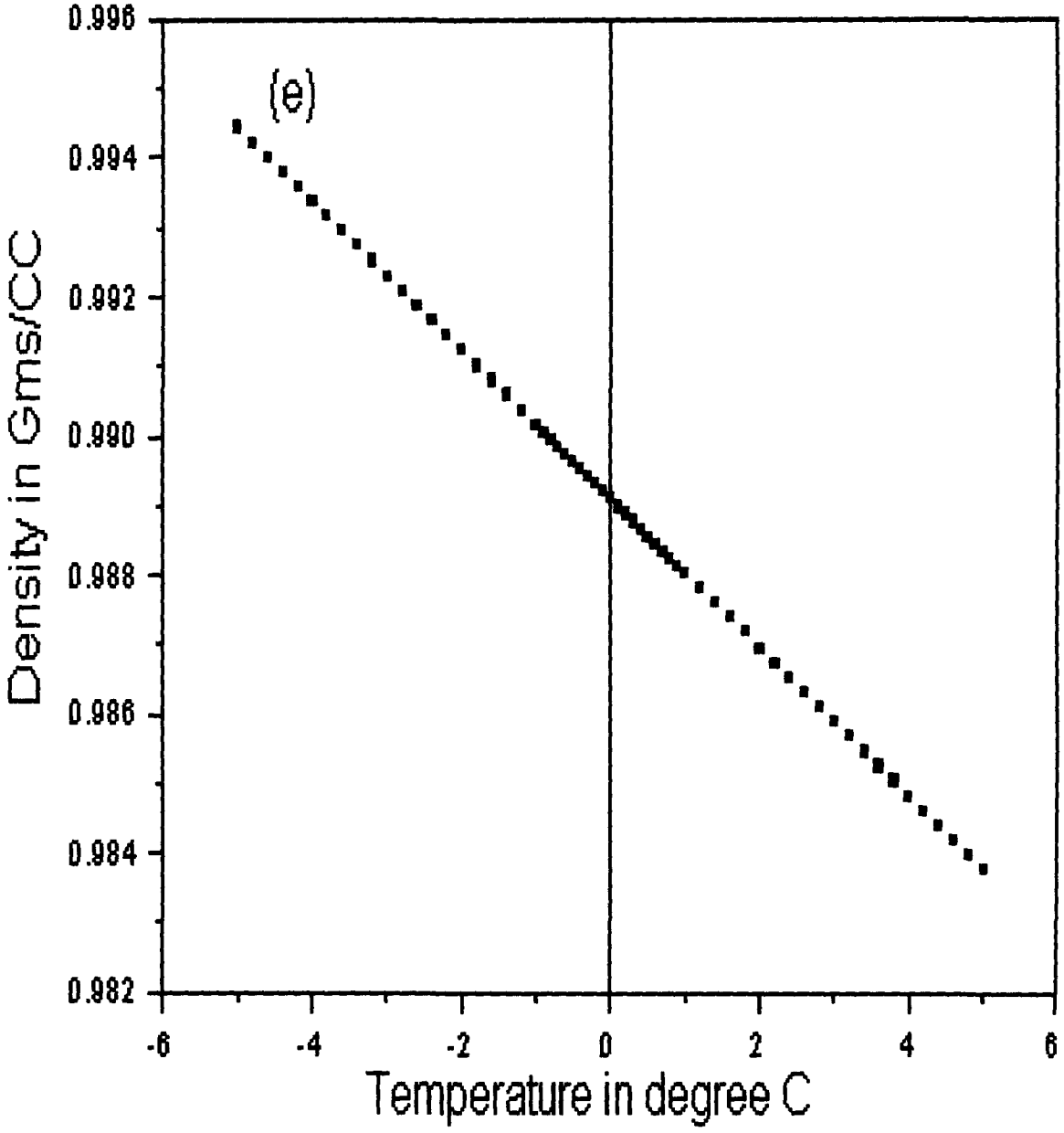

Fig. 5.6e Variation of density as a function of temperature in the binary mixtures of TBDA + TBBA: (e) 80.05%TBDA

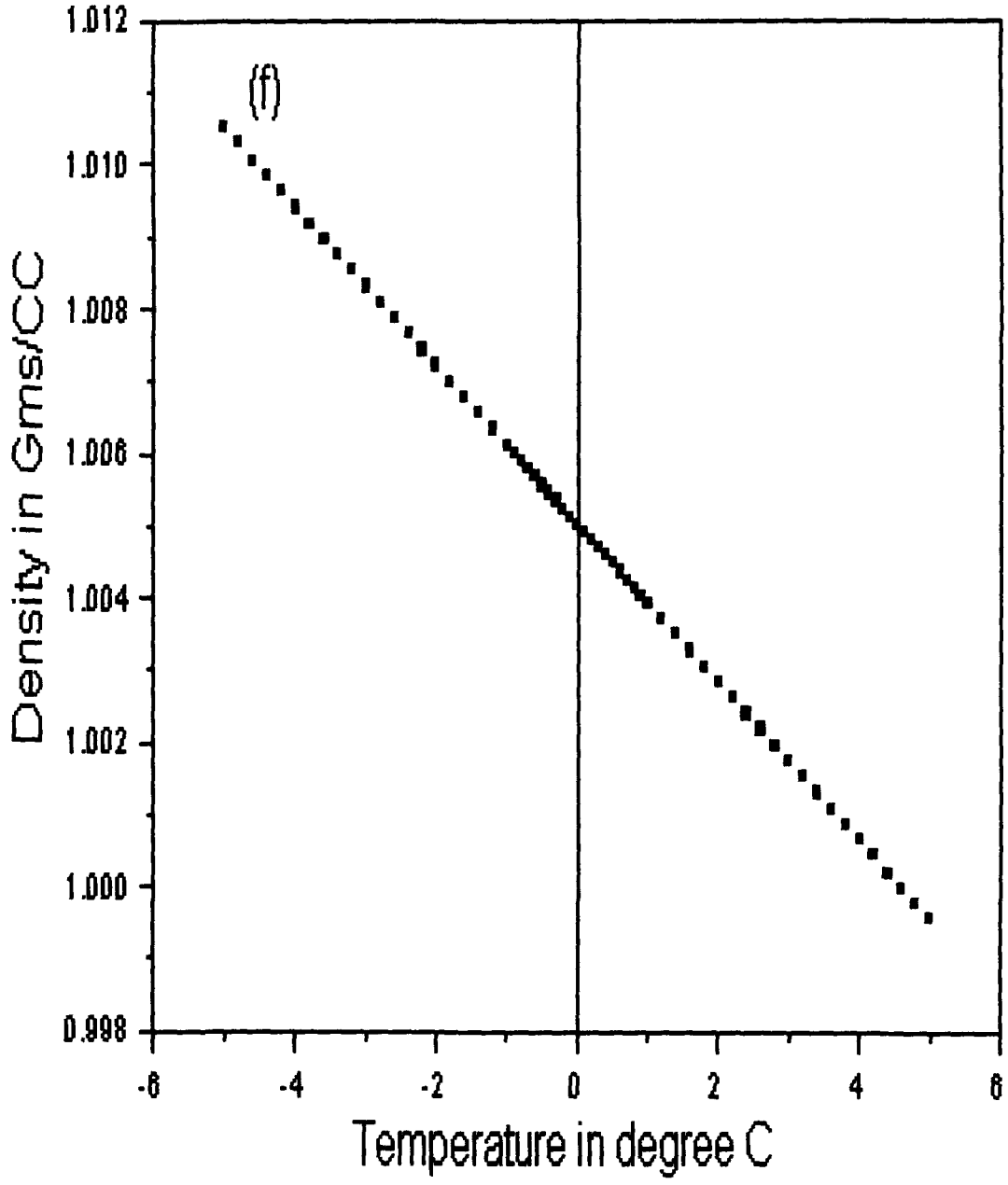

Fig. 5.6f Variation of density as a function of temperature in the binary mixtures of TBDA + TBBA: (f) 75.39%TBDA

CHAPTER - 6

SUMMARY AND CONCLUSION

The main purpose of this chapter is to summarize the discussion in the previous chapters and to highlight the major conclusions drawn from each chapter. As recorded from the discussion in previous chapters, this thesis basically highlights the molecular structure and phase transitions in some liquid crystals. Five members of liquid crystal dimers of the α,ϖ-bis(4-alkylanilinebenzylidene-4′-oxy)alkane (m.OnO.m) homologous series and binary mixtures of the terepthalylidene–bis-p-n-alkylaniline (TBAA) homologues series of liquid crystal compounds have been exhaustively studied. The starting chemicals/ ingredients needed for the synthesis of these compounds have been imported from Aldrich, USA and TCI, Japan. All the compounds used in this work have been synthesized in our laboratory. The phases, phase transition temperatures and purity of the compounds were confirmed by observing the optical textures through a polarizing thermal microscope and DSC studies.

In case of m.OnO.m series compounds, 7.O4O.7, 7.O5O.7, 10.O4O.10, 10.O10O.10 and 10.O12O.10, have been chosen to study using two different experimental techniques. All these m.OnO.m series compounds have been studied using bicapillary pyknometer whereas the compounds 7.O4O.7 and 7.O5O.7 have been studied using Raman spectroscopic technique. On the other hand, in case of TBAA homologues series, TBBA and TBDA have been chosen. The binary mixtures of these compounds at different weight percent have been studied to explore tricritical point at Sm A – Sm C transition by using DSC and bicapillary pyknometer techniques.

The major conclusions drawn on each chapter are given as follows.

In chapter 1, a brief introduction on liquid crystals is given. In this chapter the various basic requirements of liquid crystalline molecules along with their important properties have been explained briefly. A description of the different liquid crystalline phases based on their structural characteristics and optical textures observed under polarizing microscope is given. Some theoretical aspects of liquid crystals like the various order parameters have been briefly discussed to facilitate the understanding of their classification. A section has been dedicated to explain the importance and significance of schiff base liquid crystal dimers and TBAA homologues series which were chosen for present study. Some earlier works on liquid crystals have also been described with an emphasis on the Raman spectroscopy and density measurement techniques.

Chapter 2 can broadly be divided into two sections. First part of this chapter is dedicated to explanation of the actual experimental techniques used in the present study. This portion includes sections on synthesis of the liquid crystalline compounds, their characterization and brief discussion on the phase transition sequence. The construction details of high temperature cells for both Polarizing Thermal Microscopy and Raman Spectrometer for studies on liquid crystals have been described. The measurement of density as a function of temperature using bicapillary pyknometer are also discussed. Another section of this chapter deals extensively with the theoretical background of the

experimental techniques used. The basic principles and the instrumentation used for recording Raman spectra have been described.

Chapter – 3 describes the phase transition study by DSC and density measurements as a function of temperature on five symmetric liquid crystal dimers viz. 7.O4O.7, 7.O5O.7, 10.O4O.10, 10.O10O.10 and 10O.12O.10. at various phase transitions. It was found from the DSC studies that the entropy values at different phase transitions for the dimeric compounds are larger than that for other monomeric compounds. Further, the entropy value of even spacer dimer (7.O4O.7) at the Isotropic – Sm A transition is nearly double compared to the odd spacer dimer (7.O5O.7). These very large entropy values suggest that both the orientational and translational ordering in the smectic A phase are high for even spacers and also affect the alternation of entropies in varying the flexible spacer for any given length of terminal chain. The density studies with variation of temperature using bicapillary pyknometer technique across the phase transitions include I – Sm A, I – Sm C, Sm C - Sm F with the very rare I – G and Sm A – Sm F transitions have been discussed. In all the compounds, the density increases as the temperature decreases, except in the vicinity of the phase transitions. It was found that the all the transitions are of first order in nature but smaller density jumps than expected in the density across certain transitions.

In chapter 4, experimental results on the liquid crystalline compounds, 7.O4O.7 and 7.O5O.7 obtained from Raman spectroscopy are discussed. It is established that though the only difference between the 7.O4O.7 and 7.O5O.7 is an extra methylene unit in the spacer region of the molecule, this extra methylene unit has shown profound

effect on the molecular structure. The spectral analysis indicates a first order nature of phase transition for both the compounds at the crystalline - Sm F and Sm F – Sm A phase transitions. However, the Raman spectra of these compounds at room temperature remarkably highlight the odd – even effect. The results satisfy the molecular topology of the dimeric molecule and it is found that the molecular shape of the odd spacer dimer is bent whereas for the even spacer dimer, the molecular shape is linear. The assumption of a semi-rigid core region of the dimeric molecule for the manifestation of the odd – even effect at the molecular level supports the odd spacer dimer (7.O5O.7) for bending shape of the molecules, whereas the even spacer dimer (7.O4O.7) is established to behave like monomeric compounds such as nO.ms. Also, in both the cases, it is established that the dynamics about the C = N bond have a profound effect on the molecular shape in different phases and phase behaviour.

Chapter – 5 deals with the tricritical behaviour of the Sm A – Sm C phase transition. The only other study of the Sm A – Sm C tricritical point in TBAA homologues series was reported using x-ray diffraction studies on binary mixtures of TBDA and TBOA, where TBOA was found to undergo a second order Sm A – Sm C transition. However, density studies reported later on confirm this to be a weakly first order transition in TBOA. On the other hand, the TBNA and TBDA, higher homologues of the TBAA series are the only examples of non-ferroelectric thermotropic liquid crystals which exhibit a weakly first order Sm A – Sm C phase transition. Whereas the TBBA, the lower homologue exhibits a clearly second order

Sm A – Sm C phase transition within the series. For this reason, binary mixtures of TBBA and TBDA(where TBBA has been well established to exhibit a second order Sm A – Sm C phase transition) have been chosen to explore the tricritical point (TCP) in Sm A – Sm C phase transition. In order to investigate the tricritical point (TCP) of the Sm A – Sm C phase transition, binary mixtures of TBBA and TBDA (of different weight percent) of few compositions have been studied as tricritical point is approached using DSC and density measurements as a function of temperature. The results of these studies clearly suggest the decisive role played by the Sm A thermal range in determining the nature of the Sm A – Sm C transition and location the TCP, and that the transition becomes weakly first order as the thermal range of the Sm A decreases. The important outcome of this study is the existence of tricritical point in the binary mixtures of TBBA + TBDA and its establishment in 80.05% weight percent of TBDA in TBBA at a T_{AC}/T_{IA} value of 0.959. The earlier study of TCP for TBOA was reported in the thermal range of 9.4°C, which is much lower than that of our TBDA+TBBA mixture (present study) where the Sm A thermal range is about 17°C.

Future Scope of Study

The studies on m.OnO.m and TBAA compounds established the usefulness of the various experimental techniques used for this study. In particular the Raman spectroscopy is very effective in understanding the molecular dynamics, especially at phase transitions and also, the bicapillary pyknometer is another useful tool for understanding the nature of phase transition. An elaborate study of the other homologues of the liquid crystal dimers with different terminal and spacer lengths using

Raman spectroscopy is likely to provide ample information to understand the structure-property relationship of these systems at molecular level.

The density measurement as a function of temperature are extensively useful to establish the nature of phase transitions. This technique may be useful for understanding the model compounds for main chain liquid crystal polymer, which is of basic research importance. In general, the liquid crystal dimers are very interesting and have much potential in the field of basic research as well as for technological applications.

BIO DATA

1.	**Name**	:	BULBUL GOGOI
2.	**Father's Name**	:	Mr. Bhadreswar Gogoi
3.	**Permanent Address**	:	Tengrajan P.O. Tengabari (Sarupathar) Dist. Golaghat, ASSAM PIN – 785 601
4.	**Mailing Address**	:	Department of physics NERIST, Nirjuli Itanagar – 791 109 FAX # 91-0360-257872/233407 e- mail : bul_gog@yahoo.com
5.	**Date of birth**	:	20-01-1969
6.	**Sex**	:	Male
7.	**Marital Status**	:	Unmarried
8.	**Religion**	:	Hindu
9.	**Nationality**	:	Indian
10.	**Academic Qualifications**	:	

Exam Passed	Board/Univ.	Year of Passing	Div./Class
H.S.L.C.	S.E.B.A.	1985	1st
H.S.S.L.C.	A.H.S.E.C.	1987	2nd
B.Sc. (Phy. Maj)	Dib. Univ, Assam	1990	2nd
M.Sc. (S.S.Phy)	Dib. Univ, Assam	1993*	1st

*** One-year session late**

11. **Work Experiences** :

i) Working as JRF in DST, New Delhi Sponsored research project in the Department of physics at NERIST, Nirjuli from September 2001 till date.

ii) Worked as SRF in CSIR, New Delhi sponsored research project in the Department of physics at NERIST, Nirjuli from December1997 to March 2001.

iii) Worked as JRF in DST, New Delhi sponsored research project in the Department of Applied Physics at BIT, Mesra, Ranchi from May1995 to March 1997.

iv) Worked as a Subject Teacher in Physics at Sarupathar H.S.School, Sarupathar from March 1994 to March 1995.

V) Worked as a lecturer in the Department of Physics, D.R. College, Golaghat from October 1993 to January 1994.

12. **Conference/workshop attended**:

i) International school on Powder Diffraction. Held at Calcutta (Kolkota) during 7^{th} to 10^{th} October, 1998

ii) 8^{th} National Conference on Liquid Crystals. Held at Mumbai during 28^{th} to 30^{th} *December, 2000*

iii) 3^{rd} Conference on Physics Research of North East. Held at Dibrugarh University, Dibrugarh on 9^{th} November, 2002.

13. **List of publications**

i) Density studies on two homologues of α,ω-bis(alkylanilinebenzylidene-4′-oxy) alkane
B. Gogoi, A. Arulsankar, T. K. Ghosh and P. R. Alapati
***Mol. Cryst. Liq. Cryst*, 365,561 (2001)**

ii) Investigation of rare phase transitions by density measurements
B. Gogoi, A. Arulsankar, and P. R. Alapati
***Mol. Cryst. Liq. Cryst*, 366,69 (2001)**

iii) Sm A – Sm C tricritical point in TBBA and TBDA mixtures
P. R. Alapati, A. Arulsankar, B. Gogoi, T. K. Ghosh and Nagappa
***Mol. Cryst. Liq. Cryst*, 366,61 (2001)**

iv) Phase transition studies in mesogenic dimers
B. Gogoi, P.R. Alapati and A. L. Verma
***Cryst. Res. Technol.* 37, 12(2002)**

v)Laser Raman studies in 7.O4O.7 and 7.O5O.7
B. Gogoi, A. Bhattacharjee, P. R. Alapati and A. L.Verma
***Liquid crystals* (Communicated)**

I hereby declare that all the statements made above are true, complete and correct to the best of my knowledge and belief.

(BULBUL GOGOI)

Place : Nirjuli

Date : 17-12-02